MICROCOMPUTER CONTROLLED ELECTROTHERMAL ATOMIZATION USING LASER ATOMIC FLUORESCENCE SPECTROMETRY

BY

PHILIP KIRK WITTMAN

A DISSERTATION PRESENTED TO THE GRADUATE COUNCIL OF THE UNIVERSITY OF FLORIDA IN PARTIAL FULFILLMENT OF THE REQUIREMENTS FOR THE DEGREE OF DOCTOR OF PHILOSOPHY

UNIVERSITY OF FLORIDA

1982

This dissertation is dedicated to my closest friends who most certainly know who they are.

ACKNOWLEDGEMENTS

I wish to take this opportunity to express my appreciation to the members of Dr. Winefordner's research group who, with their discussions and actions, helped make this time pass. In particular I wish to thank both Dr. Ed Voigtman and Dr. Ben Smith for their help, guidance and friendship. I especially wish to express my sincerest gratitude to Dr. James D. Winefordner, my research director, for his continual guidance and patient encouragement during the course of this work. I consider myself fortunate to have been part of his research efforts.

TABLE OF CONTENTS

		Page
ACKNOWLEDGEMENTS		iii
ABSTRACT		vi
CHAPTER		
1	INTRODUCTION	1
	Electrothermal Atomization	1
	Laser Atomic Fluorescence Spectrometry	3
	Electrothermal Atomization Using Laser Atomic Fluorescence Spectrometry	4
2	THEORETICAL CONSIDERATIONS	6
	Electrothermal Atomization	6
	Types of Atomic Fluorescence	11
	Atomic Fluorescence Expressions	15
	Saturation Spectral Irradiance	18
	Lifetime	21
3	EXPERIMENTAL	22
	General Comments	22
	Fluorescence Collection	22
	Temperature Monitoring	26
	Detection Electronics	29
	Nitrogen Laser	32
	Dye Laser	33
	Furnace System	35
	Microcomputer	36
	Quantum Efficiency	41
	Solutions	43
4	RESULTS AND DISCUSSION	44
	Signal To Noise Optimization	44
	Definitions Of Analytical Parameters	45
	Limits Of Detection	52
	Linear Dynamic Range And Sensitivity	53
	Precision	60
	Sodium Population Profile	70
	Quantum Efficiency	73
	Saturation Spectral Irradiance	81

5 SUMMARY AND FUTURE WORK 88

Summary 88
Future Work 89
Temperature Control 89
Laser Considerations. 90
Detector Calibration. 93
Sample Types. 94
Furnace Design. 94

APPENDICES

1 FURNACE HARDWARE. 96

2 FURNACE SOFTWARE. 103

3 RADIOMETER SYSTEM 111

4 DIGITAL PLOTTING PROGRAM. 130

5 DIFFRACTED STIMULATED EMISSION. 144

REFERENCES. 152

BIOGRAPHICAL SKETCH 157

Abstract of Dissertation Presented to the Graduate Council of the University of Florida in Partial Fulfillment of the Requirements for the Degree of Doctor of Philosophy

MICROCOMPUTER CONTROLLED ELECTROTHERMAL ATOMIZATION USING LASER ATOMIC FLUORESCENCE SPECTROMETRY

By

Philip Kirk Wittman

December 1982

Chairman: James Dudley Winefordner
Major Department: Chemistry

Laser atomic fluorescence spectrometry combined with a microcomputer controlled electrothermal atomizer is evaluated with respect to several analytical figures of merit. Among these are the sensitivity, the limit of detection, the linear dynamic range and relative standard deviation of the technique. The atom population distribution as well as post filter effects are investigated. Additionally the saturation irradiance curves are determined for three elements in the electrothermal atomizer. An instrumental system consisting of a graphite rod furnace, as the atomizer, a nitrogen laser pumped dye laser as the excitation source and a microcomputer to control the system is described. Quantum efficiencies are determined by comparing fluorescence intensities in two sheath gases (argon and

nitrogen) with different quenching cross sections. Experimental results for sodium, tin and manganese are presented which demonstrate the analytical utility of the described microcomputer controlled electrothermal atomization system.

CHAPTER 1
INTRODUCTION

Electrothermal Atomization

Initially the interest in electrothermal atomization (1-3) arose mainly in connection with the problem of developing absolute methods of atomic absorption analysis. Early publications (2-4) indicated an apparent freedom from matrix effects on the results of quantitative analyses. This led to great interest in the technique and consequently many researchers studied the processes involved.

Some of this work included characterization of atomic absorption signals and various methods of their measurement (5-8), the influence of the rate of heating of the atomizer on the analytical sensitivity (8-10), the effects of atomizer geometry and construction material on the signal (11-14), the mechanism of atom formation (10,12,15-17) and the interferences due to compound formation and composition of the matrix (18-22).

Some of the advantages (23) that electrothermal atomization (ETA) has over flame techniques are as follows:

1. ETA requires only a few microliters of sample per analyses.
2. Difficult to nebulize liquids can be conveniently handled.

3. The efficiency of the vaporization process is generally better than in a flame, due to the faster heating rate.

4. The efficiency of the atomization process is usually better than in a flame, especially in the cases of those elements which tend to form thermally stable oxides. This is a consequence of the rapid heating of the sample in a reducing environment provided by the argon and hydrogen diffusion flame sheath gases.

5. Enhancements in the signal to noise ratios in the electrothermal atomizer are a result of the smaller sample volume, the absence of analyte dilution by expanding flame gases and increased lifetime of the analyte within the analytical volume.

6. The chemical and thermal environment can be better controlled in ETA.

7. The capability of direct solid sampling exists.

Coupling these advantages with the possibility of determining a large number of elements with high sensitivity, selectivity, accuracy and speed, it is little wonder that electrothermal atomization with atomic absorption spectrometry has been shown to be of considerable value for the detection and quantitative determination of trace amounts of metals in a variety of matrices (24-26).

Laser Atomic Fluorescence Spectrometry

In 1963, Alkemade (27) reviewed the methods by which atoms undergo excitation in flames--one of these being radiational. He described the use of atomic fluorescence flame spectroscopy for measuring quantum efficiencies and used this method for measuring the quantum efficiency of the sodium D-lines.

Atomic fluorescence spectrometry as a method of chemical analysis was first proposed by Winefordner and Vickers (28) in 1964. At the same time, Winefordner and Staab (29) reported the determination of cadmium, mercury, thallium and zinc in solution by atomic fluorescence flame spectrometry.

The advent of the tunable dye laser (30,31) and the power it has to generate atomic fluorescence transitions has given spectroscopists a valuable tool for analyses. The general properties of lasers include

1. The laser beam has good directionality (low divergence).
2. The laser beam is highly monochromatic.
3. The laser beam is spatially and temporally coherent.
4. The laser beam has a high irradiance.

All of these laser properties have been useful for analytical atomic fluorescence spectrometry since Fraser and Winefordner (32) first used a dye laser to excite atomic fluorescence. Their work covered nine elements in

hydrogen-air and acetylene-air flames. The limits of detection obtained were within ten to one hundred fold of those obtained with conventional sources. This lack of greatly improved sensitivity over conventional sources is apparently connected with the fact that in flames the detection limit in most cases is determined by non-selective scattering of the exciting radiation by small unburnt particles and by fluctuations in the flame optical density, as well as by strong molecular fluorescence of organic species (33). Progress in both theory and experimental achievements has been rapid in the ensuing years (34-41).

Electrothermal Atomization Using Laser Atomic Fluorescence Spectrometry

Patel et al. (42) combined the advantages of graphite rod ETA with those of atomic fluorescence spectrometry for the determination of silver, cadmium, copper, mercury, lead, tin, thallium and zinc in aqueous samples and silver, lead and tin in oil-based samples. However, this work used electrodeless discharge lamps as the exciting sources.

This work did point out the usefulness of combining atomic fluorescence with electrothermal atomization, and so it was inevitable that the next step would be evaluating laser excited atomic fluorescence with ETA. The low scattering level of the exciting radiation in the analytical zone and the absence of organic compounds, which quench fluorescence and can produce a considerable background due to molecular luminescence, permits an

appreciable decrease in detection limits over laser excited atomic fluorescence flame methods.

Laser atomic fluorescence with electrothermal atomization has produced the lowest detection limits by spectroscopic methods for several elements (43-46). The present work was intended to characterize several figures of merit of such a system and to make analyses easier by the automation provided by microcomputer control.

CHAPTER 2
THEORETICAL CONSIDERATIONS

Electrothermal Atomization

Analytical signals obtained with electrothermal atomizers are, in general, curves having peaks (24), their exact shape being determined by a number of factors. To understand why this should be, L'vov (5,47,48), L'vov et al. (49,50) and Sturgeon and Chakrabarti (23) devised a mathematical model to describe the time-dependent characteristics of the atom population within an isothermal volume. For the sake of simplicity, only the process of the transfer of sample vapour through the analytical volume (defined by the beam of excitation radiation and the cell length) is considered.

Two simplifying assumptions were made in this mathematical model: the element to be determined is completely atomized and all of the atoms of the element enter the analytical volume. The following variables will be used:

N_o = number of atoms of the element to be determined in the sample, dimensionless

$N(t)$ = total number of atoms of the element within the analytical volume at the moment of time, dimensionless

τ_1 = atomization time--the length of time for the transfer of all the atoms into the analytical volume, s

τ_2 = residence time of atoms within the analytical volume, s

$n_1(t)$ = number of atoms entering the analytical volume at any time, s^{-1}

$n_2(t)$ = number of atoms escaping from the analytical volume at any time, s^{-1}

The rate of population change within the analytical volume is given by

$$dN/dt = n_1(t) - n_2(t).$$

With a diffusional mechanism of vapour loss, the function $n_2(t)$ may be approximated by

$$n_2(t) = N(t)/\tau_2$$

Since the introduction of the sample into the analytical volume takes place via a process of accelerated vaporization due to the continuously rising temperature of the eletrothermal atomizer surface, $n_1(t)$ can be approximated by

$$n_1(t) = Dt$$

where D is the atomization factor. With normalization D may be determined:

$$\int_0^{\tau_1} n_1(t)dt = N_o.$$

Therefore

$$n_1(t) = (2N_o/\tau_1^2) = Dt$$

and the rate of population change becomes

$$dN/dt = (2N_o/\tau_1^2) - N(t)/\tau_2$$

This is a general linear first order differential equation which may be solved with an integration factor $\exp(t/\tau_2)$ and then integrating and evaluating at the boundary condition N = 0 at t = 0 yields

$$N_{t<\tau_1}(t) = 2N_o\frac{\tau_2^2}{\tau_1^2}\left[\frac{t}{\tau_2} - 1 + e^{-t/\tau_2}\right] .$$

When the sample has been completely atomized ($t = \tau_1$), $N(t)$ attains a maximum given by

$$N_{t=\tau_1}(t) = 2N_o\frac{\tau_2^2}{\tau_1^2}\left[\frac{\tau_1}{\tau_2} - 1 + e^{-\tau_1/\tau_2}\right] .$$

However at $t > \tau_1$ the rate of population change loses the term that accounts for the addition of new atoms since they have now all been atomized. Taking this into account, at times $t > \tau_1$, $N(t)$ is defined by

$$N_{t>\tau_1}(t) = 2N_o\frac{\tau_2^2}{\tau_1^2}\left[\frac{\tau_1}{\tau_2} - 1 + e^{-\tau_1/\tau_2}\right] e^{(\tau_1 - t)/\tau_2} .$$

These last three equations describe the change in the number of atoms within the analytical volume as a function of time. From these equations, it can be seen that the signal grows in an exponential manner and also decays away exponentially (see Figure 1).

Because of the type of atom population change, it can be shown that by measuring signal peak areas as opposed to signal peak heights, one often avoids the problem of

Figure 1

Curves representing the change in atom population within the analytical volume of the electrothermal atomizer for different τ_1 / τ_2 ratios.

A--τ_1/τ_2 = 1/5 B--τ_1/τ_2 = 1/1 C--τ_1/τ_2 = 5/1

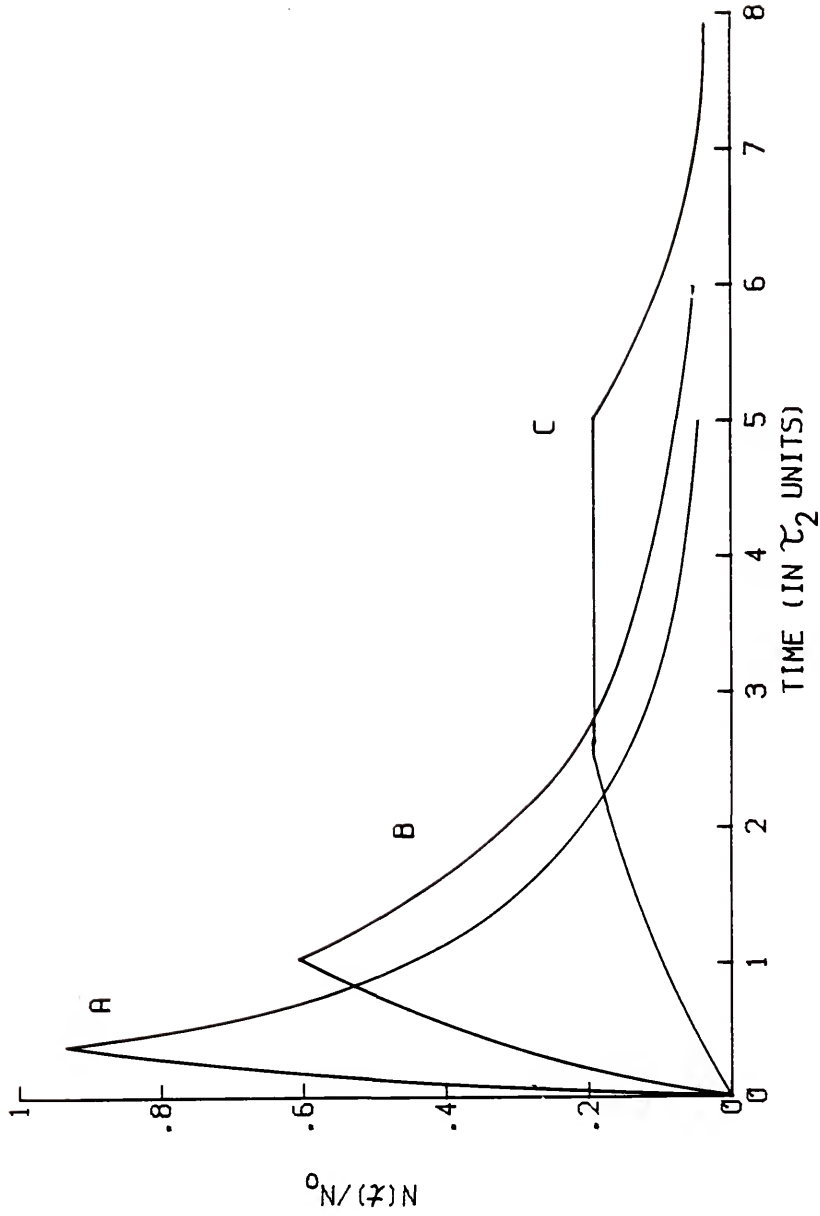
A
B
C
1
.8
.6
.4
.2
0
0
1
2
3
4
5
6
7
8
TIME (IN τ_2 UNITS)
$N(t)/N_o$

varying sample composition on the analytical results (23). This is due to fact that the integrated signal is neither dependent on the rate, n ( ), nor the time, , of entry of sample atoms into the analytical volume.

Types of Atomic Fluorescence

There are five basic types of atomic fluorescence (51-53). These are illustrated in Figure 2. Resonance fluorescence results when atoms are radiationally excited to some excited state and then undergo radiational deactivation back to the ground state, releasing a photon of light of the same energy as was absorbed. The most intense resonance fluorescence is typically from the first excited state. The transition probabilities for resonance transitions are generally much greater than those for non-resonance transitions, which then leads to much greater fluorescence signals. A variation of resonance occurs when the lower state is not the ground state, but rather a low-lying, thermally populated state. This is referred to as thermally assisted resonance fluorescence.

Another type of atomic fluorescence is direct-line fluorescence. This results when an atom is radiationally excited to a state much above the ground state and undergoes radiational deactivation to a lower excited state and emits a photon of light with an energy different from that which was initially absorbed. This lower state then, most often, collisionally deactivates to the ground state (54).

Figure 2

Types of atomic fluorescence: a--resonance, b--excited state resonance, c--Stokes direct-line, d--excited state Stokes direct-line, e--anti-Stokes direct-line, f--excited state anti-Stokes direct-line, g--Stokes stepwise line, h--excited state Stokes stepwise line, i--anti-Stokes stepwise line, j--excited state anti-Stokes stepwise line, k--thermally assisted Stokes or anti-Stokes stepwise line (depending upon whether the absorbed radiation has shorter or longer wavelengths, respectively, than the fluorescence radiation), l--excited state thermally assisted Stokes or anti-Stokes stepwise line (depending upon whether the absorbed radiation has shorter or longer wavelengths, respectively, than the fluorescence radiation), m--sensitized (D = donor, D^* = excited donor, A = acceptor, A^* = excited acceptor, h_E = exciting radiation, h_F = fluorescence radiation), n--two-photon excitation via a virtual level, o--two-photon excitation via a real level.

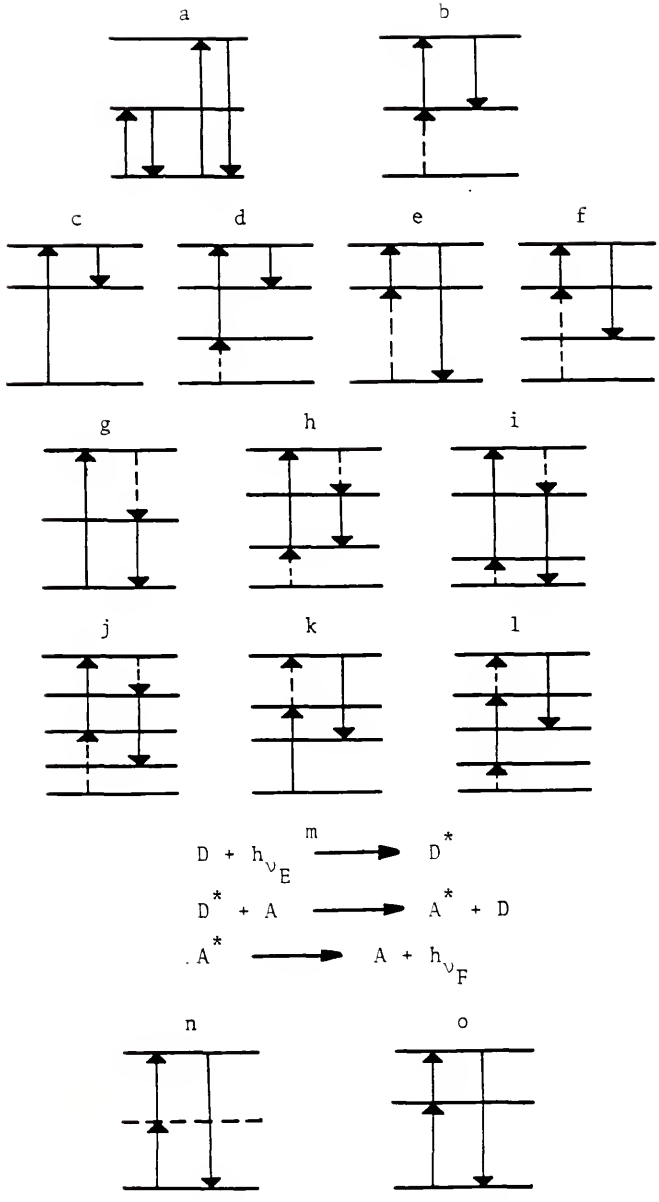
a
b
c
d
e
f
g
h
i
j
k
l
m
$D + h\nu_E \longrightarrow D^*$
$D^* + A \longrightarrow A^* + D$
$A^* \longrightarrow A + h\nu_F$
n
o

The third type of atomic fluorescence is stepwise line fluorescence. This occurs when an atom is radiationally excited to a state considerably above the ground state, is then collisionally (although it could also be radiationally) deactivated to some intermediate state from which it then radiationally deactivates to a still lower electronic state, emitting a photon of wavelength different from that which was initially absorbed. Several variations of stepwise line fluorescence are shown in Figure 2.

The fourth type of atomic fluorescence is multiple-photon fluorescence. This requires the simultaneous absorption of two (or more) photons which combined contain an amount of energy equal to the difference in the energy levels of the absorbing atom. This is different from direct-line and stepwise line fluorescence because these two pass through specific quantized energy levels whereas multiple-photon absorption does not. However there is also a two-photon fluorescence which does pass through a specific energy level. This occurs when an atom is radiationally excited by a photon of energy, $h\nu_1$, and then undergoes additional radiational excitation to a higher level by the absorption of another photon but of a different energy, $h\nu_2$. Two-photon fluorescence then occurs when the atom undergoes radiational deactivation to a lower level (see Figure 2).

The last type of atomic fluorescence is called sensitized fluorescence. This results when donor atoms or

molecules excited by an external light source collide with the analyte atom transferring energy and exciting the analyte atom. The analyte atom then undergoes radiational deactivation resulting in fluorescence.

Atomic Fluorescence Expressions

The basic fluorescence expression (55) is

$$B_F = \left(\frac{\ell}{4\pi}\right) Y_{21}\ E_{\nu_{12}} \int_0^\infty k_\nu d\nu$$

where

B_F = fluorescence radiance, J $s^{-1}m^{-2}sr^{-1}$

ℓ = path length in direction of detection system, m

4π = number of steradians in a sphere (fluorescence is isotropic), sr

Y_{21} = fluorescence power (quantum) efficiency, W fluoresced/W absorbed

$E_{\nu_{12}}$ = spectral irradiance of exciting radiation at absorption line, $_{12}$, W $m^{-2}Hz^{-1}$ (1W = J s^{-1})

$\int_0^\infty k_\nu d\nu$ = integrated absorption coefficient over absorption line, $m^{-1}Hz$

The product $E_{\nu_{12}} \int_0^\infty k_\nu d\nu$ is the power absorbed from the source by the analyte atoms per meter cubed of atomic species. The integrated absorption coefficient is given by

$$\int_0^\infty k_\nu d\nu = n_1 \left(\frac{h\nu_{12}}{c}\right) B_{12} \left[1 - \frac{g_1 n_2}{g_2 n_1}\right]$$

where

$h\nu_{12}$ = energy of the exciting photon, J

c = speed of light, m s^{-1}

B_{12} = Einstein coefficient of stimulated absorption, $m^3\ J^{-1} s^{-1} Hz$

g_1, g_2 = statistical weights of states 1 and 2, respectively, dimensionless

n_1, n_2 = concentration of states 1 and 2, respectively, m^{-3} ($n_1 + n_2 = n_T$, the total concentration of atoms in all states, assuming a two level model).

The bracketed quantity corrects for the effective decrease in absorption caused by stimulated emission from the upper state.

Assuming steady state, the number of upward transitions can be set equal to the number of downward transitions thereby giving

$$\left(k_{12} + \frac{B_{12}E_{\nu 12}}{c}\right) n_1 = \left(k_{21} + A_{21} + \frac{B_{21}E_{\nu 12}}{c}\right) n_2$$

where

k_{12}, k_{21} = excitation and deexcitation non-radiational (collisional) rate constants, s^{-1}

A_{21} = Einstein coefficient of spontaneous emission, s^{-1}

B_{21} = Einstein coefficient of stimulated emission, $m^3\ J\ s^{-1}\ Hz$

B_{12} = Einstein coefficient of stimulated absorption,

m^3 J s^{-1} Hz

n_1, n_2 = concentration of states 1 and 2, respectively, m^{-3}

c = speed of light, m s^{-1}

The quantum efficiency of a two level transition is defined as

$$Y_{21} = \frac{A_{21}}{A_{21} + k_{21}}$$

and A_{21} is related to B_{21} and B_{12} by

$$A_{21} = \left(\frac{8\pi h\nu_{12}}{c^3}\right) B_{21} = \left(\frac{8\pi h\nu_{12}}{c^3}\right)\left(\frac{g_1}{g_2}\right) B_{12}$$

where h is the Planck constant. Consolidating expressions, B_F for two level atoms is given by

$$B_F = \left(\frac{\ell}{4\pi}\right) Y_{21}\, E_{\nu_{12}} \left[n_1 \left(\frac{h\nu_{12}}{c}\right) B_{12} \left(\frac{E^*_{\nu_{12}}}{E^*_{\nu_{12}} + E_{\nu_{12}}} \right) \right]$$

where $E^*_{\nu_{12}}$ is a modified saturation spectral irradiance (W $m^{-2}Hz^{-1}$) and is defined as

$$E^*_{\nu_{12}} = \frac{cA_{21}}{B_{21}Y_{21}} .$$

If the modified saturation spectral irradiance is expressed in terms of the saturation spectral irradiance $E^s_{\nu_{12}}$, which is that source spectral irradiance that causes the fluorescence signal to be fifty per cent of the

maximum possible value, the expression

$$E^{*}_{\nu_{12}} = E^{s}_{\nu_{12}} \left(\frac{g_2 + g_1}{g_1} \right)$$

is obtained.

Now substituting for n_1 in terms of n_T, B_F is given by

$$B_F = \left(\frac{\ell}{4\pi} \right) Y_{21} \, E_{\nu_{12}} \, n_T \left(\frac{h\nu_{12}}{c} \right) \left[\frac{B_{12}}{1 + \frac{E_{\nu_{12}}}{E^{s}_{\nu_{12}}}} \right]$$

Saturation Spectral Irradiance

Complete saturation means that the populations of an excited state and the ground state are equalized. Therefore, radiationless and radiational (spontaneous) drains on the excited state are neglible with respect to the optical pumping rate. A further increase in source irradiance cannot effect an increase in the fluorescence radiance (56,57).

If the saturation plateau can be reached, i.e., the plateau resulting when the fluorescence radiance is plotted versus the source spectral irradiance (See Figure 3), then the saturation spectral irradiance, $E^{s}_{\nu_{12}}$ can be obtained by finding that source spectral irradiance where B_F equals one-half $B_{F_{max}}$. Here $B_{F_{max}}$ is the maximum fluorescence radiance (on the plateau).

Figure 3

Theoretical plot of fluorescence radiance versus source irradiance.

$B_{F_{max}}$ = maximum attainable fluorescence radiance

$E^{s}_{\nu_{12}}$ = saturation spectral irradiance

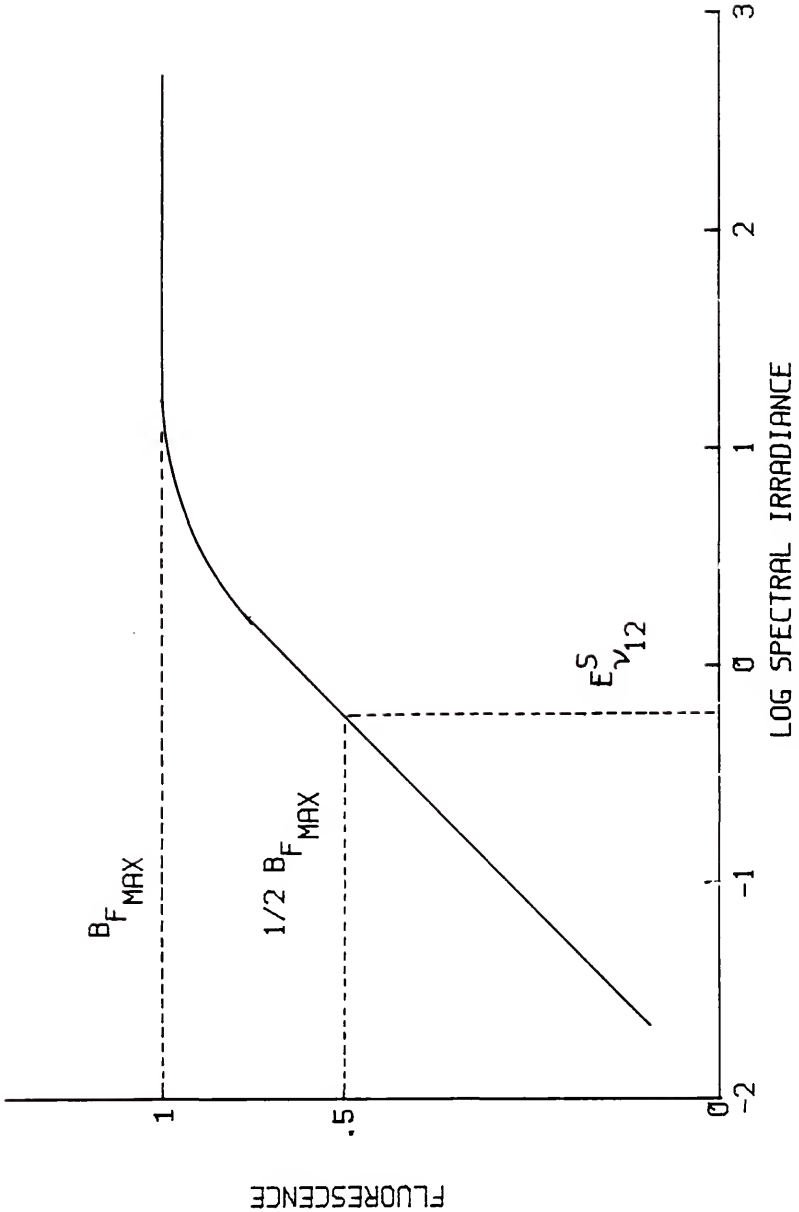
FLUORESCENCE
1
.5
0
$B_{F_{MAX}}$
1/2 $B_{F_{MAX}}$
$E^S_{\nu_{12}}$
-2
-1
0
1
2
3
LOG SPECTRAL IRRADIANCE

Lifetime

Lifetimes of excited states can be measured by the pulse method; this is when a pulsed source of excitation is used and the fluorescence decay is followed upon termination of the source excitation (58). The decay time of the fluorescence signal can be measured and if the temporal influence of the source and detection-measurement system is known, then these instrumental effects can be deconvoluted leaving a decay curve indicative of only the fluorescent species (58,59). The fluorescence lifetime, τ, is given by

$$\tau_j = \frac{1}{\sum_i A_{ji} + \sum_i k_{ji}}$$

where j is the upper state and i represents other states involved in the deactivation process (generally $j > i$). For a two level atom, τ_2 is given by

$$\tau_2 = \frac{1}{A_{21} + k_{21}} .$$

In the case where there is no collisional deactivation, i.e., $k_{21} = 0$, the lifetime is at its maximum value and this is referred to as the natural lifetime, τ_{sp}. This can be used in the measurement of quantum efficiencies since the observation of the natural lifetime occurs only when the quantum efficiency is one ($Y_{21} = 1$).

CHAPTER 3
EXPERIMENTAL

General Comments

The basic setup shown in Figure 4 is the microcomputer controlled electrothermal atomization system used in this work. A listing of the equipment used is found in Table 3-1. In order to minimize the fluctuating nature of the wings of a Gaussian laser beam, the atomizer was placed ten feet away from the dye laser. By using an iris diaphragm, the center of the beam was selected and focussed over the graphite rod.

Due to space constrictions a pair of front surface planar mirrors were used to fold the dye laser beam and direct it to the atomizer. By defining the path of interaction of the laser beam with the atomizer as a line between the aperture and a predefined spot on the beam stop, it was possible to easily realign the laser beam after dye changes or equipment sharing.

The collection system was aligned at a 90^{o} angle to the incoming beam by the use of a helium-neon laser crossed with the dye laser beam.

Fluorescence Collection

A 0.5 m monochromator (Jarrell-Ash, Newtonville, MA), with a spectral dispersion of 1.4 nm/mm, was used to

Figure 4

Microcomputer controlled electrothermal atomization system using laser atomic fluorescence spectrometry. Component symbols are as follows: A1 and A2 = diaphragm apertures, L1 and L2 = focussing lenses, M1 and M2 = front surface planar mirrors, PMT = photomultiplier tube, H.V. = high voltage power supply.

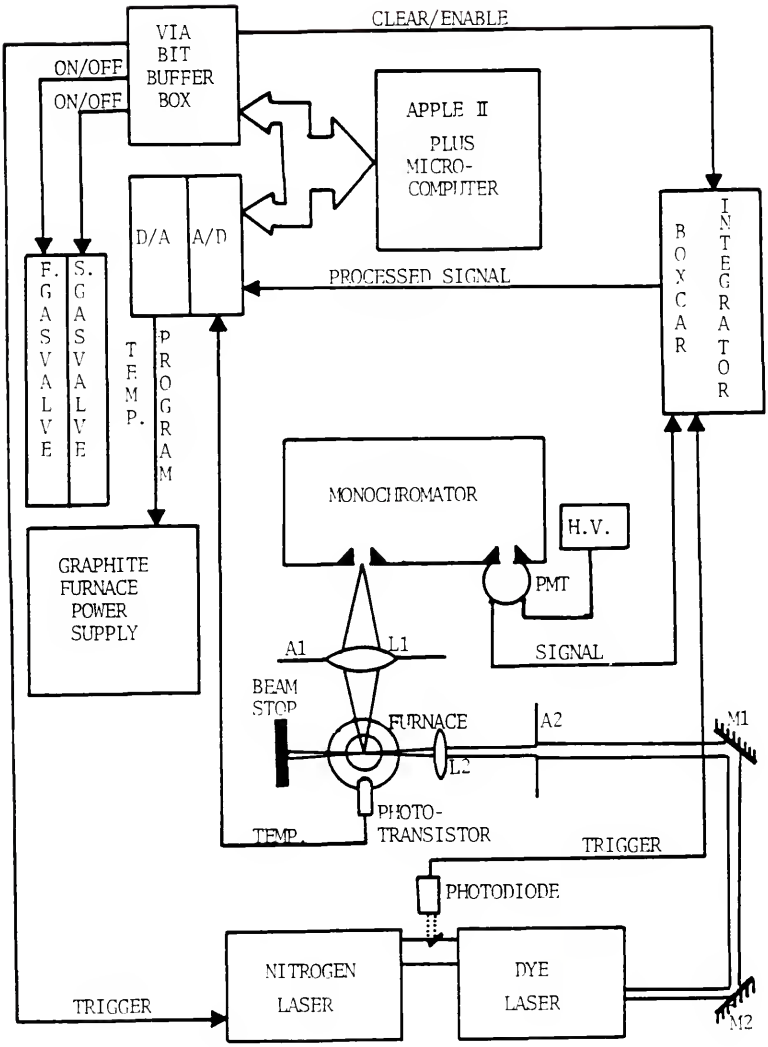
VIA
BIT
BUFFER
BOX
CLEAR/ENABLE
ON/OFF
ON/OFF
APPLE II
PLUS
MICRO-
COMPUTER
D/A
A/D
PROCESSED SIGNAL
BOXCAR INTEGRATOR
F.G.
GAS
VALVE
S.G.
GAS
VALVE
TEMP.
PROGRAM
MONOCHROMATOR
H.V.
PMT
GRAPHITE
FURNACE
POWER
SUPPLY
A1
L1
SIGNAL
BEAM
STOP
FURNACE
A2
M1
L2
PHOTO-
TRANSISTOR
TEMP.
TRIGGER
PHOTODIODE
NITROGEN
LASER
DYE
LASER
TRIGGER
M2

TABLE 3-1

Microcomputer Controlled Electrothermal Atomization using Laser Atomic Fluorescence Spectroscopy Equipment List

Item	Manufacturer
Apple II Plus Microcomputer	Apple Computer, Cupertino, CA
Video 100 Monitor	Leedex Corporation, Elk Grove Village, IL
Analog/Digital Converter	Laboratory Built
Digital/Analog Converter	Laboratory Built
VIA Interface Board	Laboratory Built
Model UV-24 Nitrogen Laser	Molectron Corp., Sunnyvale, CA
Model DL-II Dye Laser	Molectron Corp., Sunnyvale, CA
Furnace Assembly	Laboratory Built
Model 20-250 Power Supply	Electronic Measurements, Oceanport, MA
Gas Solenoid Valves	Laboratory Built
Graphite Rods	Poco Graphite, Decatur, TX
J-A 0.5 m Monochromator	Jarrel-Ash Company, Newtonville, MA
Model R1P28 Photomultiplier Tube	RCA Corp., Lancaster, PA
Model 130 Photomultiplier Tube Housing	Princeton Applied Research, Princeton, NJ
Model 226 High Voltage Power Supply	Pacific Precision Instr., Concord, CA
Model 162 Boxcar Mainframe	Princeton Applied Research, Princeton, NJ
Model 164 Boxcar plug-in module	Princeton Applied Research, Princeton, NJ
Photodiode Trigger	Laboratory Built

collect the fluorescence. The slits were curved and typically set at 100 μm width and 10 mm height. When setting the wavelength on the monochromator, the final setting was always approached from a lower setting.

One quartz lens was used to produce an image of unit magnification at the entrance slit of the monochromator. A fixed 2 in aperture was coupled to this lens to reduce both scatter and broadband emission of the heated graphite rod from entering the monochromator. In addition, curtains of black felt cloth were used to reduce scatter, which can be especially important in resonance fluorescence cases. A baffle was placed horizontally and immediately in front of the slit to eliminate any broadband emission from dirctly entering the monochromator.

Temperature Monitoring

Initially a TIL 67 phototransistor (Texas Instr., Dallas, TX) was mounted in a Macor machineable ceramic block (Accuratus Ceramic, Washington, NJ) viewing the center of the graphite rod (see Figure 5). The signal generated was fed into an A/D converter which was then read by the microcomputer. This was calibrated using an optical pyrometer (Pyrometer Instr., Northvale, NJ) also focussed at the center of the graphite rod. This temperature calibration was then compared to the voltage sent out by the D/A converter to the furnace power supply. This information was then used to allow a simple selection of temperature and have the microcomputer calculate and send

Figure 5

Circuit diagram for the phototransistor used to monitor the graphite rod temperature. The positive bias voltage was typically 12 V.

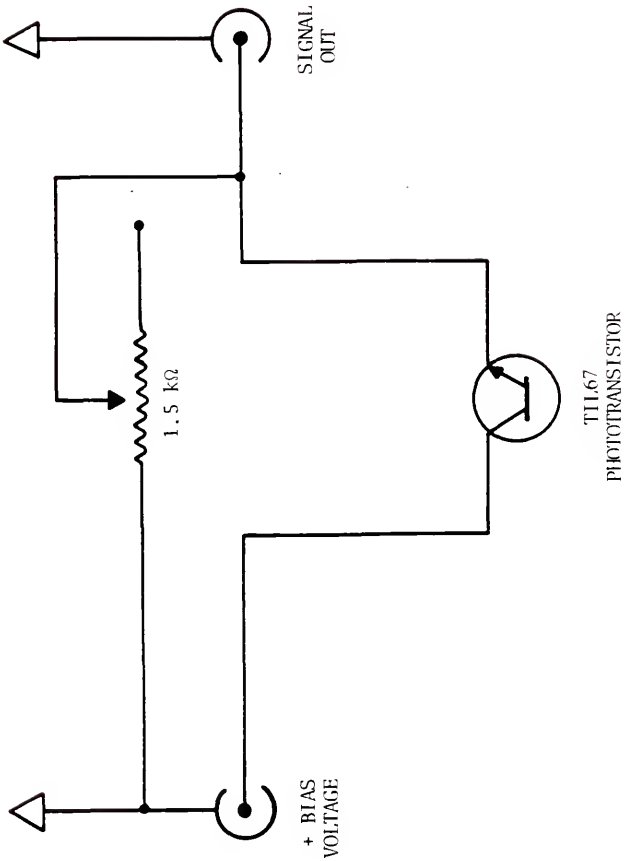
SIGNAL
OUT
1.5 kΩ
TIL67
PHOTOTRANSISTOR
+ BIAS
VOLTAGE

out the control voltage required to produce this temperature.

Encountering problems with the reproducibility of the phototransistor after prolonged use, due to excessive heating and melting of the epoxy dome-shaped lens of the phototransistor, it was replaced with a tungsten-5%rhenium vs. tungsten-26%rhenium thermocouple (Omega Engineering, Stamford, CT). This was also placed at the center of the rod, but offset to one side by 1 mm. This offset was necessary because the thermocouple would not function when in contact with the graphite since it is part of an electrical circuit. Again using the optical pyrometer, the thermocouple output was cross calibrated. The thermocouple output, since it was in the millivolt range, was fed through a laboratory built scaler set at a gain of 100 fold so that the output more nearly filled the A/D converter's input range. It was then sent to channel two of the A/D converter's four channels. This calibration enabled the construction of a plot of D/A control voltage versus furnace temperature (see Figure 6). The temperature readings were collected within a few hundred microseconds of each individual laser pulse so that each fluorescence pulse could be associated with a particular temperature.

Detection Electronics

A PAR Model 162 boxcar averager with Model 164 gated integrator plug-in module was used for the detection and measurement of the fluorescent pulses. The Model 164

Figure 6

Calibration curve for the D/A's output voltage versus furnace temperature.

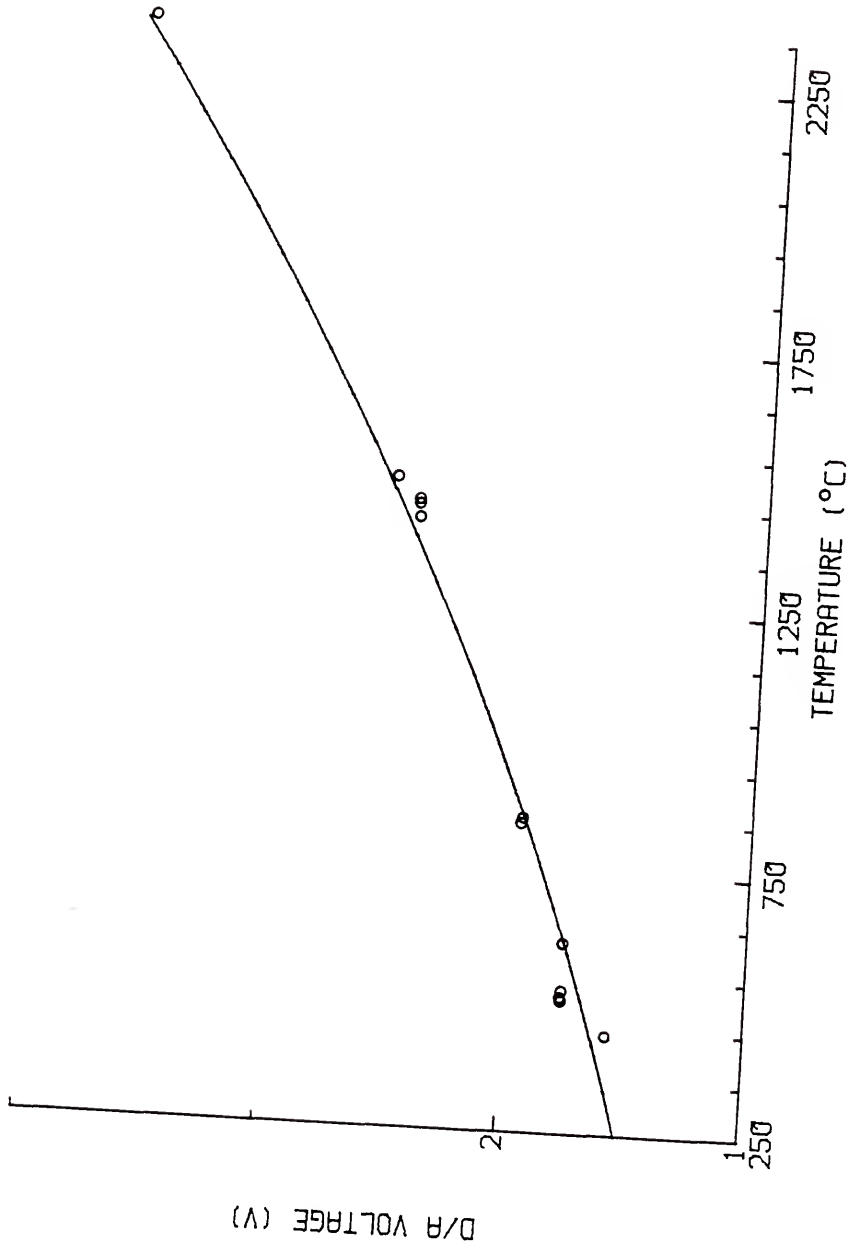
D/A VOLTAGE (V)
2
1
250
750
1250
1750
2250
TEMPERATURE (°C)

plug-in offered a fixed sensitivity (100 mV full scale) and several integration times and gate delay times. The 50 Ω input impedance was always used to match the connecting cables (RG-58U coaxial) and minimize ringing. The gate most commonly used was 50 ns with an aperture delay of 0.2 μs. This was necessary to avoid the huge ringing RF interference caused by the electrical breakdown in the spark gap of the nitrogen laser. The jitter in the time between triggering and the the laser actually firing was circumvented by using an optical trigger between the nitrogen laser and the dye laser. This enabled correct timing between laser firing and boxcar gating. The output of the boxcar was fed through a voltage inverter and then into channel zero of the A/D converter.

Nitrogen Laser

The nitrogen pump laser was run according to the manufacturer's instructions. The nitrogen flow rate was 26 L/min for all experiments. Operating pressure was maintained at 60 torr.

The laser repetition rate was controlled by the microcomputer and for ease of operation only three repetition rates, 10, 20, and 29 Hz, were user selectable. The 29 Hz was the upper limit because of the speed at which the compiled BASIC control program operated. Between samples the repetition rate would default to 16 Hz, the slowest that the software independent clock of the Versatile Interface Adapter could be run; but this still

satisfied the requirement that the nitrogen laser be triggered at least once every 30 s while in the run mode.

Dye Laser

The dye laser was also operated according to the manufacturer's instructions. The laser dyes used are listed in Table 3-2. Adjustments of both the oscillator dye cell and amplifier dye cell carriage were made after each new dye cell was introduced into the beam line. Since the Model DL-II dye laser operates in the third through seventh order, it is necessary to determine which order you can best operate in to be able to set correctly the wavelength dial of the dye laser. Having done this, it is simply a matter of following the manufacturer's instructions to maximize the energy output. However some difficulty was encountered with the frequency doubling accessory. The doubling crystal and focussing lens assembly is extremely sensitive to movement which foiled early attempts to utilize this valuable accessory. Additionally when doubling to a wavelength below 270 nm the polarization of the fundamental beam must be vertical. Because the DL-II laser normally produces a horizontally polarized beam, an intracavity polarization rotator (half-wave plate) had to be installed. Once installed, it only takes a flick of a small lever to rotate the polarization from horizontal to vertical and back again. In cases where it is not being used, it can be removed totally in order to achieve the highest energy output.

Table 3-2

Laser Dyes

Dye	Concentration (Moles/Liter)	Solvent	Wavelength Range (nm)
Rhodamine 6G	5×10^{-3}	Ethanol	568--605
Rhodamine B	5×10^{-3}	Ethanol	594--643
Coumarin 460	1×10^{-2}	Ethanol	440--478
PBD	5×10^{-3}	Ethanol/Toluene (1/1)	360--386
DPS	1×10^{-3}	p-dioxane	390--416

The only problem with dye deterioration occurred with Coumarin 460, and therefore it was changed frequently in order to avoid undue energy loss. Although the manufacturer recommends exchanging the old dye via pipet, rinsing with fresh dye, and refilling with fresh dye, it was found that the dyes performed better by flushing the cell with pure solvent before rinsing and refilling with fresh dye.

Furnace System

The gas flow control system consisted of one solenoid valve for the sheath and flame diluant gas and another solenoid valve for the flame gas. Each gas had its own individual rotameter. The entire system was calibrated by means of a linear mass flow meter (ALK-50K, Hastings, Hampton, VA). The flow rate of the sheath gas, the flame diluant gas and the flame gas was set on their respective rotameters while the solenoid valves were used to turn this flow on or off. In this way, it was possible to conserve the gases when not actually in use. Both the sheath gas (argon) and flame diluant gas (argon) were used to provide a sheath of an inert atmosphere around the graphite rod. The flame gas (hydrogen) was used to provide a reducing environment and to burn off any entrained oxygen. The sheath gas flow was optimized at 1.2 L/min, the flame gas was optimized at 0.50 L/min and the flame gas diluant was optimized at 0.31 L/min. The flame gas and flame diluant gas were introduced under the center of the graphite rod via a multi-capillary tube burner, and this burner was

surrounded by several concentric rings which encased the length of the rod with sheath gas only (See Figure 7).

The graphite furnace consisted of a cylindrical bakelite block 8.2 cm in diameter and 2.6 cm high with water-cooled, copper blocks on either side to support the graphite rod and provide electrical contact with the SCR power supply. The SCR Model 20-250 power supply was wired in the external voltage program control mode to permit the use of a microcomputer driven D/A converter in controlling the power supply's output and thus the furnace temperature.

A modification in the graphite rod design was made to facilitate machining of the rods as well as to reduce the turbulent flow in the sheath gases caused by sharp edges. Additionally the small sample hole was eliminated due to the irreproducibilty in its depth and because the removal of the graphite by drilling this hole caused the rod to burn unnecessarily fast at this point. Due to the small sample volume (μL) used, the sample formed a droplet which was small enough to place on top of the graphite rod without any spillage. The dimensions of the simplified rod design are shown in Figure 8.

The furnace was mounted on a riser capable of translational and vertical movement. This allowed easy optimization of rod position under the laser beam.

Microcomputer

The Apple II Plus was used to control as much of the electrothermal atomization system as possible. The ability

Figure 7

Drawing showing the physical configuration of the graphite rod furnace. The dye laser beam passes lengthwise over the graphite rod.

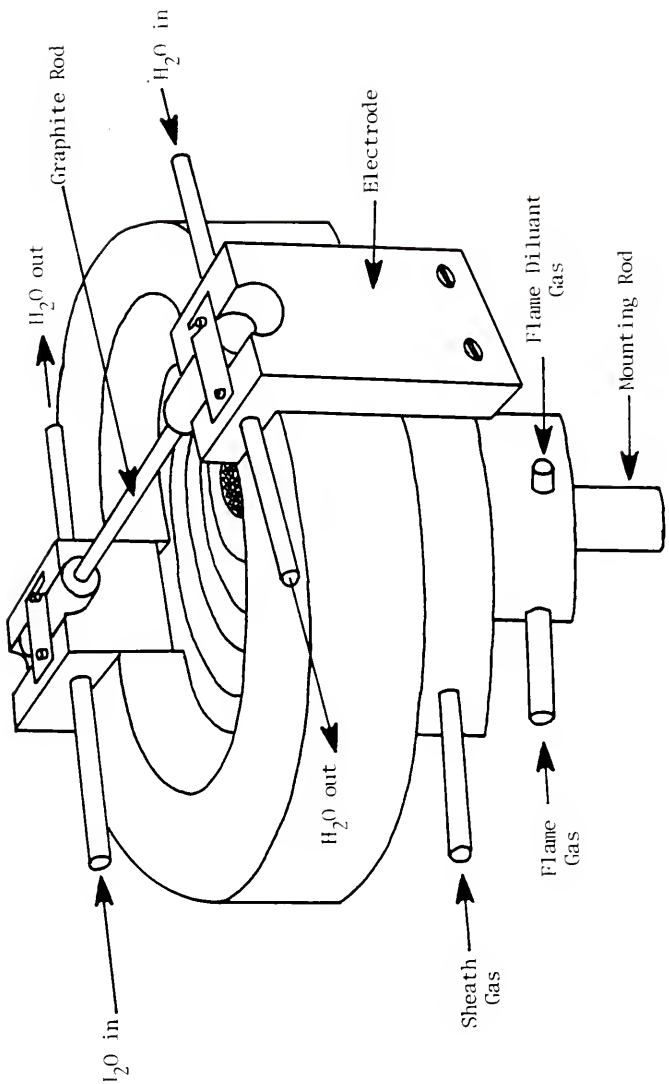
H_2O in
H_2O out
Graphite Rod
H_2O in
Electrode
Flame Diluant Gas
Mounting Rod
H_2O out
Flame Gas
Sheath Gas
H_2O in

Figure 8

Simplified graphite rod design. All dimensions are in inches.

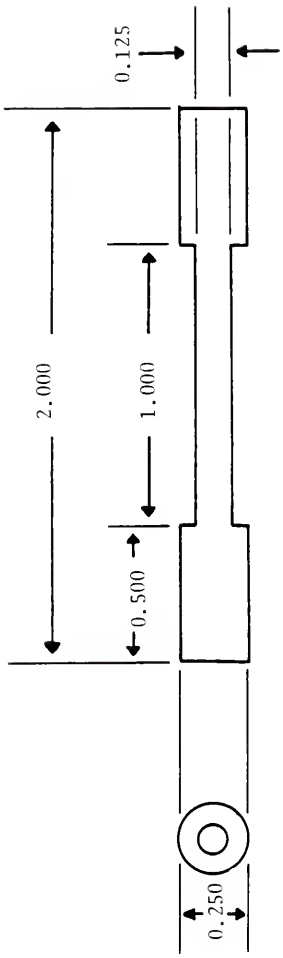
0.125
2.000
1.000
0.500
0.250

of the microcomputer to communicate with the outside world was made possible by the Versatile Interface Adapter (VIA) board (see Appendix 1). Through this interface the nitrogen laser was triggered, the graphite rod temperature was controlled, the sheath, flame diluant and flame gases were turned on/off, the boxcar was enabled/cleared, and both the temperature monitor output and boxcar output were read. All data as well as the operating parameters could be stored on disk for later retrieval or dumped to the video monitor for immediate consideration or to a printer for a hard copy. The control program was formatted so that after it was loaded into the microcomputer the data could be stored on a disk in either drive one or two (see Appendix 2).

This particular Apple II Plus was outfitted with a parallel interface board (for printers), a serial interface board (for the digital plotter), the VIA interface board, an Integer BASIC ROM board, and a Videoterm 80-column board (for the word processor). The microcomputer itself was mounted in a wheeled rack so that it could be used in various other experiments in the laboratory, such as the radiometer system (see Appendix 3).

Quantum Efficiency

In order to determine the efficiency of the fluorescence process in the electrothermal atomizer, two different sheath gases were used. Argon which has a small quenching cross section (60) was used in all of the

calibration and fluorescence studies. By replacing argon with nitrogen, which has a much larger quenching cross section (60-64), it was possible to obtain relative quantum efficiencies for the two environments.

To make this relative information more definitive, the fluorescence lifetime of the sodium 3P-3S transition (65) in the electrothermal atomizer was measured. To do this a fast photomultiplier tube with a known rise time had to be used. The Nitromite nitrogen laser (Photochemical Research Asc., Ontario, Canada) was used to measure the rise time of an R1414 photomultiplier tube seated in a fast wired E850-03 base (Hamamatsu, Middlesex, NJ). The laser pulse is typically 350 ps (when the spark gap is operated at atmospheric pressure) and it was scattered into a monochromator onto which the R1414 tube had been mounted.

The resulting signal was monitored using a Model 7834 storage oscilloscope (Tektronix, Beaverton, OR) with a Model 7A19 plug-in amplifier (500 MHz bandwidth) which has a rise time of 0.9 ns. From this signal, it was determined that the response time of the photomultiplier tube and base combination was 1.8 ns. This compares favorably to the manufacturer's specification of 1.4 ns.

This detector then replaced the RCA 1P28 photomultiplier tube used for all the other measurements on the furnace system. The Molectron dye laser beam was then scattered into the monochromator and the photocurrent was fed directly into the 50 Ω input of the Model 7A19

amplifier. This yielded a signal with a full-width half-maximum of 4 ns for the dye laser pulses. A 5 µL aliquot of 1000 ppm Na was then placed on the graphite rod and atomized.

Solutions

Stock solutions of 1000 µg/mL for all elements were prepared from reagent grade chemicals in deionized water as per Parsons et al. (66). Working solutions were prepared by serial dilution from the stock solutions on a daily need basis.

CHAPTER 4
RESULTS AND DISCUSSION

Signal To Noise Optimization

As mentioned in Chapter 3, the intersection of the center of the excitation optics and the center of the luminescence optics (L2, L1 and A1, respectively of Figure 4) was determined; this intersection could be located to better than 1 mm by using graduated markings on the furnace mount. The graphite furnace was coarsely positioned using these markers, and then, by means of the translational and vertical screw adjusts, the fluorescence signal was finely tuned to a maximum.

Because ideally a fluorescence signal should be measured against "no" background signal, two apertures (A1 and A2 of Figure 4) were used to minimize the source laser radiation from being scattered about the room and eventually finding its way to the photomultiplier tube. Care was excercised to ensure that the apertures did not limit the solid angle of fluorescence collection.

No mirrors were used to increase fluorescence intensity by reflecting the exciting laser beam back upon the analytical volume or in collecting a larger solid angle of fluorescence radiation from the analytical volume. An improvement in SNR of a factor of 3-10 by employing mirrors in this manner has been reported (41,67,68).

The atomic fluorescence SNR of sodium was examined for graphite rods of two different designs. The SNR for the round design (see Figure 8) was better than for the previous rectangular design (69). This is attributable to the less turbulent gas flow around the rod and a resultant decrease in analyte transport noise into the analytical volume of the electrothermal atomizer. Therefore, the round design was used for all subsequent atomic fluorescence measurements.

Typical atomic fluorescence data for the three elements obtained with the microcomputer controlled electrothermal atomizer are presented in Figures 9, 10 and 11. These data (as all data used in this work) were reconstructed from data files collected and stored by ETA PS7.1.OBJ (see Appendix 2) on floppy minidisks. The data were plotted on a digital plotter by a BASIC plotting program found in Appendix 4.

The optimum temperatures of the graphite rod were determined for each element by comparing fluorescence signal to noise ratios. The graphite rod lifetime was also taken into account here; higher temperatures led to shorter lifetimes of the graphite rod.

Definitions of Analytical Parameters

The atomic fluorescence concentration (ng/ml) limit of detection (LOD) was defined as that concentration (in ng/ml) giving a signal of 3X the rms noise of the background (blank) noise. Each LOD was found by preparing

Figure 9

Typical fluorescence signal versus time curve for manganese. This particular curve was obtained using a 5 L aliquot of 50 ppm solution.

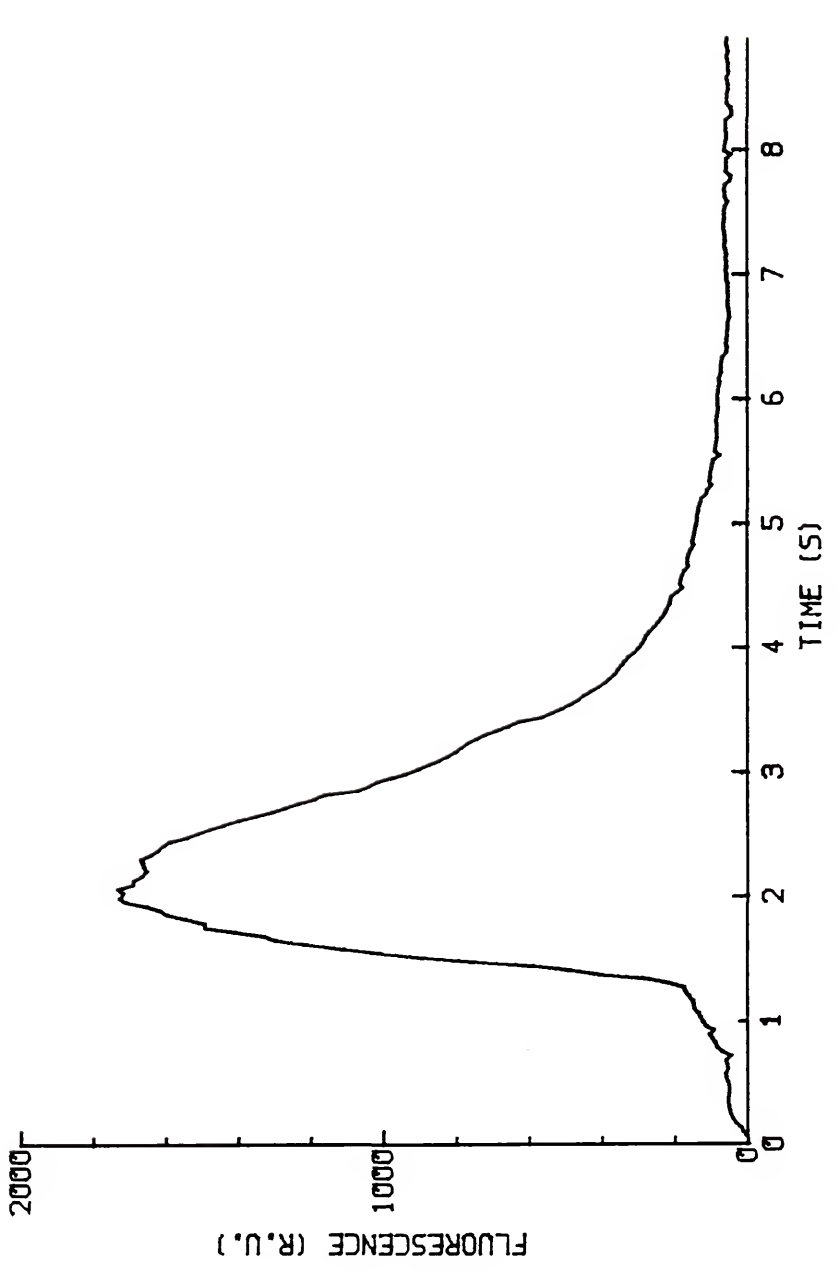
FLUORESCENCE (R.U.)
2000
1000
0
0
1
2
3
4
5
6
7
8
TIME (S)

Figure 10

Typical fluorescence signal versus time curve for sodium. This particular curve was obtained using a 5 L aliquot of 50 ppm solution.

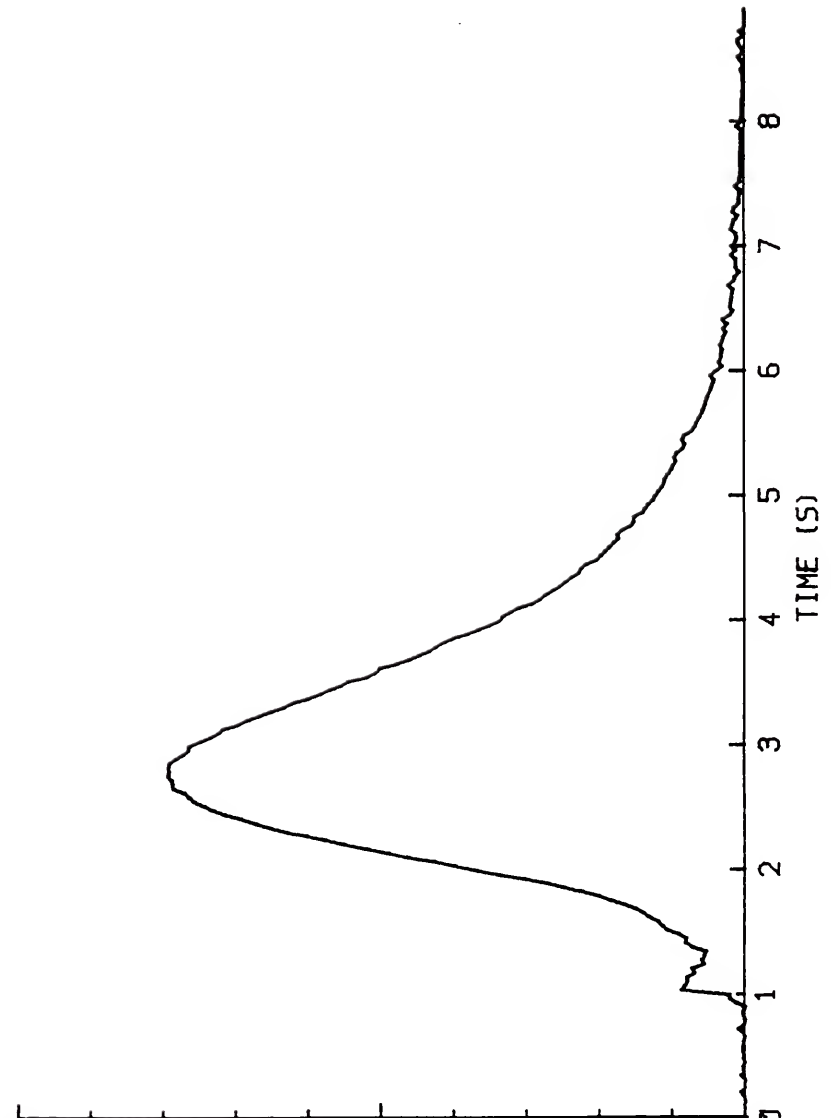
FLUORESCENCE (R.U.)
2000
1000
0
0
1
2
3
4
5
6
7
8
TIME (S)

Figure 11

Typical fluorescence signal versus time curve for tin. This particular curve was obtained using a 5 L aliquot of 50 ppm solution.

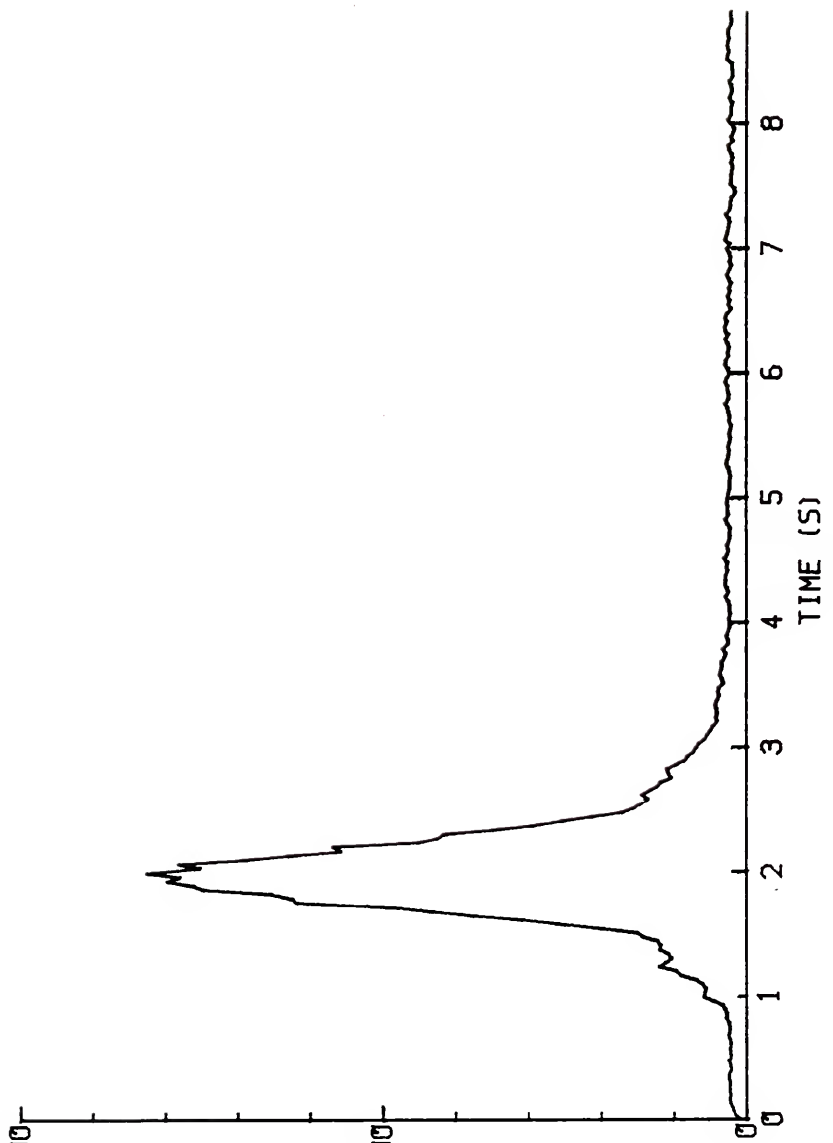
FLUORESCENCE (R.U.)
2000
1000
0
0
1
2
3
4
5
6
7
8
TIME (S)

analytical curves for each element and then extrapolating back to a signal level which corresponded to that of three times the rms noise. The concentration associated with this signal was the limit of detection. Atomic fluorescence measurements of the three elements were determined for concentrations ranging from 1000 µg/mL to 1 µg/mL. Solutions of lower concentrations were not used because of the problem associated with accurately making the required dilutions and concern with how well the small aliquot (5 µL) would represent the bulk of a dilute solution. The upper concentation limit was determined by the beginning of serious curvature (greater than 4 per cent deviation from linearity) of the analytical curve. The linear dynamic range (LDR) was the difference between the upper concentration limit and the limit of detection, and the sensitivity was the slope of the analytical curve. The precision of the system (relative standard deviation) was determined for the lowest concentration available.

Limits of Detection

The resulting LOD's for the three elements are given in Table 4-1 along with the linear dynamic ranges, relative standard deviations, sensitivities and the wavelengths used. Both concentration limits of detection (CLOD--in ng/ml) and absolute limits of detection (ALOD--in pg) are listed in Table 4-1. In general, the concentration limits of detection are about one order of magnitude poorer (higher) than those reported by Winefordner (70) for laser

excited atomic fluorescence. Compared to the best reported values to date (46) for furnace laser atomic fluorescence spectrometry, the concentration limit of detection is 2 or more orders of magnitude poorer. However, when the aliquot size is considered, then the absolute limits of detection can be compared to these other values. In this comparison, the detection limits are better than those reported by Browner (71) and within a factor of 5 of those of Bolshov et al. (46).

It should be noted here that since the LOD depends upon the signal intensity as well as the background (blank) noise, it was important to have as pure a graphite rod as possible. It was noticed that it took as many as three sequential heatings of a new graphite rod to atomize and remove any surface contamination. After the third heating the blank level was a rather flat constant offset with only the background noise on it. This contamination was especially evident at the sodium wavelength presumably from the handling during the final machining of the graphite rods. The contamination as well as the effect of these presample heatings are clearly seen in Figures 12, 13 and 14.

Linear Dynamic Range and Sensitivity

The atomic fluorescence analytical calibration curves were constructed for the resonance fluorescence of manganese and sodium and for both excited state Stokes direct-line fluorescence and excited state anti-Stokes

Figure 12

Fluorescence signal versus time curve obtained during the first heating of a new graphite rod (no sample). The broad peak from that occurs from 1 s to 5 s is sodium contamination due to handling during machining.

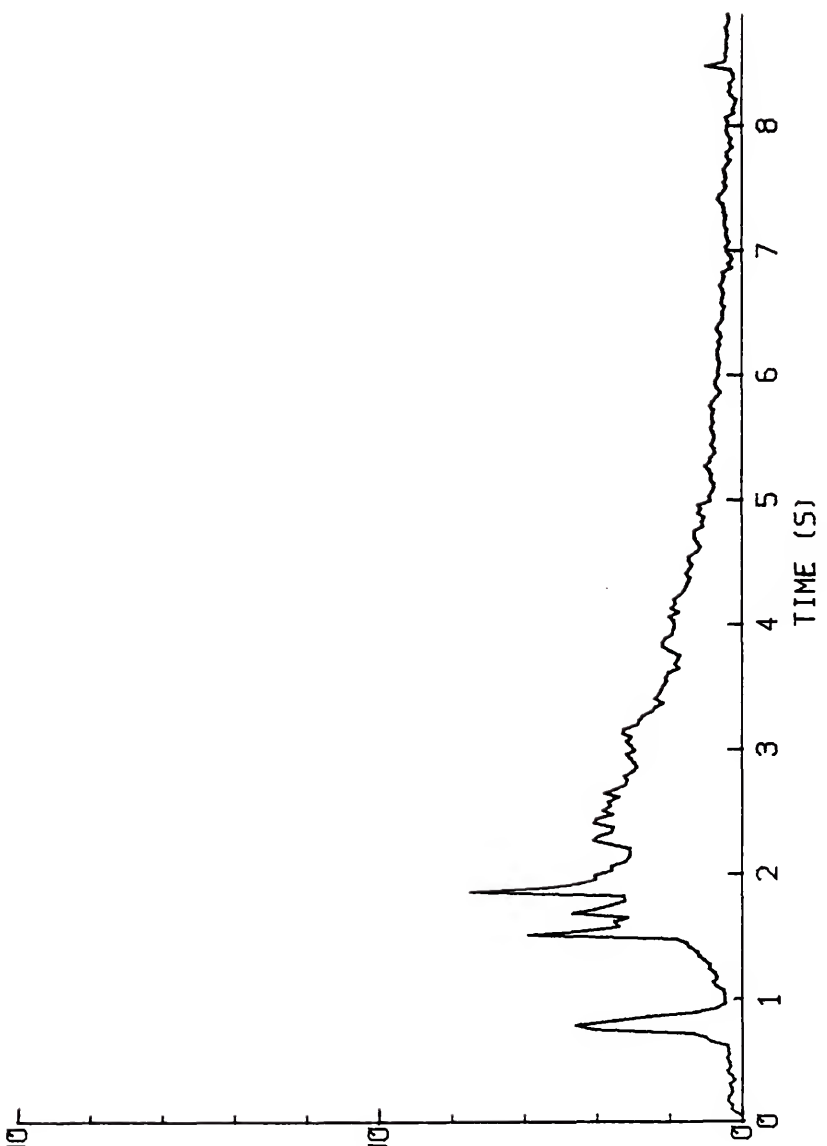
FLUORESCENCE (R.U.)
2000
1000
0
0
1
2
3
4
5
6
7
8
TIME (S)

Figure 13

Fluorescence signal versus time curve obtained during the second heating of a new graphite rod (no sample). It can be seen that the broad peak present during the first heating is gone.

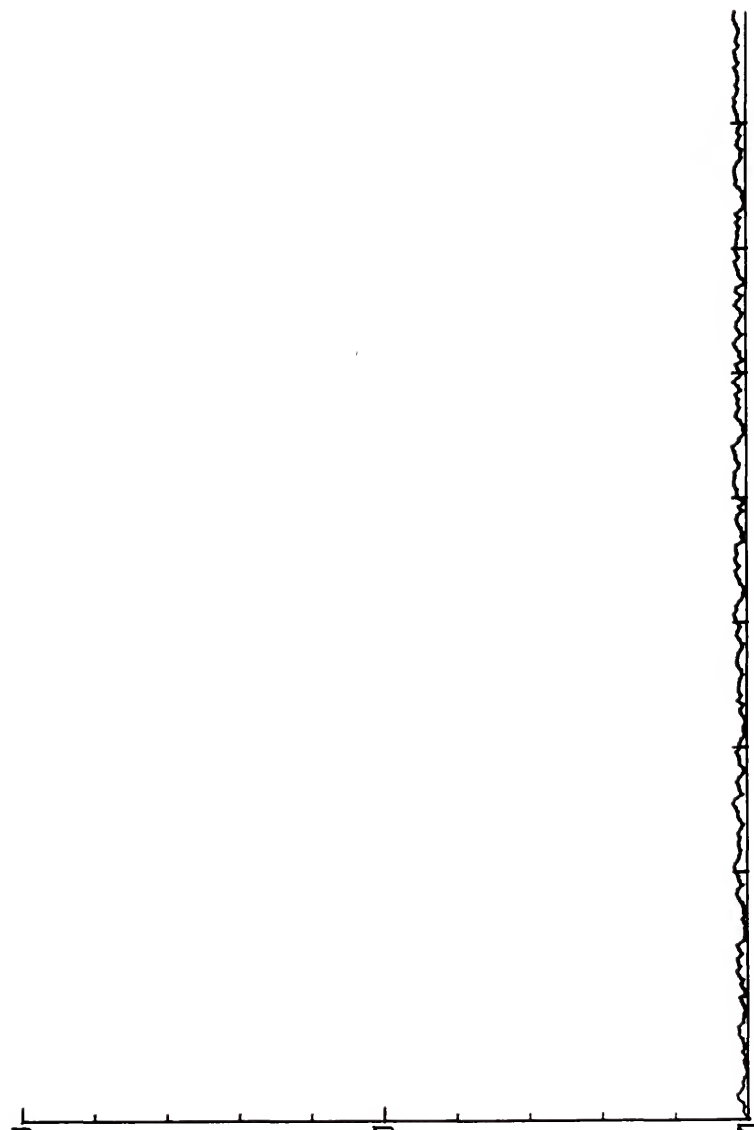
FLUORESCENCE (R.U.)
2000
1000
0
0
1
2
3
4
5
6
7
8
TIME (S)

Figure 14

Fluorescence signal versus time curve obtained during the third heating of a new graphite rod (no sample). It can be seen that the background level is a flat constant level with random noise upon it.

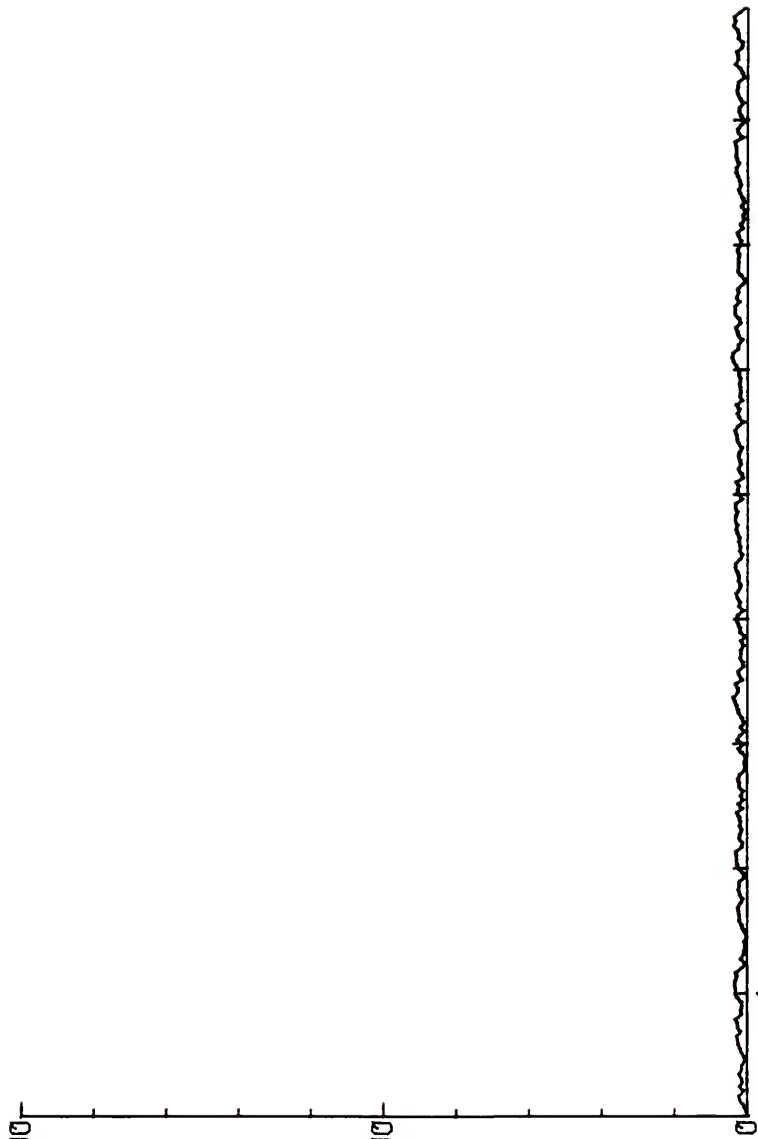
FLUORESCENCE (R.U.)
2000
1000
0
0
1
2
3
4
5
6
7
8
TIME (S)

direct-line fluorescence of tin. These curves are shown in Figures 15, 16, 17 and 18, respectively. It should be noted that the excited state anti-Stokes direct-line fluorescence of tin was not analytically useful in the concentration range and system conditions investigated. It is shown here to emphasize that care must be taken in the selection of atomic transitions to ensure that a linear relationship exists between the atom concentration and the fluorescence signal. It can be seen that the curves for both sodium and manganese do not include the upper concentration limit--all that can be said for these elements is that it is above 1000 g/mL. However the linear dynamic range for both manganese and sodium was over 5.5 orders of magnitude. The LDR for tin was determined to be only 4 orders of magnitude.

Precision

The precisions for the three elements are listed in Table 4-1. The precision obtained is competitive with other atomization devices used in atomic fluorescence. For the elements examined the relative standard deviation was 0.064 to 0.088 which is typical of graphite rod atomic fluorescence spectrometry. Two of the factors which contribute to this high relative standard deviation are errors in sample placement on the graphite rod and the fluctuations in the laser beam irradiance from pulse to pulse.

Figure 15

Analytical calibration curve for the resonance fluorescence of manganese at 403.1 nm.

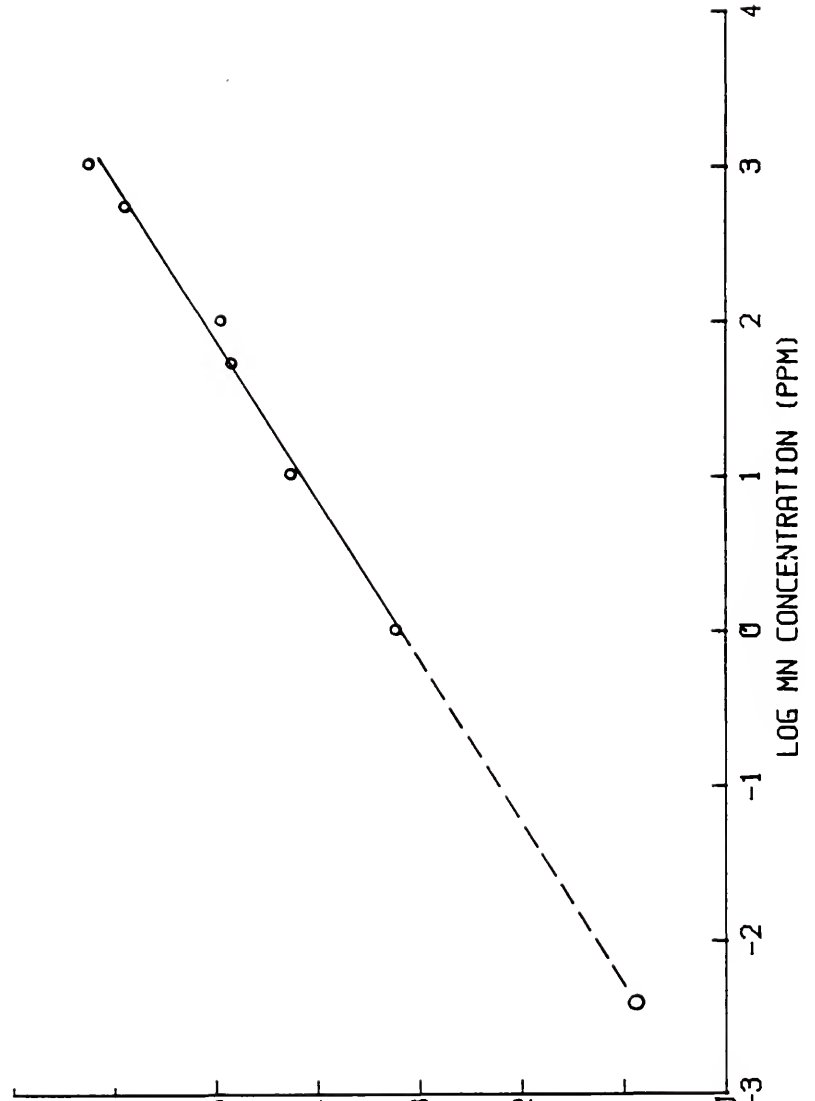
LOG FLUORESCENCE (R.U.)
7
6
5
4
3
2
1
0
-3
-2
-1
0
1
2
3
4
LOG MN CONCENTRATION (PPM)

Figure 16

Analytical calibration curve for the resonance fluorescence of sodium at 589.0 nm.

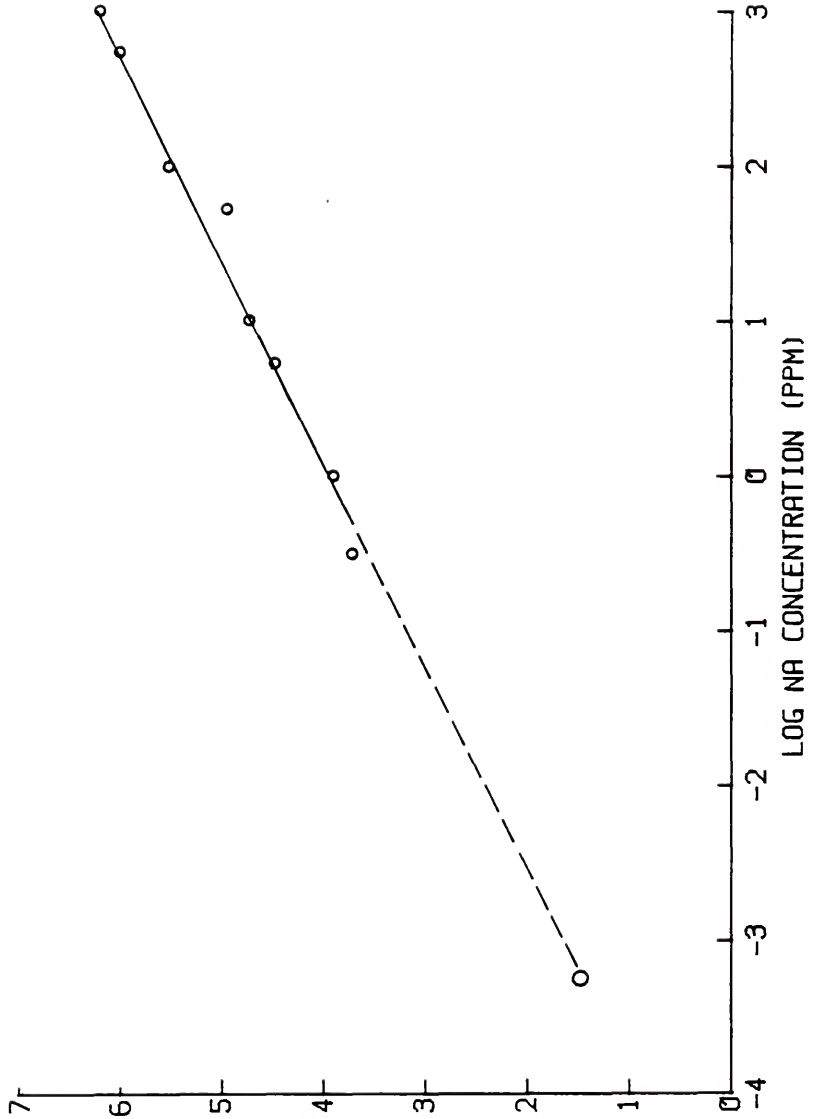
LOG FLUORESCENCE (R.U.)
7
6
5
4
3
2
1
0
-4
-3
-2
-1
0
1
2
3
LOG NA CONCENTRATION (PPM)

Figure 17

Analytical calibration curve for the excited state Stokes direct-line fluorescence of tin.

300.9 nm excitation
317.5 nm fluorescence

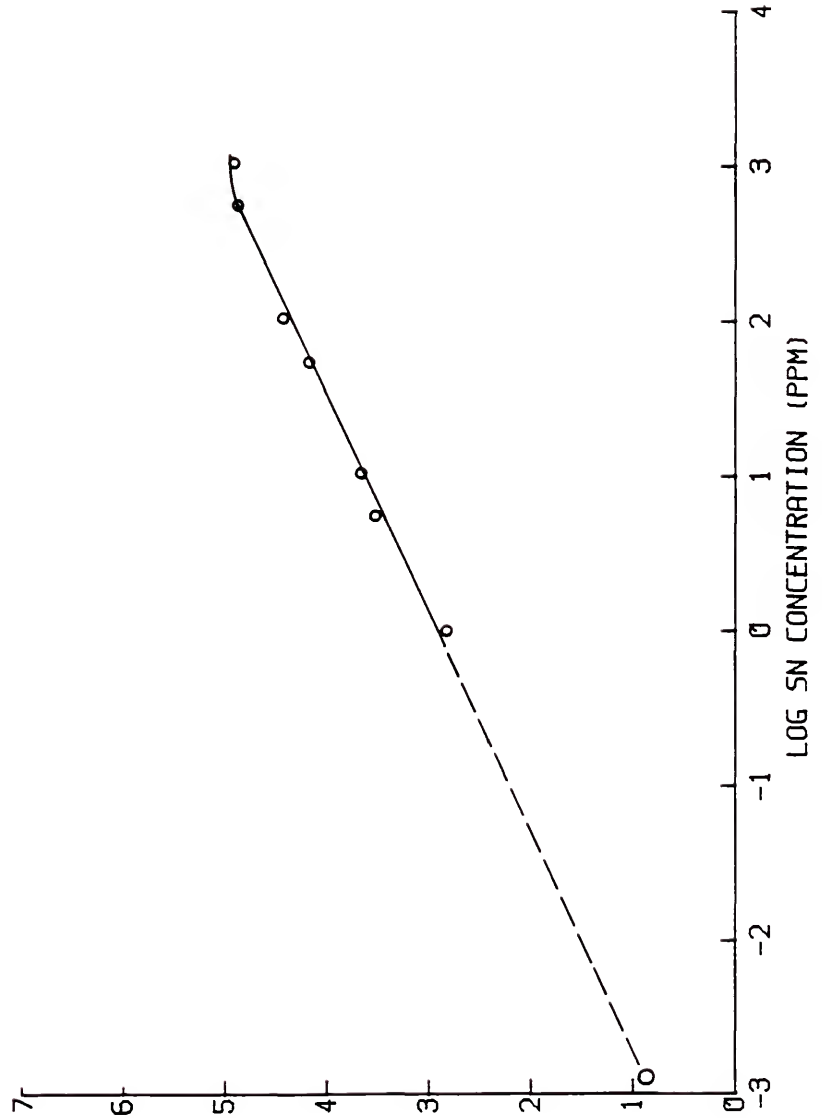
LOG FLUORESCENCE (R.U.)
LOG SN CONCENTRATION (PPM)
7
6
5
4
3
2
1
0
-3
-2
-1
0
1
2
3
4

Figure 18

Analytical calibration curve for the excited state anti-Stokes direct-line fluorescence of tin.

300.9 nm excitation
286.3 nm fluorescence

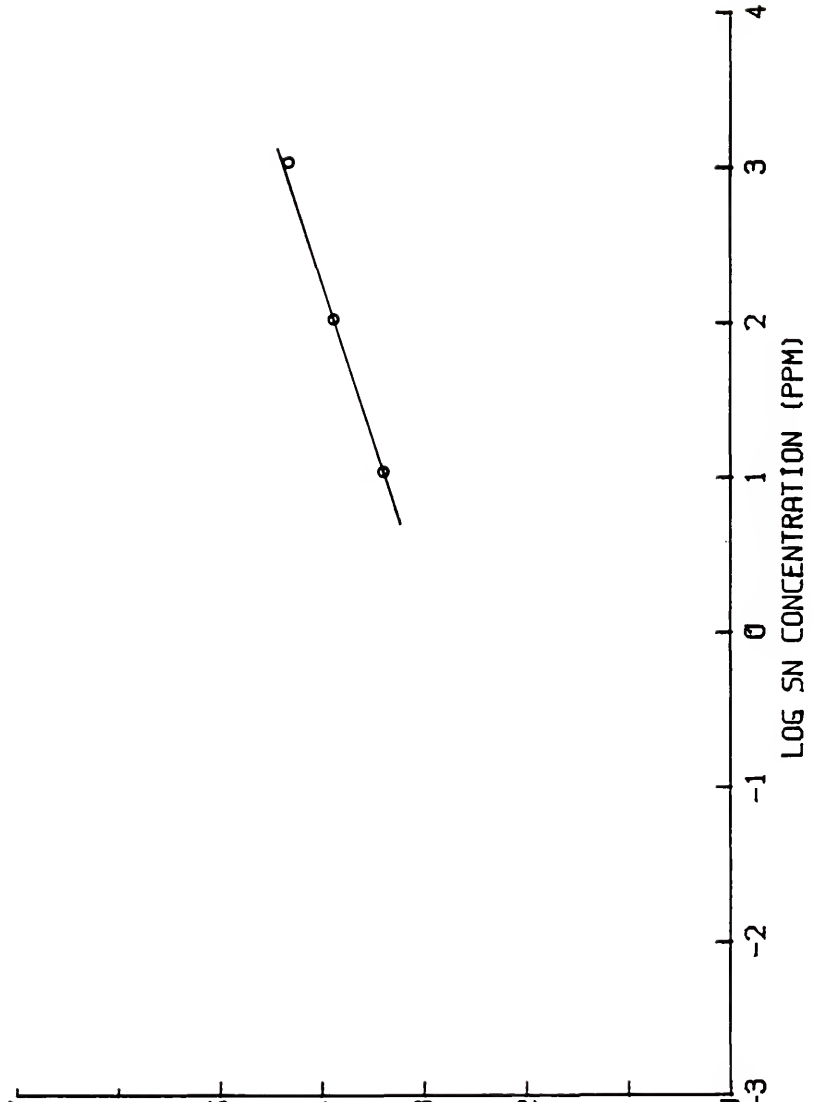
LOG FLUORESCENCE (R.U.)
7
6
5
4
3
2
1
0
-3
-2
-1
0
1
2
3
4
LOG SN CONCENTRATION (PPM)

TABLE 4-1

Experimental conditions and analytical results for measurements of three elements by means of microcomputer controlled electrothermal atomization using laser atomic fluorescence spectrometry.

Element	Excitation Wavelength (nm)	Fluorescence Wavelength (nm)	CLOD[a] (ng/ml)	ALOD[b] (pg)	LDR[c]	RSD[d]	Sensitivity[e]
Mn	403.1	403.1	4	20	>5.5	0.088	0.97
Na	589.6	589.6	0.6	3	>5.5	0.064	0.77
Sn	300.9	317.5	1	5	4	0.070	0.74
	300.9	286.3	--	--	-	0.070	0.42[f]

[a] CLOD = concentration limit of detection (see text for definition).

[b] ALOD = absolute limit of detection (see text for definition).

[c] LDR = linear dynamic range (see text for definition).

[d] RSD = relative standard deviation (taken at 1 g/ml).

[e] Sensitivity = slope of the analytical calibration curves.

[f] This value indicates that CLOD and ALOD values would be misleading.

Sodium Population Profile

The method used to measure the decay of sodium atom population as a function of height has been previously described (72). The profile was determined to aid in the positioning of the electrothermal atomizer in the optical path of the excitation and emission optics. The same atomization conditions were used for this study as for the analytical calibration curve measurements.

The factors contributing to the decrease in the measured integrated atomic fluorescence as the graphite rod is lowered include

1. The loss of atoms due to chemical reaction.
2. The transport of atoms outside of the analytical volume due to diffusion.
3. The decrease of the solid angle subtended by the atoms in the analytical volume.
4. The loss of excited state atoms due to collisional quenching.

Even in the absence of condensation, oxide formation and other possible chemical losses, a gradual decrease of the fluorescence signal from factors 2 and 3 would be expected.

The decay of atom populations with height above the electrothermal atomizer was measured by atomic fluorescence spectrometry, and the results are shown in Figure 19. The decay of the sodium population was gradual, reaching 50 per cent at a height of 12 mm above the graphite rod.

Figure 19

Decay of sodium atom population with height above the graphite rod atomizer as measured by atomic fluorescence spectrometry. This profile was taken 1 mm off center of the graphite rod. The offset was towards the monochromator side of the graphite rod.

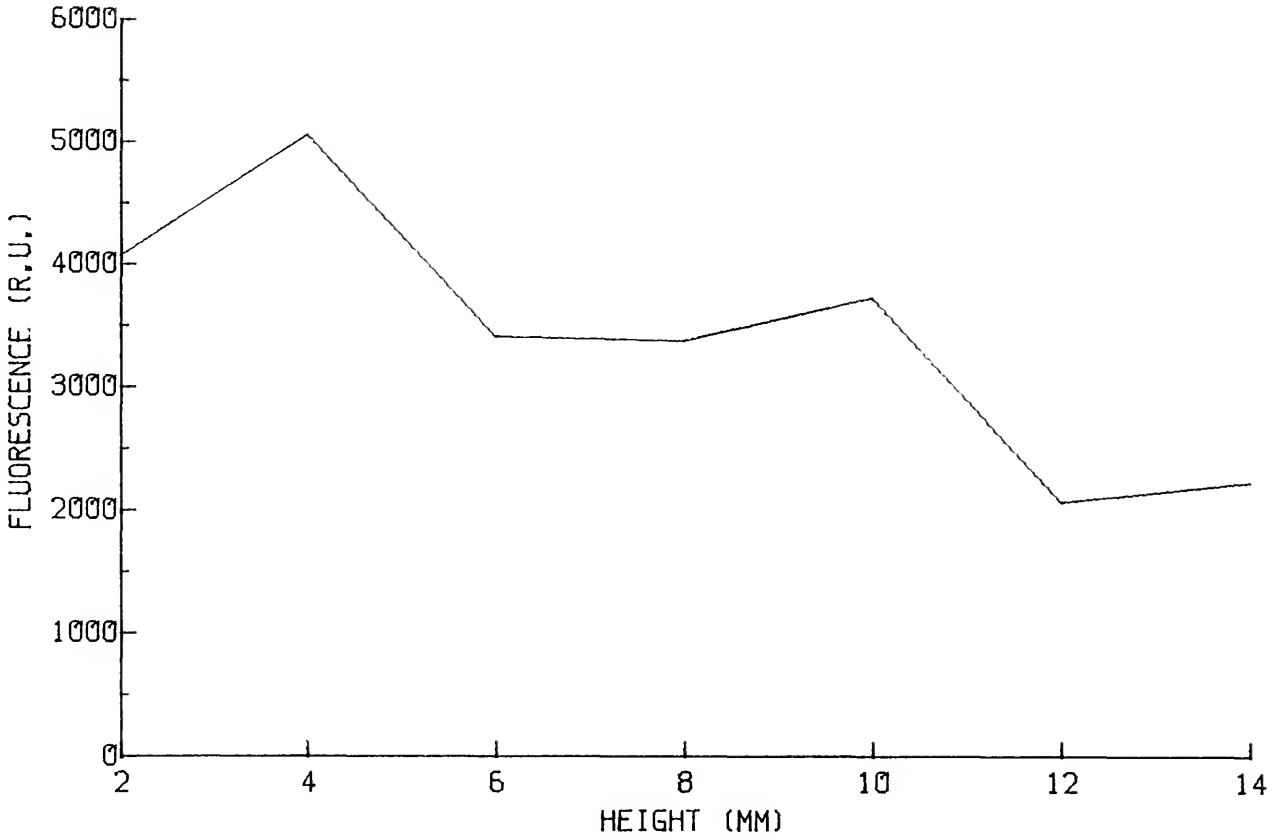
6000
5000
4000
3000
2000
1000
0
FLUORESCENCE (R.U.)
2
4
6
8
10
12
14
HEIGHT (MM)

In addition to investigating the sodium population as a function of height it was also studied as a function of displacement from the center of the graphite rod. This displacement was investigated to determine what effects, if any, post-filtering may have. Figures 20, 21 and 22 show the sodium fluorescence as a function of displacement at three different heights above the rod. It can be seen that there is some attenuation of the fluorescence signal when the path of the exciting laser beam over the graphite rod is on the opposite side from the monochromator. This shows up as a skewing of the fluorescence intensity towards the side of the graphite rod closest to the monochromator; in the absence of any post-filter effects a totally symmetric distribution of sodium atoms about the center of the graphite rod would be expected.

The atom population distribution was adopted as the general pattern that other atoms would follow; consequently, the optimum position for sodium fluorescence was used as the initial position of the furnace for both manganese and tin.

Quantum Efficiency

In order to obtain an idea of the efficiency of the fluorescence process in this electrothermal atomizer, two different sheath gases were (argon and nitrogen) used. By comparing the fluorescence intensity of a standard solution in these two gases the relative quenching effects of the two gases were obtained. Since nitrogen has a much larger

Figure 20

Sodium atom population distribution at a height of 2 mm above the graphite rod with a displacement of up to 4 mm to each side of the center of the graphite rod.

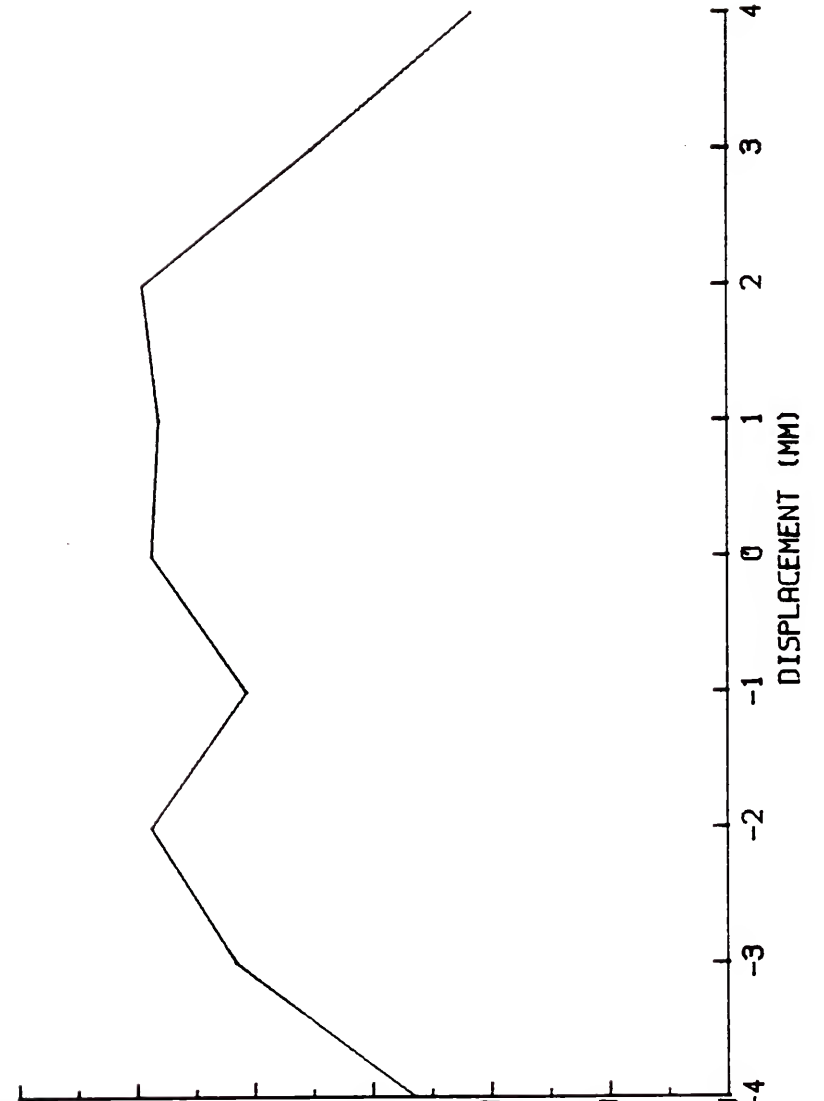
FLUORESCENCE (R.U.)
6000
5000
4000
3000
2000
1000
0
-4
-3
-2
-1
0
1
2
3
4
DISPLACEMENT (MM)

Figure 21

Sodium atom population distribution at a height of 4 mm above the graphite rod with a displacement of up to 4 mm to each side of the center of the graphite rod.

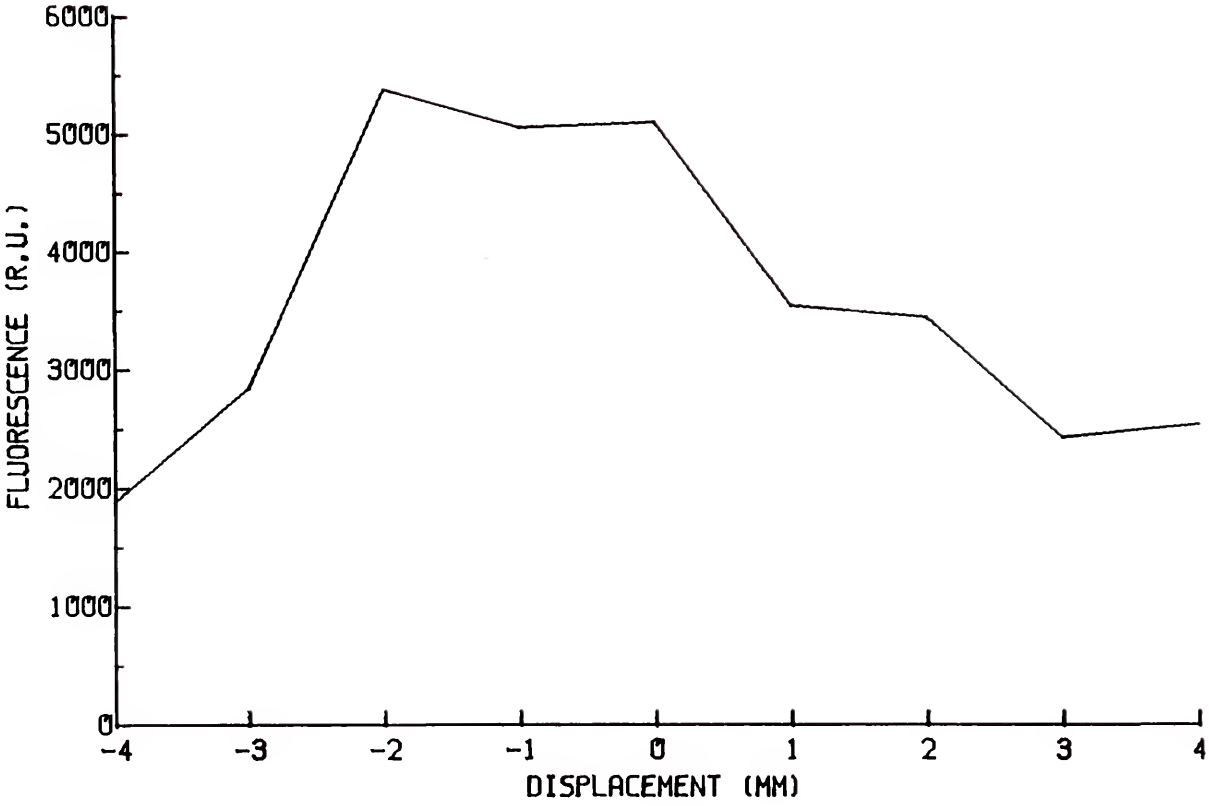
6000
5000
4000
3000
2000
1000
0
FLUORESCENCE (R.U.)
-4
-3
-2
-1
0
1
2
3
4
DISPLACEMENT (MM)

Figure 22

Sodium atom population distribution at a height of 6 mm above the graphite rod with a displacement of up to 4 mm to each side of the center of the graphite rod.

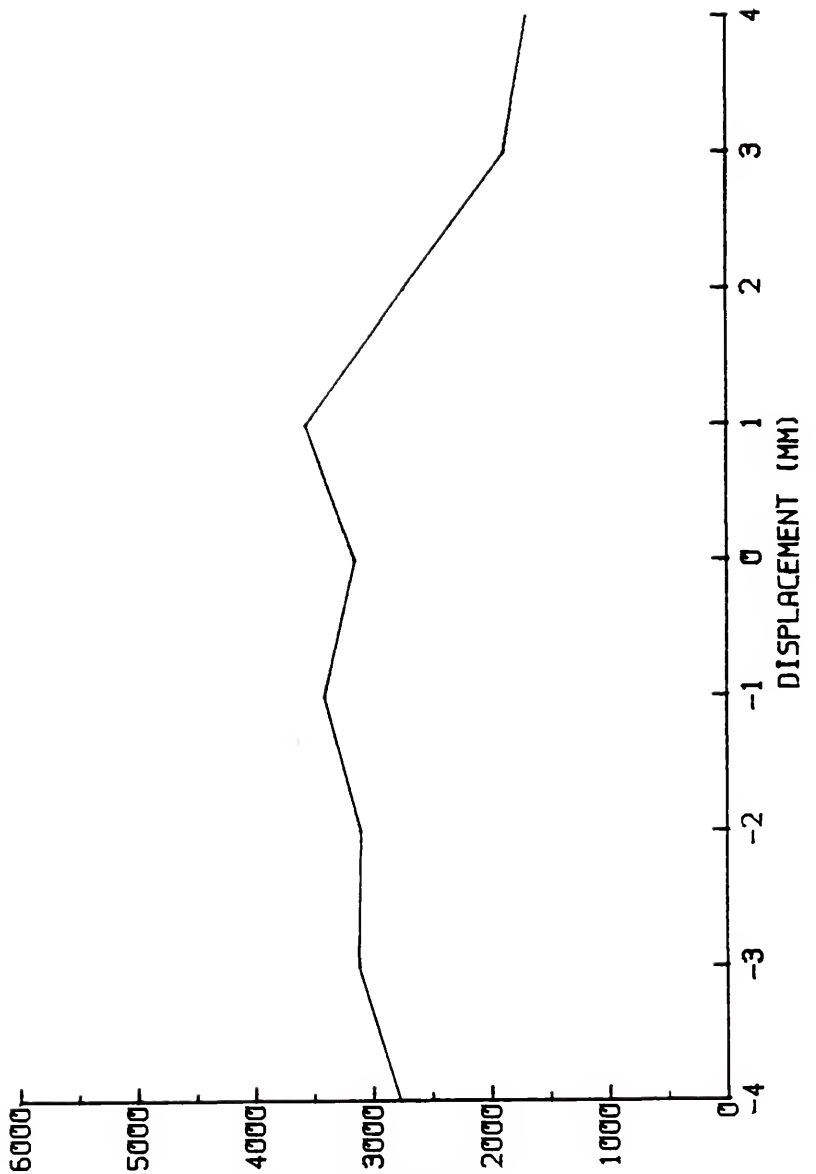
FLUORESCENCE (R.U.)
6000
5000
4000
3000
2000
1000
0
-4
-3
-2
-1
0
1
2
3
4
DISPLACEMENT (MM)

quenching cross section, it was expected to have lower fluorescence signals and this was found to be the case. The relative quenching ratios (fluorescence in nitrogen/fluorescence in argon) for a 1000 ppm tin solution and a 100 ppm tin solution were 0.76 and 0.80, respectively. A 100 ppm solution of manganese yielded a quenching ratio of 0.61. The difference in quenching for the two elements may be attributed to the different effective cross sections that these gases have with different atoms (63).

So that this relative quenching information may be made more definitive, the fluorescence lifetime of sodium in an argon sheath was measured in the electrothermal atomizer. The observed lifetime was 6 ns. Comparing this to the natural lifetime of 16.2 ns (73), it is obvious that a significant amount of quenching does occur in an argon sheath. The ratio of observed sodium fluorescence lifetime to the natural fluorescence lifetime is 0.37 and is indicative of the magnitude of the radiationless deactivation processes in the electrothermal atomizer. Since the quenching processes in the two different sheath gases would have the same effect on the other elements, the quenching factor found for sodium can also be applied to the other elements determined in this system. Therefore, for manganese and tin, it is implied that their respective quantum efficiencies in an argon sheath are also 0.37 (i.e., reduced from the maximum value of 1 by a factor of

3). The quantum efficiency in a nitrogen sheath is then found to be 0.23 and 0.30 for manganese and tin, respectively.

Saturation Spectral Irradiance

The plots of fluorescence intensity versus source spectral irradiance for sodium, tin and manganese are shown in Figures 23, 24 and 25, respectively. These were obtained using an argon sheath with a hydrogen diffusion flame around the electrothermal atomizer. Of the three elements examined only manganese clearly showed the saturation plateau. This indicates that it would be possible to determine the absolute number density of the manganese atoms if the detection system were calibrated in absolute units. This would also then provide a means to calculate an actual quantum efficiency for manganese in addition to the relative quantum efficiency determined in this work.

In order to perform these calculations for sodium and tin, since they do not reach saturation, it would be necessary to use the slope method (near saturation irradiance method) (59). Again, however, this requires the detection system to be calibrated in absolute units.

Figure 23

Plot of fluorescence intensity versus source spectral irradiance for the resonance fluorescence of sodium at 589.0 nm.

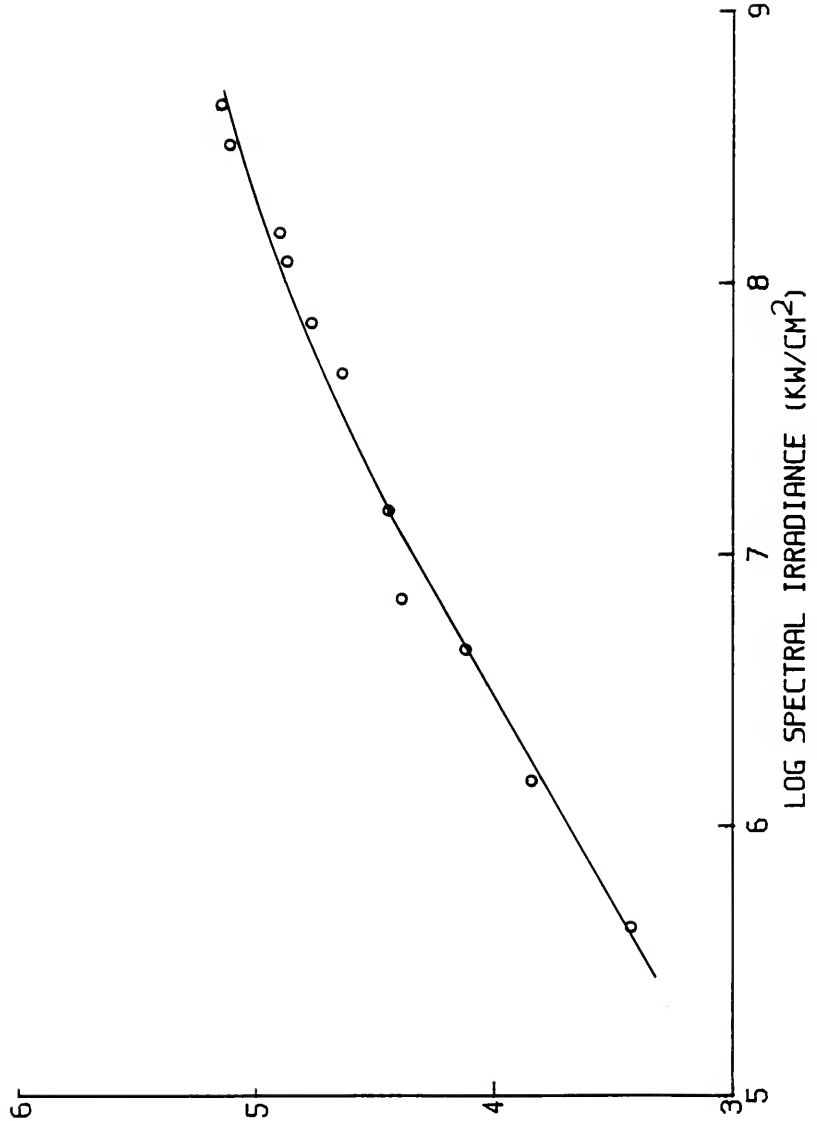
LOG FLUORESCENCE (R.U.)
6
5
4
3
5
6
7
8
9
LOG SPECTRAL IRRADIANCE (KW/CM2)

Figure 24

Plot of fluorescence intensity versus source spectral irradiance for the excited state Stokes direct-line fluorescence of tin.

300.9 nm excitation
317.5 nm fluorescence

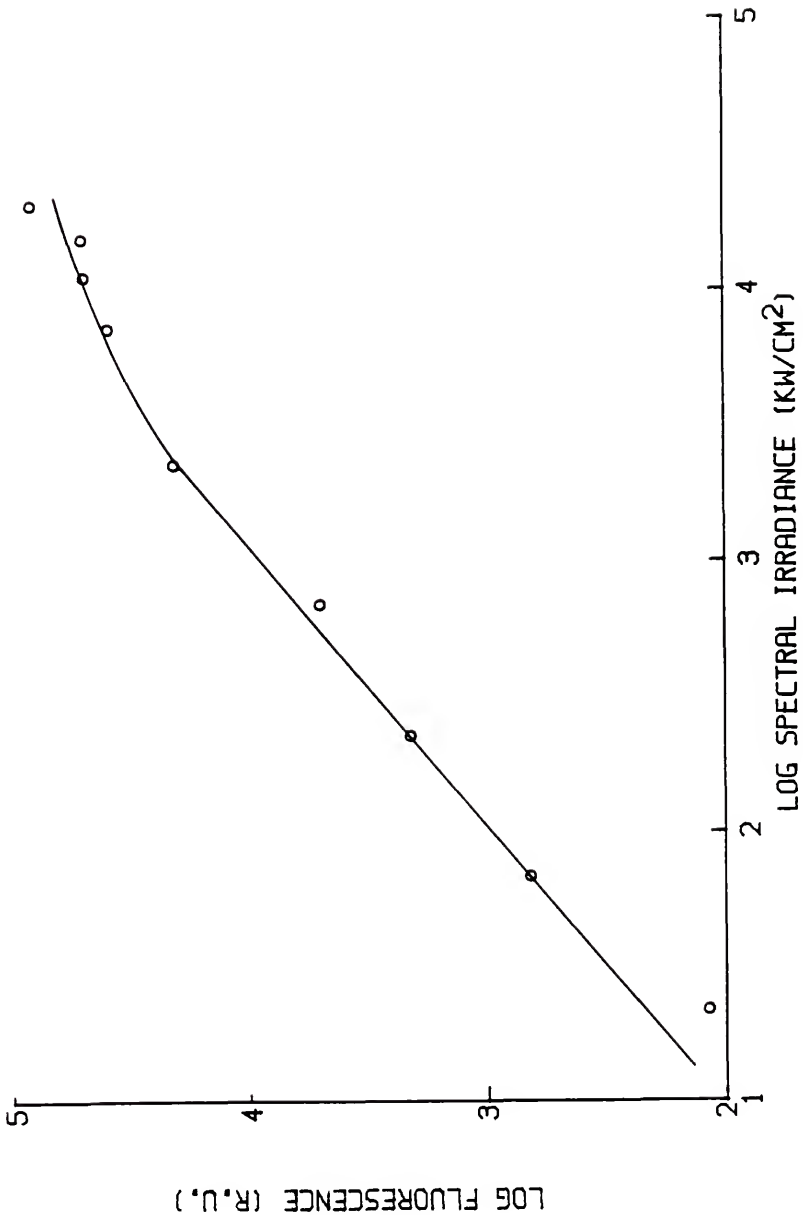
LOG FLUORESCENCE (R.U.)
LOG SPECTRAL IRRADIANCE (KW/CM2)
1
2
3
4
5

Figure 25

Plot of fluorescence intensity versus source spectral irradiance for the resonance fluorescence of manganese at 403.1 nm.

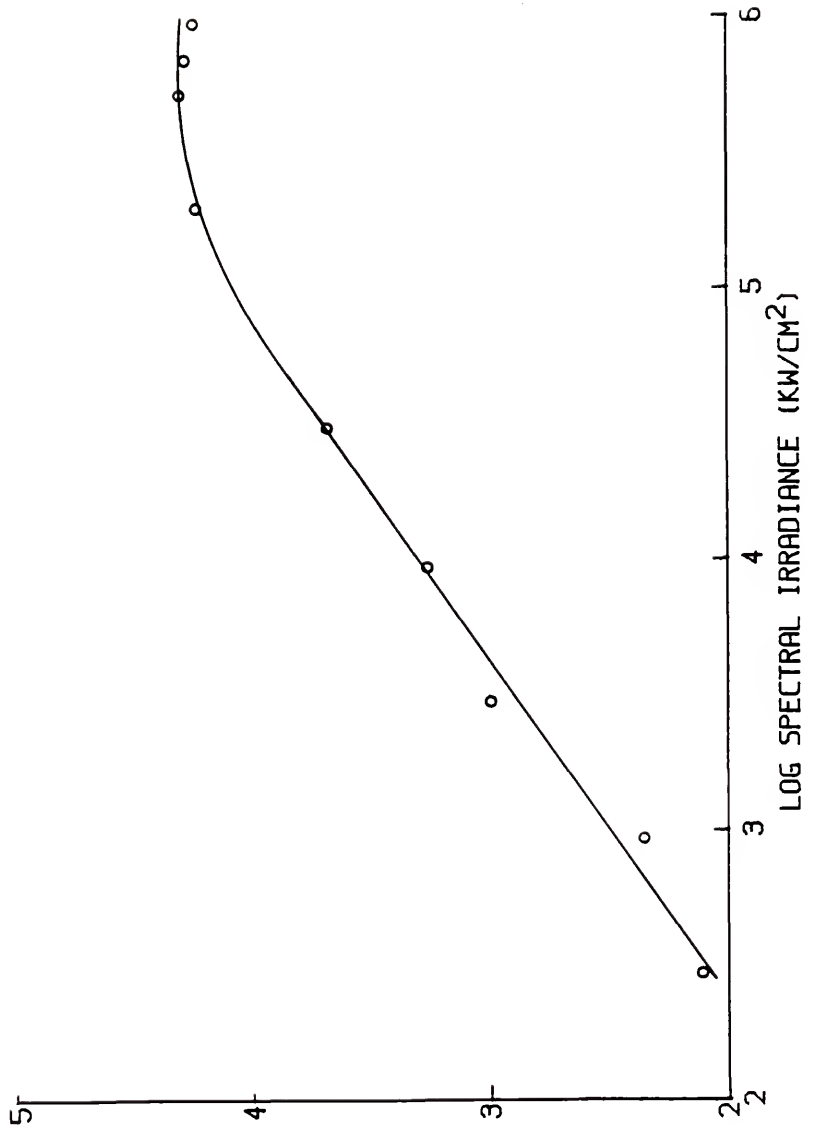
LOG FLUORESCENCE (R.U.)
5
4
3
2
2
3
4
5
6
LOG SPECTRAL IRRADIANCE (KW/CM2)

CHAPTER 5
SUMMARY AND FUTURE WORK

Summary

A microcomputer controlled electrothermal atomization system has been described and several analytical parameters in atomic fluorescence spectrometry have been given.

The theory of the transport of the analyte to the analytical volume and the resulting fluorescence signal was reviewed, along with some reasons why non-flame cells in atomic fluorescence should attain better figures of merit than flame atomic fluorescence spectrometry. The method used for obtaining the maximum signal to noise ratio was described.

The design, construction and evaluation of the new microcomputer controlled electrothermal atomizer were discussed. The analytical figures of merit, precision, sensitivity, linear dynamic range and limits of detection were examined for three elements. The decay of sodium atom population above the electrothermal atomizer as well as a function of horizontal displacement using an argon and hydrogen diffusion flame sheath were determined, and the results were discussed.

A major advantage of the present system over some past electrothermal atomization systems is that the operator has the power of a microcomputer at his disposal. This allows

faster and much more reproducible parameter changes, such as furnace temperatures and laser repetition rate. This ease of operation coupled with the long linear dynamic range and the low limits of detection make this system attractive for routine use. A more extensive use of the microcomputer for data reduction and presentation would only serve to increase the appeal of this system.

Future Work

Temperature Control

An immediate improvement in temperature control would be realized by adding a real time feedback feature to the temperature monitor that the controlling microcomputer uses. By using this feature, it would be possible to increase the heating rate from the present rate of approximately 300 K/s to a much higher value (dependent on the power supply used). This could be accomplished by operating the power supply at full power until the temperature monitor senses that the desired temperature has been reached. At this point, the microcomputer would then regain control of the power supply and maintain the desired temperature via the voltage programming mode of the power supply.

This would also eliminate temperature variations due to the aging of the graphite rod. This aging results in an increase in the resistance and a consequential drop in the current since the voltage is being held constant (voltage programming mode). This overall drop in power results in a

lower and varying temperature, especially towards the end of the lifetime of the graphite rod.

Laser Considerations

In the course of this work, many accessories had to be added to the dye laser in order to obtain the desired laser wavelength. However, one feature that would have made the elements requiring frequency doubling easier to determine was a scan drive for the doubling crystal turret. Since the angle of incidence of the fundamental laser beam on the doubling crystal is a function of the wavelength, it is necessary to change the doubling crystal angle in unison with the wavelength scanning of the fundamental beam. Unfortunately, the rate of angle change with respect to the wavelength change is a non-linear function which is different for each type of doubling crystal (see Figure 26).

However, it should be possible to use the same microcomputer that controls the other parts of the system to change the doubling crystal angle at the proper rate. This would be done using the stepper motor on the doubling crystal turret in conjunction with a software controlled digital output line from the VIA board. Using the equations that define the curves in Figure 26, the microcomputer could perform the necessary calculations and activate the stepper motor to take the required number of steps at the necessary rate. This of course could only be of use if the dye laser wavelength scan drive were also

Figure 26

Tuning curves for the frequency doubling crystals. The letters designate the different types of doubling crystals.
A--C = KPB crystals which require a vertically polarized fundamental beam.
D--F = KDP crystals which require a horizontally polarized fundamental beam.
(from DL-II Series Dye Laser instruction manual, Molectron Corp., Sunnyvale, CA)

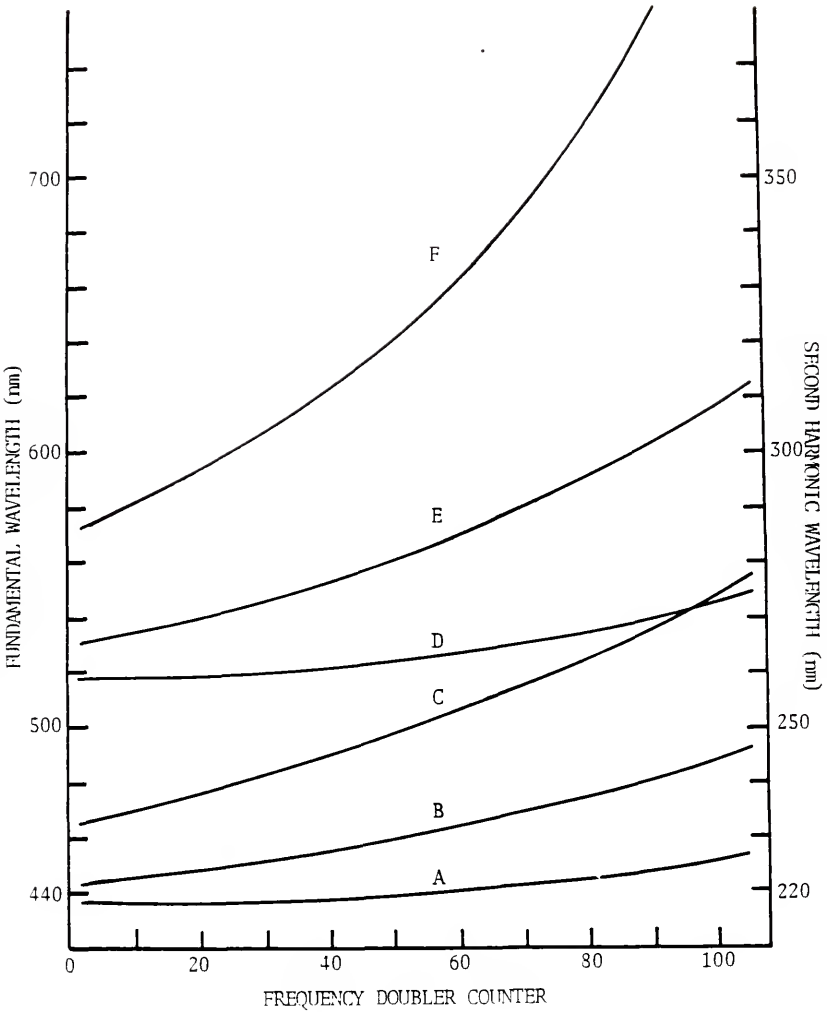
700
600
500
440
350
300
250
220
F
E
D
C
B
A
0
20
40
60
80
100
FUNDAMENTAL WAVELENGTH (nm)
SECOND HARMONIC WAVELENGTH (nm)
FREQUENCY DOUBLER COUNTER

under the microcomputer's control (an external control connector is provided by the manufacturer).

Improvements in the actual output of the laser would also improve the analytical parameters of this system. This would most easily be accomplished by an increase in the laser repetition rate. For example, it has been predicted that in the determination of lead, an increase in the laser repetition rate from 50 Hz to 10 kHz should result in an lowering of the limit of detection by 15 fold (74). This, however, would necessitate using a laser other than a nitrogen laser to pump the dye laser. One of the most promising in this regard is the Cu laser which can operate with repetition rates of several kHz. Another possibility would be using a cavity-dumped continuous-wave laser to pump a dye laser. In this manner, it would be possible to obtain repetition rates of several MHz.

Detector Calibration

As mentioned in Chapter 4, if the detection system had been calibrated in absolute units, it would have been possible to calculate quantum efficiencies and absolute number densities. In addition, the bandwidth of the laser beam needs to be measured (by scanning the monochromator across the laser wavelength). In further work, this calibration seems to be of utmost importance to allow a more definitive characterization of the electrothermal atomization system.

Sample Types

In addition to the calibration of the detection system, other elements need to be characterized in this electrothermal atomizer. These would include high volatility elements, such as lead or cadmium and refractory elements, such as vanadium or molybdenum.

Some preliminary work had been done on cadmium, but results were elusive. This was attributed to the difficulties encountered with the required frequency doubling of the fundamental laser beam and the attempt to then separate the two beams. The separation was required in order to ascertain when the frequency doubling had been accomplished and to reduce second order scatter into the monochromator. It is expected that with the previously mentioned laser wavelength scan control, it will be possible to overcome the difficulties associated with doubling near the lower limit (217 nm) of the doubling crystal. Additionally, several sensitive lines for each element (when available) should be investigated in order to characterize the analytical parameters for each line. This characterization was done for two lines of tin in the present work.

Furnace Design

A further increase in signal to noise ratios of furnace atomic fluorescence spectrometry could be obtained by improving the atomizer design. This improvement would consist of producing a less dynamic analytical volume, i.e.,

one where the residence time of the analyte is greatly increased. By having this more static design, the atomization temperature would be experienced by the analyte atoms for this increased time, resulting in fewer losses of the free analyte due to recombination processes. In addition, the increased residence time would allow greater fluorescence signals to be obtained and perhaps even allow cyclic interaction between analyte atoms and the exciting radiation.

APPENDIX 1
FURNACE HARDWARE

To be able to control the various aspects of the electrothermal atomization system several pieces of equipment were needed which were not commercially available at the time or if available were prohibitively priced. Therefore the required equipment was built in the laboratory. The most important piece was the VIA interface board. Using two SY6522 Versatile Interface Adapter chips (Synertek, Santa Clara, CA) along with the associated buffers, inverters, and data transceivers, an interface consisting of 32 independent I/O lines was built on a single prototyping board (see Figure 27). The overall design was based on a previous Peripheral Interface Adapter (PIA) board by Voigtman and Bolton (75). Although the VIA has many more functions than the PIA, the upgrade was primarily prompted by the added feature of a sixteen bit programmable clock. Every aspect of the present work was controlled by twenty of the 32 I/O lines leaving twelve I/O lines free to control additional devices as added, e.g., an autosampler.

By using hardware selectable (8 position mini-dip switch) addressing, the VIA interface board was extremely mobile and could be located in any of the Apple's peripheral slots except slot zero and six which are

Figure 27

Versatile Interface Adapter board schematic. Component symbols are as follows:
R1 = 1.0 k resistor network, S1 = 8 position mini-dip switch, AD1 and AD2 = 74LS85 four-bit decoder, V1 and V2 = Vesatile Interface Adapter chip, B1 = 74LS241 inverting buffer, D1 = 74LS245 data transceiver, C1 and C2 = off-board connector for V1 and V2, respectively. The A and D line connections originate from the Apple II microcomputer bus as do the Res and R/W lines.

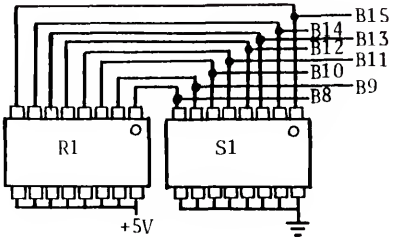
B15
B14
B13
B12
B11
B10
B9
B8
R1
S1
+5V

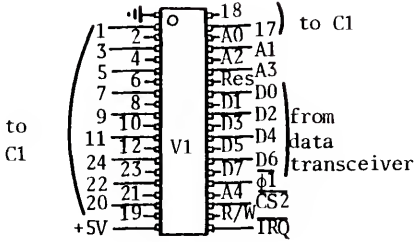
to C1
to C1
V1
A0
A1
A2
A3
Res
D0
D1
D2
D3
D4
D5
D6
D7
A4
R/W
φ1
CS2
IRQ
+5V
from data transceiver

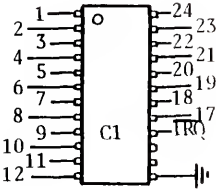
C1
IRQ

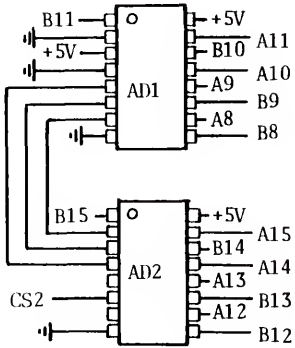
B11
+5V
AD1
+5V
B10
A11
A9
A10
B8
A9
B8
B15
AD2
+5V
B14
A15
A13
A14
A12
B13
CS2
B12

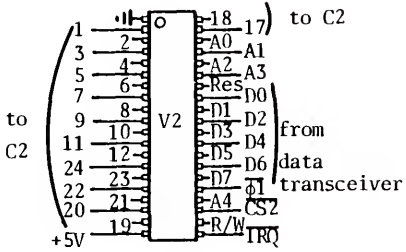
to C2
to C2
V2
A0
A1
A2
A3
Res
D0
D1
D2
D3
D4
D5
D6
D7
A4
R/W
φ1
CS2
IRQ
+5V
from data transceiver

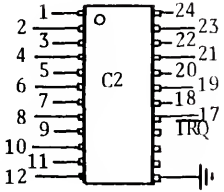
C2
IRQ

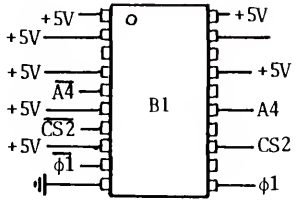
+5V
+5V
+5V
+5V
+5V
A4
CS2
φ1
B1
+5V
+5V
A4
CS2
φ1

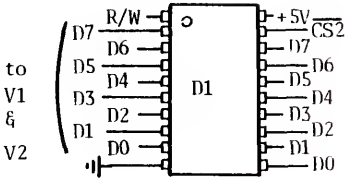
to V1 & V2
R/W
D7
D6
D5
D4
D3
D2
D1
D0
D1
+5V
CS2
D7
D6
D5
D4
D3
D2
D1
D0

reserved for memory expansion and the disk drive controller, respectively. One rare problem was encountered while assembling the VIA interface board; it was found that the timing on the Apple II I/O SELECT did not meet the minimum timing specifications required by the VIA chip select line. In order to overcome this problem, it was necessary to decode an additional address line to act as a replacement for the Apple II I/O SELECT.

Both the A/D converter and D/A converter were designed by E. Voigtman (76) and were then built into NIM bin modules to make them portable throughout the laboratory. The A/D converter was wired to have four independent channels with a twelve bit resolution over a 0-10 V range. The acquisition time of this A/D converter (MDAS-8D, Datel, Mansfield, MA) was 6 μs and the conversion time was 14 μs. The A/D's twelve bits were typically read in a high byte, low byte order and the data reconstructed to base ten format before storage on disk. Since the minimum number of steps to control and read the A/D converter took almost a 100 μs, there was no possiblity of overrunning the A/D converter. The D/A converter actually consisted of four independent D/A converters (DAC-IC8BC, Datel, Mansfield, MA) each with an eight bit resolution over a range of 0-5 V.

Another NIM bin module was used to contain several buffers for all of the I/O lines not used for the A/D or D/A converters. These lines were used to trigger the

nitrogen laser, clear/enable the boxcar and activate/deactivate the gas solenoid valves. The buffers were required to maintain TTL levels over long cable lengths. These buffers were required to trigger the gas solenoid valves as well as reliably trigger the nitrogen laser. The NIM bin, in addition to buffering the lines, separated the 16 I/O lines from a 25 pin connector into sixteen separate BNC connectors to facilitate use of individual lines.

In order to conserve gas, it was decided to use solenoid valves to stop the flow of gas when the furnace was not actually on. Because the available solenoid valves operated at 110 V and 60 Hz, a TTL interface had to be built to allow microcomputer control. Using an optoisolator (MOC 3010, Motorola, Phoenix, AR), a circuit was designed and built to meet the requirements of a TTL to line voltage interface (see Figure 28). Because of the on/ off nature of the interface it was controlled directly by one of the VIA I/O lines.

Figure 28

Schematic for the microcomputer controlled gas solenoid valves. All resistor values are in ohms and all capacitor values are in microfarads.

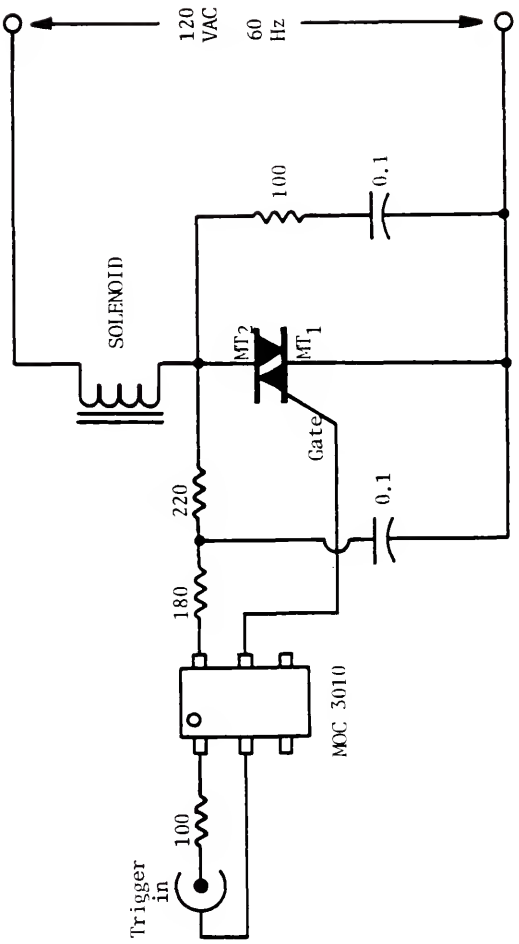
120
VAC
60
Hz
100
0.1
SOLENOID
MT2
MT1
Gate
220
0.1
180
MOC 3010
100
Trigger
in

APPENDIX 2
FURNACE SOFTWARE

A useful and practically required aspect of software is that it be very user friendly; with this in mind the electrothermal atomization control software (ETA PS7.1.OBJ) was written. Program names should be indicative of the function they perform and ETA PS7.1.OBJ follows this convention--Electrothermal Atomization (ETA), Peripheral Slot 7 location (PS7) , .1 is the version number and .OBJ indicates that the program has been compiled. The original version was written in Applesoft BASIC and when executed in this form the fastest the nitrogen laser could be triggered was 5 Hz. Compilation overcame this slowness in execution by converting the BASIC into machine language. This resulted in an increase of approximately six fold allowing laser triggering at a rate of 29 Hz.

The BASIC version used as the source program for the compiler is listed here in its entirety. In order to facilitate understanding of this program, the key sections are briefly explained below (in addition to the remarks imbedded within the program).

Lines 100--200

This section defines certain variables as integer values for the BASIC compiler.

Lines 380--480

This is the initialization section. It sets the various registers to default values to await further commands later in the program.

Lines 490--740

This section asks the user for the experimental parameters that are to be used for this particular analysis.

Lines 770--910

The VIA board selects the D/A channel that controls the electrothermal atomizer and outputs the voltage needed to produce the temperature requested.

Lines 920--950

The VIA board now has the D/A output rise to produce the atomization temperature requested.

Lines 980--1120

The VIA board triggers a laser shot and then initiates the A/D to read the boxcar output.

Lines 1130--1180

The datum is read from the A/D in a high byte, low byte order.

Line 1190

This line checks to see if the requested number of laser shots have been done.

Line 1200

The boxcar output is reconstructed to a base ten format and stored in an array.

Lines 1240--1340

The VIA board initiates the A/D to read the temperature monitor output.

Lines 1350--1410

The temperature monitor datum is reconstructed to a base ten format and stored in an array.

Lines 1530--1600

The VIA turns electrthermal atomizer power off as well as the hydrogen gas. After a 6 s cooling delay, the argon gas is also turned off.

Lines 1610--1660

The VIA clock is set in its slowest cycle and is set to trigger the laser once every clock cycle.

Lines 1700--1750

These lines dump the most recent data to the video monitor.

Lines 1760--1820

These lines dump the most recent data to a printer for a hard copy.

Lines 1840--2080

This section saves the most recent data on a disk in a format which places all of the user selected experimental parameters first, followed by the boxcar output alternated with the temperature data.

```
100  REM ! INTEGER T,LS,P,A,B,DT,BT,VT,F
110  REM ! INTEGER SS,CN,F1,F2
120  REM ! INTEGER DZ(1100),DT(1100)
130  REM
140  REM       WRITTEN AS A SOURCE PROGRAM FOR TASC
150  REM  ***************************
155  REM  *                         *
160  REM  *         ETA PS7.1       *
165  REM  *                         *
170  REM  ***************************
180  REM       PROGRAM TO CONTROL THE FURNACE POWER SUPPLY,
      THE LASER, THE BOXCAR,
190  REM       THE GAS SOLENOID VALVES, AND READ DATA FROM
     THE BOXCAR AND
200  REM    A W5%RE/W25%RE THERMOCOUPLE.
210  REM WRITTEN JANUARY 1982 BY PKW.MODIFIED JULY 1982.
220  REM
230  REM     A/D CHANNEL ZERO = BOXCAR OUTPUT
240  REM     A/D CHANNEL TWO = THERMOCOUPLE OUTPUT
250  REM     D/A CHANNEL ONE = FURNACE POWER CONTROL
260  REM     BIT BUFFER B0 = BOXCAR CLEAR/ENABLE
270  REM BIT BUFFER B1 = SHEATH GAS SOLENOID CLOSED/OPEN

280  REM BIT BUFFER B2 = FLAME GAS SOLENOID CLOSED/OPEN
290  REM     BIT BUFFER B7 = LASER TRIGGER ON/OFF
300  REM      VIA #1 (50944 - PER. SLOT 7) GOES TO THE BIT
     BUFFER NIM BIN
310  REM      VIA #2 (50960 - PER. SLOT 7) GOES TO THE A/D
     & D/A NIM BIN
320  REM
330  REM
340  REM
350 Q1 = 50944:Q2 = 50960
360  DIM DZ(1100),DT(1100)
370 P = 1:K = 0: REM     INITIALIZE LASER SHOT COUNTER AND
      LASER SHOT FLAG
380  REM      INITIALIZE VIA'S IN PER. SLOT 7
390  POKE Q1 + 11,0: REM   DISABLE TIMER 1 & 2 ON VIA #1
400  POKE Q2 + 11,0: REM   DISABLE TIMER 1 & 2 ON VIA #2
410  POKE Q1 + 3,255: REM   #1 DDRA OUTPUTS
420  POKE Q1 + 2,255: REM   #1 DDRB OUTPUTS
430  POKE Q1 + 1,0: REM    #1 PA0-7 TO LOW
440  POKE Q1,0: REM   #1 PB0-7 TO LOW
450  POKE Q2 + 3,255: REM   #2 DDRA OUTPUTS
460  POKE Q2 + 2,255: REM   #2 DDRB OUTPUTS
470  POKE Q2 + 1,0: REM   #2 PA0-7 TO LOW
480  POKE Q2,0: REM   #2PB0-7 TO LOW
490  REM  ENTER EXPERIMENTAL PARAMETERS
500  INPUT " HOW MANY LASER SHOTS ?";LS
510  PRINT " TRIGGER FREQUENCY ?"
520  INPUT "1-10 HERTZ  2-20 HERTZ  3-29 HERTZ ";F1
530  IF F1 < 1 OR F1 > 3 THEN 520
540  IF F1 = 1 THEN F2 = 3.4
```

```
550  IF F1 = 2 THEN F2 = 15
560  IF F1 = 3 THEN F2 = 1000
570 FR =  INT (1000 / F2): REM    DELAY TIME FOR COMPILED
     VERSION
580  INPUT " DRYING TEMPERATURE (F) ?";D1
590 DT =  INT (53.3755646 + 0.0367097355 * D1 - ((3.359217
     7 * 10 ^  - 6) * D1 ^ 2))
600  INPUT " DRYING TIME IN SECONDS ?";D2
610 DS = D2 * 4800
620  INPUT " ASHING TEMPERATURE (F) ?";B1
630 BT =  INT (53.3755646 + 0.0367097355 * B1 - ((3.359217
     7 * 10 ^  - 6) * B1 ^ 2))
640  INPUT " ASHING TIME IN SECONDS ?";B2
650 BS = B2 * 4800
660  INPUT " ATOMIZATION TEMPERATURE (F) ?";V1
670 VT =  INT (53.3755646 + 0.0367097355 * V1 - ((3.359217
     7 * 10 ^  - 6) * V1 ^ 2))
680  INPUT " ATOMIZATION TIME IN SECONDS ?";V2
690 VS = V2 * 65
700  INPUT " SAMPLE ELEMENT ?";SE$
710  INPUT " ALIQUOT SIZE (MICROLITER) ?";SS
720  INPUT " EXCITATION WAVELENGTH (NM) ?";EW
730  INPUT " FLUORESCENCE WAVELENGTH (NM) ?";FW
740  INPUT " SAMPLE CONCENTRATION (PPM) ?";CN
750  REM
760  PRINT : PRINT "PLACE SAMPLE ON GRAPHITE AND PRESS KEY
      TO START.";: GET A: PRINT
770  REM  TURN ON SHEATH GAS SOLENOID - #1 B1
780  POKE Q1,2: REM    SHEATH OPEN, BOXCAR CLEAR
790  REM  FURNACE TO DRY - #2
800  POKE Q2,16: REM   SELECT D/A CHANNEL 1
810  POKE Q2,0
820  POKE Q2 + 1,DT: REM    POKE DRYING TEMP
830  POKE Q2,16
840  POKE Q2,0: REM   SELECT D/A CHANNEL 1
850  FOR PK = 1 TO DS: NEXT PK: REM    DRYING TIME DELAY
860  POKE Q2 + 1,BT: REM    POKE ASHING TEMP
870  POKE Q2,16
880  POKE Q2,0: REM   SELECT D/A CHANNEL 1
890  FOR PK = 1 TO BS: NEXT PK: REM    ASHING TIME DELAY
900  REM   TURN ON FLAME GAS SOLENOID #1 B2
910  POKE Q1,6: REM       SHEATH OPEN, FLAME OPEN, BOXCAR
     CLEAR
920  REM  FURNACE TO ATOMIZE
930  POKE Q2 + 1,VT: REM   POKE ATOMIZATION TEMP
940  POKE Q2,16
950  POKE Q2,0: REM   SELECT D/A CHANNEL 1
960  GOSUB 980
970  GOTO 1480
980  FOR TT = 1 TO VS
990  REM  START DATA COLLECTION LOOP
1000  REM  TRIGGER LASER, ENABLE AND READ BOXCAR
```

```
1010  POKE Q1,7: REM       SHEATH OPEN, FLAME OPEN, BOXCAR
    ENABLED
1020  POKE Q1,135: REM     SHEATH OPEN, FLAME OPEN, BOXCAR
    ENABLED, LASER TRIGGERED
1030  POKE Q1,7: REM       SHEATH OPEN, FLAME OPEN, BOXCAR
    ENABLED
1040  POKE Q2 + 1,160
1050  POKE Q2,1
1060  POKE Q2,0
1070  POKE Q2 + 1,161: REM     TRIGGER A/D CHANNEL ZERO FOR
    DATA CONVERSION OF BOXCAR
1080  POKE Q2,1
1090  POKE Q2,0
1100  POKE Q2 + 1,160
1110  POKE Q2,1
1120  POKE Q2,0
1130  POKE Q2 + 3,0: REM   #2 DDRA INPUTS
1140  POKE Q2,8: REM       STROBE B PORT TO LATCH A PORT ON
    HIGH 4 BITS
1150 A =  PEEK (Q2 + 1): REM   SET A = HIGH 4 BITS
1160  POKE Q2,4: REM       STROBE B PORT TO LATCH A PORT ON
    LOW 8 BITS
1170 B =  PEEK (Q2 + 1): REM   SET B = LOW 8 BITS
1180  POKE Q2,0: REM     INHIBIT DAS LINES
1190  IF P =  > LS THEN 1210: REM  LASER DONE NO MORE DATA
    TO BE TAKEN
1200 DZ(P) =  INT (A * 16 + B / 16): REM  RECONSTRUCT A/D
    12 BITS TO 0-4095
1210  POKE Q2 + 3,255: REM   #2 DDRA OUTPUTS
1220  POKE Q1,7: REM       SHEATH OPEN, FLAME OPEN, BOXCAR
    CLEAR
1230  FOR F = 1 TO FR: NEXT F: REM   FREQUENCY DELAY
1240  REM   READ THERMOCOUPLE
1250  POKE Q2 + 1,164
1260  POKE Q2,1
1270  POKE Q2,0
1280  POKE Q2 + 1,165: REM TRIGGER A/D CHANNEL 2 FOR DATA
    CONVERSION OF THERMOCOUPLE
1290  POKE Q2,1
1300  POKE Q2,0
1310  POKE Q2 + 1,164
1320  POKE Q2,1
1330  POKE Q2,0
1340  POKE Q2 + 3,0: REM   #2 DDRA INPUTS
1350  POKE Q2,8: REM       STROBE B PORT TO LATCH A PORT ON
    HIGH 4 BITS
1360 A =  PEEK (Q2 + 1): REM   SET A = HIGH 4 BITS
1370  POKE Q2,4: REM       STROBE B PORT TO LATCH A PORT ON
    LOW 8 BITS
1380 B =  PEEK (Q2 + 1): REM   SET B = LOW 8 BITS
1390  POKE Q2,0: REM   INHIBIT DAS LINES
```

```
1400  IF P =  > LS THEN 1430: REM  LASER DONE NO MORE DATA
      TO BE TAKEN
1410 DT(P) =  INT (A * 16 + B / 16): REM  RECONSTRUCT A/D
     12 BITS TO 0-4095
1420 P = P + 1: REM  INCREMENT LASER SHOT COUNTER
1430  POKE Q2 + 3,255: REM   #2 DDRA OUTPUTS
1440  IF K = 1 THEN 1470: REM  CHECK LASER SHOT FLAG
1450  IF P =  > LS THEN 1490: REM        LASER SHOTS DONE
     FINISH ATOMIZATION TIME
1460  NEXT TT: REM   CONTINUE ATOMIZATION TIME
1470  RETURN
1480  GOTO 1530
1490 K = 1
1500  FOR W = TT TO VS
1510  GOSUB 1030
1520  NEXT W
1530  REM  PROCEED TO SHUT DOWN
1540  REM  TURN FURNACE OFF
1550  POKE Q2 + 1,0: REM   FURNACE OFF
1560  POKE Q2,16
1570  POKE Q2,0: REM   SELECT D/A CHANNEL 1
1580  POKE Q1,3: REM    SHEATH OPEN, BOXCAR CLEAR
1590  FOR T = 1 TO 25000: NEXT T: REM  COOLING OFF DELAY
1600  POKE Q1,1: REM    SHEATH CLOSED, BOXCAR CLEAR
1610  REM  ENABLE TIMER 1 IN FREE RUNNING MODE ON #1  PB7
1620  POKE Q1,128
1630  POKE Q1 + 11,192
1640  POKE Q1 + 4,255: REM    SET T1C-L TO MAXIMUM COUNT
     VALUE
1650  POKE Q1 + 5,255: REM   SET T1C-H TO MAXIMUM COUNT
     VALUE
1660  POKE Q1 + 6,255
1670  GOTO 1700
1680  POKE Q1,128: REM    SET #1  PB7 HIGH
1690  POKE Q1 + 11,128: REM    #1 ACR BIT7 HIGH TO ENABLE
     TIMER
1700  REM   DATA LISTING AND STORAGE
1710  INPUT " LIST DATA TO CONSOLE ?";LD$
1720  IF LD$ <  > "Y" THEN 1760
1730  FOR T = 1 TO P - 1
1740  PRINT "R#";T; TAB( 7);"BOXCAR IS ";DZ(T); TAB( 23);"
     THERMO IS ";DT(T)
1750  NEXT T
1760  INPUT " LIST DATA TO PRINTER ?";DP$
1770  IF DP$ <  > "Y" THEN 1840
1780  PRINT  CHR$ (4);"PR#1": REM  SELECT PRINTER IN PER.
     SLOT 1
1790  FOR T = 1 TO P - 1
1800  PRINT "RECORD #";T; TAB( 13);"BOXCAR IS ";DZ(T); TAB(
     29);"THERMO IS ";DT(T)
1810  NEXT T
1820  PRINT  CHR$ (4);"PR#0": REM  DESELECT PRINTER
1830  REM  CHANGE TO PR#3 IF USING VIDEOTERM
```

```
1840  INPUT " IS THIS DATA WORTH SAVING ?";SD$
1850  IF SD$ <  > "Y" THEN 2090
1860  INPUT " NAME OF DATA FILE ?";NA$
1870  INPUT " DATA DISK IN DRIVE 1 OR 2 ? ";DR
1880  PRINT  CHR$ (4);"OPEN ";NA$;".DAT,D";DR
1890  PRINT  CHR$ (4);"WRITE ";NA$;".DAT"
1900  PRINT (2 * (P - 1)) + 20
1910  PRINT DT
1920  PRINT DS
1930  PRINT BT
1940  PRINT BS
1950  PRINT VT
1960  PRINT VS
1970  PRINT SS
1980  PRINT EW
1990  PRINT FW
2000  PRINT CN
2010  FOR T = 1 TO 9
2020  PRINT T
2030  NEXT T
2040  FOR T = 1 TO P - 1
2050  PRINT DZ(T)
2060  PRINT DT(T)
2070  NEXT T
2080  PRINT  CHR$ (4);"CLOSE "
2090  INPUT " ANOTHER SAMPLE ?";AS$
2100  IF AS$ <  > "N" THEN 2120
2110  END
2120  INPUT " SAME CONDITIONS ?";SC$
2130 P = 1:W = 0:K = 0: REM     REINITIALIZE LASER SHOT
     COUNTER , ATOMIZATION FINISH
2140  REM      COUNTER AND LASER SHOT COUNTER
2150  IF SC$ <  > "Y" THEN 390
2160  POKE Q1 + 11,0: REM DISABLE TIMER 1 & 2 ON VIA #1
2170  GOTO 740
```

APPENDIX 3
RADIOMETER SYSTEM

In the course of becoming familar enough with the Apple II Plus microcomputer to enable the construction of the electrothermal atomization system discussed earlier, a microcomputer controlled radiometer system was assembled. This system was built to examine the spatial and spectral characteristics of various sources (77).

The Eimac xenon arc lamp was evaluated with respect to its use as an excitation source for atomic spectroscopy. Both the spatial output of the Eimac lamp at several wavelengths and the spatial variations in the output were investigated. The radiometer was designed according to the one described by Stair et al. (78), including the auxiliary optics for radiation transport from the source of concern to the spectrometer.

A block diagram of the radiometer system is shown in Figure 29. The Eimac lamp was mounted onto a turntable to allow motion in the x, y and z directions as well as rotation about its central axis. The light from the source passes through a pinhole aperture to an optical train consisting of front surface mirrors. This optical train is shown in Figure 30. The first mirror M1 was 16 in from the source on the turntable. The distance between mirrors M1 and M2 as well as M3 and M4 was 13.8 in. The distance

Figure 29

Block diagram of the radiometer system.

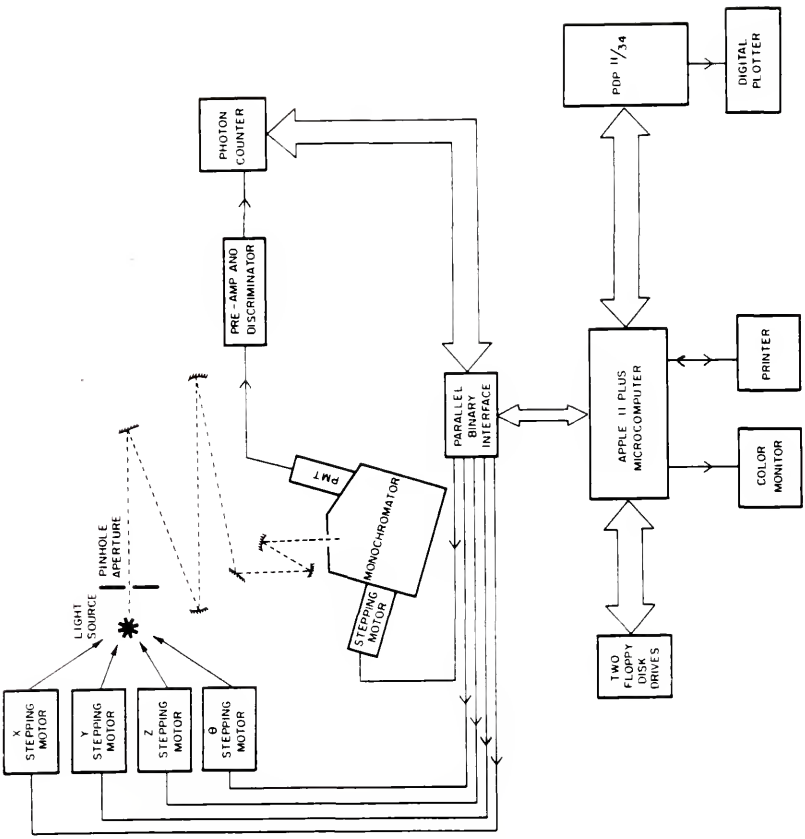
X STEPPING MOTOR
Y STEPPING MOTOR
Z STEPPING MOTOR
θ STEPPING MOTOR
LIGHT SOURCE
PINHOLE APERTURE
PMT
MONOCHROMATOR
STEPPING MOTOR
PRE-AMP AND DISCRIMINATOR
PHOTON COUNTER
PARALLEL BINARY INTERFACE
APPLE II PLUS MICROCOMPUTER
TWO FLOPPY DISK DRIVES
COLOR MONITOR
PRINTER
PDP 11/34
DIGITAL PLOTTER

Figure 30

The source turntable and optical train of the radiometer system.

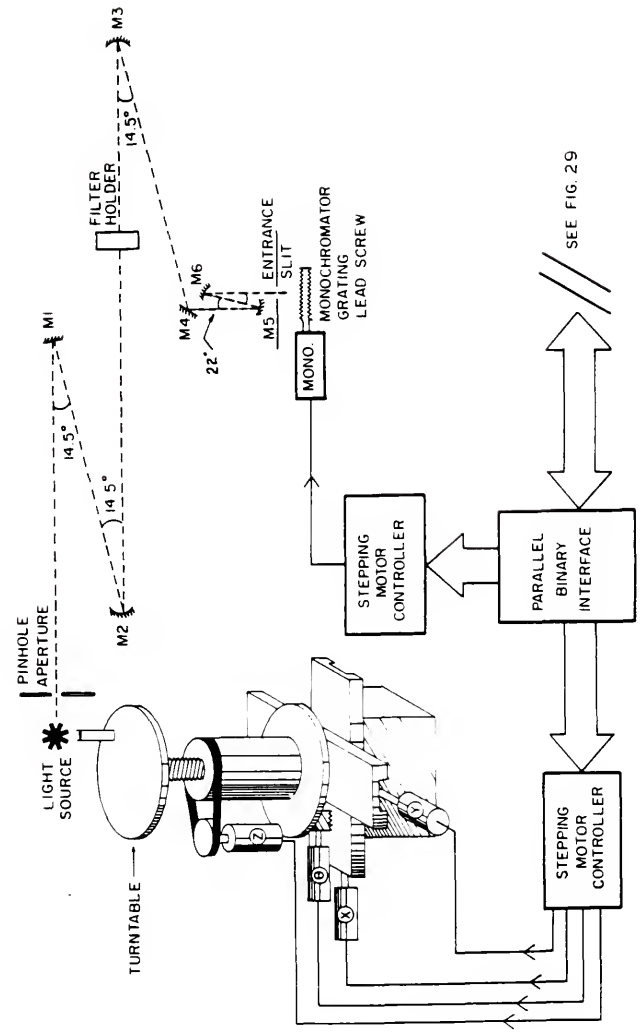
LIGHT SOURCE
PINHOLE APERTURE
TURNTABLE
M1
M2
M3
M4
M5
M6
14.5°
14.5°
14.5°
22°
FILTER HOLDER
ENTRANCE SLIT
MONOCHROMATOR GRATING LEAD SCREW
MONO.
STEPPING MOTOR CONTROLLER
PARALLEL BINARY INTERFACE
STEPPING MOTOR CONTROLLER
SEE FIG. 29

between mirrors M4 and M5 as well as M6 and the slit was 6.5 in and the distance from mirrors M5 to M6 was 4.5 in. The 28 in expanse between mirrors M2 and M3 contained collimated light and was equipped with a slotted filter holder. In order to minimize stray light, the optical path from the pinhole aperture to the entrance slit of the monochromator (f5.3, 0.3 m Czerny-Turner with 600 g/mm grating) was enclosed in blackened aluminum tubing (2.25 in I.D.) and black felt cloth. The monochromator slits were 10 mm by 20 μm with a bandpass of 0.1 nm.

The equipment used is listed in Table A3-1. The Eimac lamp used was a 300 W model. Except for the current dependent studies, it was operated at manufacturer's recommended settings (12 V, 12 A) using an Eimac power supply.

An Apple II Plus microcomputer was used to control the stepping motors via a laboratory constructed interface (four 8-bit input latches and four 8-bit output buffers) and to process data from and control the functions of the photon counter. All stepping motors were operated at a rate of less than 500 steps per second and no problems were encountered with missing steps at this speed. Monochromator control was through a stepping motor attached directly to the grating drive lead screw after disengaging the normal wavelength drive. Turntable control was by means of four stepping motors attached to the appropiate drive screws of the turntable. The source was scanned

TABLE A3-1

Radiometer System Equipment List

Item	Manufacturer
Apple II Plus Microcomputer	Apple Computer, Cupertino, CA
Model EMI 6256S Photo-multiplier Tube	Gencom Division, Plainview, NY
Model 1151 Photomultiplier Tube Housing	SSR Instruments, Princeton, NJ
Model 1105 Photomultiplier Tube Power Supply	SSR Instruments, Princeton, NJ
Model 1120 Amplifier-Discriminator	SSR Instruments, Princeton, NJ
Model 1110 Digital Synchronous Computer	SSR Instruments, Princeton, NJ
Xenon Arc Lamp	Eimac, Div. of Varian, San Carlos, CA
Lamp Power Supply	Eimac, Div. of Varian, San Carlos, CA
Parellel Binary Interface	Laboratory Built
Model M063-FD06 Turntable Stepping Motor	Superior Electric Co., Bristol, CT
Model M063-FC06 C2 Mono-chromator Stepping Motor	Superior Electric Co., Bristol, Ct
PDP 11/34 Minicomputer	DEC, Maynard, MA

horizontally while alternating up and down (vertical) movement (at each horizontal point) allowing gravity to minimize the effect of freeplay in the gears of the turntable.

When using an Eimac lamp as a source of excitation some optical considerations need to be taken into account. Although most of the light output is collimated, there is a fraction which has not been collected by the parabolic reflector and comes directly from the arc plasma. The arc light is diverging and complicates any optical arrangement using an Eimac lamp. Another complication is the "hole" in the light beam caused by the electrode assembly.

In Figures 31, 32 and 33 three dimensional (x, y and z where x = intensity) projection (A) and contour (B) plots of an Eimac lamp at three wavelengths are presented. All figures of the Eimac are as observed from the front, i.e., mirror images of the source radiation. It is apparent that the spatial intensity distribution becomes flatter at longer wavelengths; there are "holes" in the intensity distributions where the three supports hold the central arc electrode and there are greater intensity flucuations in the upper left quadrant near the support where the convective gas flow is greatest, as mentioned previously by Cochran and Hieftje (79), than in other regions of the Eimac lamp. This is more evident by observing several similar, independently measured plots. In Figures 33, 34 and 35 the effect of arc current is shown. It is apparent

Figure 31

Three dimensional (A) and contour (B) plots of an Eimac lamp at a wavelength of 213.9 nm and operation at a current of 12 A. Plot A is a 3-D projection (y--horizontal, z--vertical, x--relative intensity) of the Eimac lamp output. The y and z axes correspond to the emitting surface of the lamp. The x axis corresponds to a linear relative intensity axis. The maximum relative intensity is shown by the length of the left hand relative intensity axis. The maximum relative intensity in this figure is 5.8×10^5 counts (counting time = 1 s). The contour plot is obtained from the 3-D projection plot by dividing the relative intensity of the 3-D plot into 4 equal segments. The change in relative intensity between segments is represented by a change from white to black or vice versa. Note that the 3-D plot has been expanded compared to the contour plot for greater clarity. However any y-z point on the 3-D plot will correspond to a similar y-z point on the contour plot.

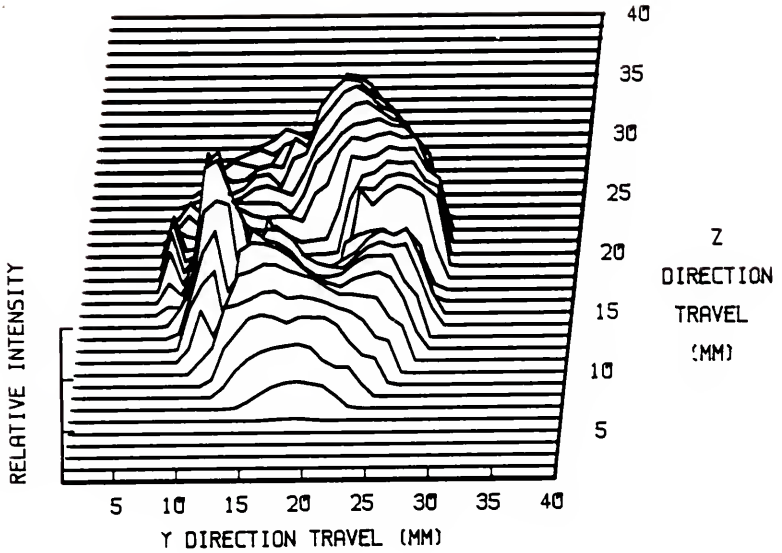
RELATIVE INTENSITY
40
35
30
25
20
15
10
5
Z
DIRECTION
TRAVEL
(MM)
5 10 15 20 25 30 35 40
Y DIRECTION TRAVEL (MM)

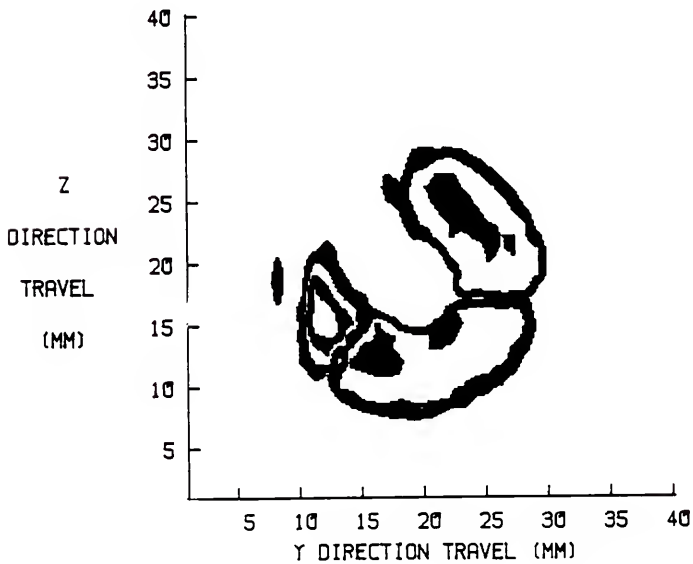
Z
DIRECTION
TRAVEL
(MM)
40
35
30
25
20
15
10
5
5 10 15 20 25 30 35 40
Y DIRECTION TRAVEL (MM)

Figure 32

Three dimensional projection (A) and contour (B) plots of an Eimac lamp at a wavelength of 328.1 nm and operation at a current of 12 A. The maximum relative intensity on this figure is 2.8×10^5 counts (counting time 0.05 s). Refer to Figure 31 caption for explanation of plots.

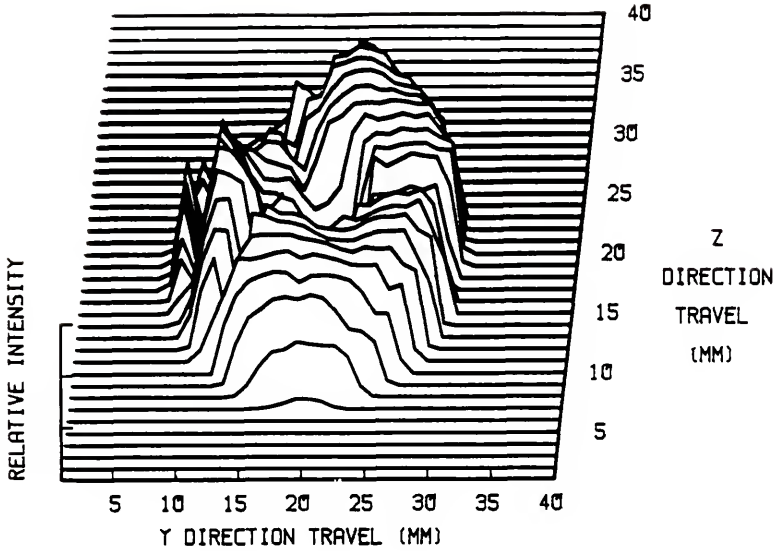
RELATIVE INTENSITY
40
35
30
25
20
15
10
5
Z
DIRECTION
TRAVEL
(MM)
5 10 15 20 25 30 35 40
Y DIRECTION TRAVEL (MM)

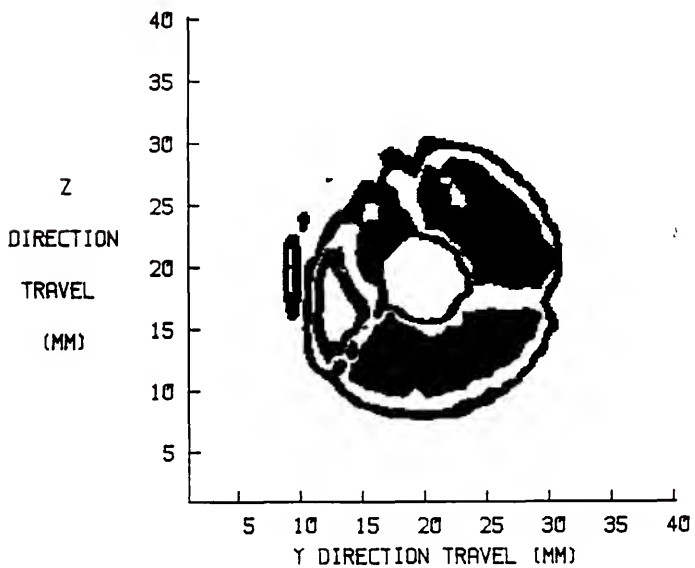
Z
DIRECTION
TRAVEL
(MM)
40
35
30
25
20
15
10
5
5 10 15 20 25 30 35 40
Y DIRECTION TRAVEL (MM)

Figure 33

Three dimensional projection (A) and contour (B) plots of an Eimac lamp at a wavelength of 589.6 nm and operation at a current of 12 A. The maximum relative intensity on this figure is 2.4×10^5 counts (counting time 0.05 s). Refer to Figure 31 caption for explanation of plots.

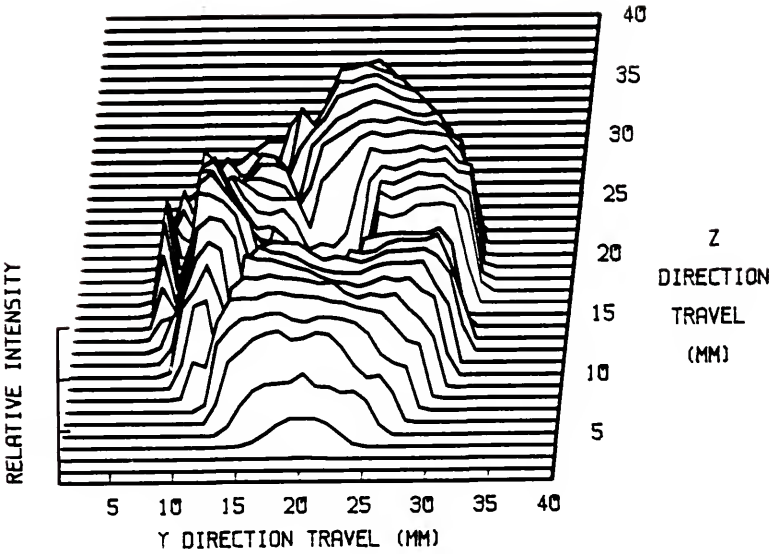
RELATIVE INTENSITY
40
35
30
25
20
15
10
5
Z
DIRECTION
TRAVEL
(MM)
5 10 15 20 25 30 35 40
Y DIRECTION TRAVEL (MM)

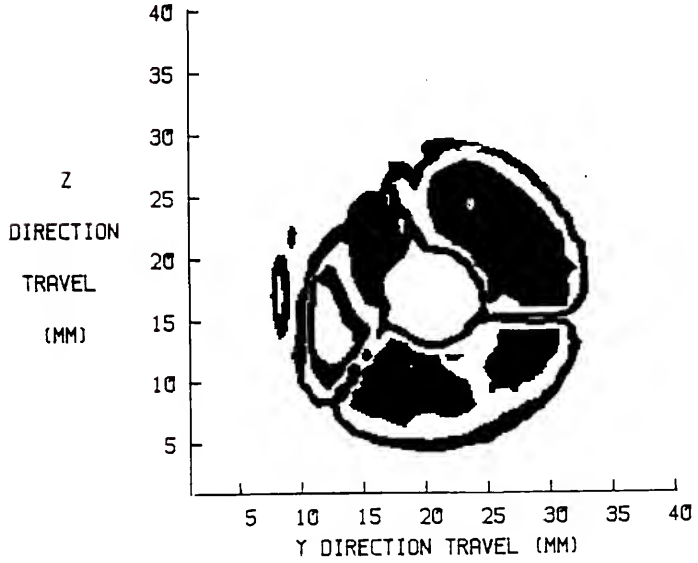
Z
DIRECTION
TRAVEL
(MM)
40
35
30
25
20
15
10
5
5 10 15 20 25 30 35 40
Y DIRECTION TRAVEL (MM)

Figure 34

Three dimensional projection (A) and contour (B) plots of an Eimac lamp at a wavelength of 589.6 nm and operation at a current of 11 A. The maximum relative intensity on this figure is 2.3×10^5 counts (counting time 0.05 s). Refer to Figure 31 caption for explanation of plots.

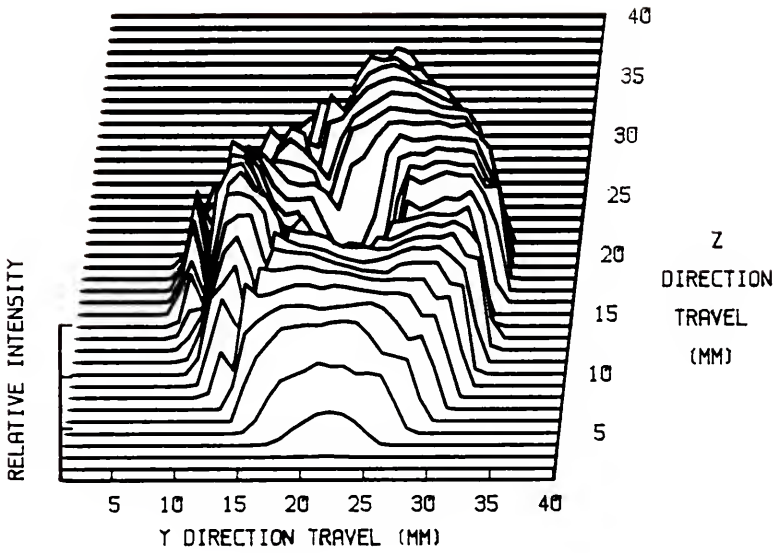
RELATIVE INTENSITY
40
35
30
25
20
15
10
5
Z
DIRECTION
TRAVEL
(MM)
5 10 15 20 25 30 35 40
Y DIRECTION TRAVEL (MM)

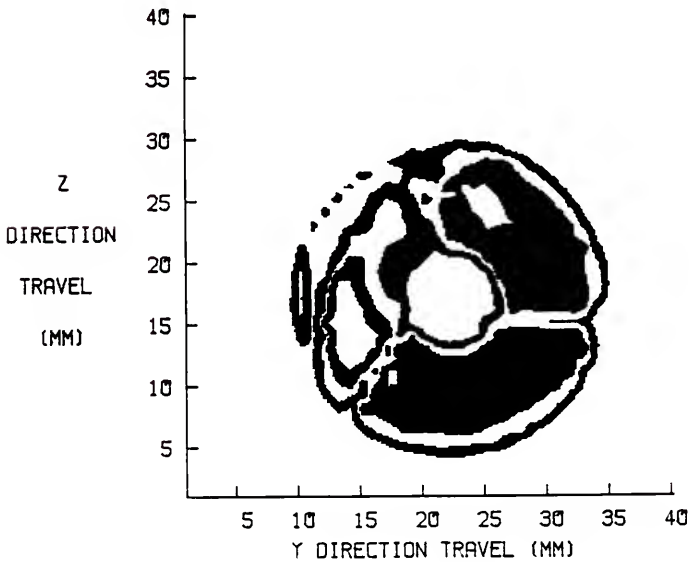
Z
DIRECTION
TRAVEL
(MM)
40
35
30
25
20
15
10
5
5 10 15 20 25 30 35 40
Y DIRECTION TRAVEL (MM)

Figure 35

Three dimensional projection (A) and contour (B) plots of an Eimac lamp at a wavelength of 589.6 nm and operation at a current of 13 A.5The maximum relative intensity on this figure is 2.5 X 10^5 counts (counting time 0.05 s). Refer to Figure 31 caption for explanation of plots.

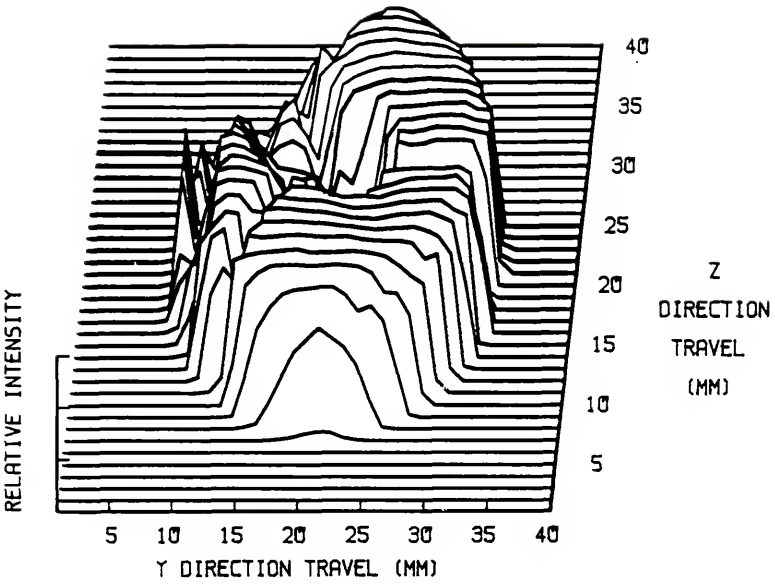
RELATIVE INTENSITY
40
35
30
25
20
15
10
5
Z
DIRECTION
TRAVEL
(MM)
5 10 15 20 25 30 35 40
Y DIRECTION TRAVEL (MM)

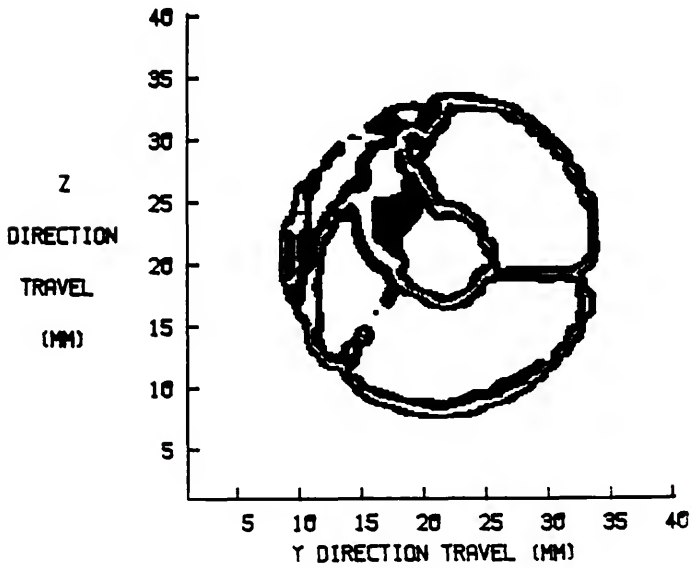
Z
DIRECTION
TRAVEL
(MM)
40
35
30
25
20
15
10
5
5 10 15 20 25 30 35 40
Y DIRECTION TRAVEL (MM)

that arc current (between 11 A and 13 A) has a rather small effect upon the spatial distribution or on the stability; an increase in arc current primarily causes an increase in total spectral output.

APPENDIX 4
DIGITAL PLOTTING PROGRAM

A useful and necessary function of a computer system is the ability to express the results of its computations in a way which is intelligible to the programmer and the user. To this end the DATA PLOTTER.11 program was written.

This program takes data stored on disk in a format which is compatible to other commercial software (Graphpak, Interactive Microware, State College, PA) and plots it on a digital plotter (DMP-4, Houston Instruments, Houston, TX). The BASIC program is listed in its entirety at the end of this Appendix. To facilitate in the understanding of the workings of this program, some of the key sections are briefly explained below.

Lines 100--240

All variables are set to their respective default values.

Lines 600--760

This section (repeated after all input statements) sets the last answer to a particular question as the default value (useful for repetitious plotting).

Lines 1000-1140

These lines read the data from disk if it is stored as x, y pairs.

Lines 1460--2020

These lines read the data from the disk if it is stored as y values at a constant x interval.

Lines 2060--2220

This section finds the maximum and minimum value for both the x and y data.

Lines 2820--2960

This section finds the maximum and minimum value of x, y data for the x interval the user wishes to examine (x scale expand).

Lines 5300--5460

These lines scale the data to fit within a 5.25 by 8 inch area (with labels, the entire plot fits within a 6 by 9 inch area).

Lines 5800--5900

This section selects the digital plotter as an output device of the microcomputer amd draws the x and y axes.

Lines 6800--7860

This section allows the selection of up to three lines of identifying text to be placed anywhere on the plot.

Lines 7880--8160

Again the digital plotter is selected to place the identifying text on the plot.

Lines 8660--8900

These lines calculate if the present x axis tick mark is one that is to be labeled and if it is, the tick mark length is doubled and labeled.

Lines 8920--9180

These lines do for the y axis what lines 8660--8900 do for the x axis.

Lines 10000--10180

This subroutine accepts the input from all the input statements and echoes it to the video screen.

```
100  REM  SET ALL INPUT DEFAULTS VALUES
120 MM$ = "NONE":XY$ = "N":LL$ = "N"
140 Z1$ = "0":Z2$ = "1":S1$ = "0":S2$ = "9"
160 NT$ = "Y":XQ$ = "X AXIS":XN$ = "2"
180 XP$ = "50":YQ$ = "Y AXIS":S3$ = "0":S4$ = "99"
200 YN$ = "2":YP$ = "50":L3$ = "N"
220 LQ$ = "Y":W1$ = " ":W3$ = " ":W5$ = " ":I1$ = "6.5":I3
    $ = "6"
240 Q1$ = "N":Q2$ = "Y"
260  REM
280  REM  ****************************
300  REM  *                          *
320  REM  *     DATA PLOTTER.11      *
340  REM  *                          *
360  REM  ****************************
380  REM
400  REM  PROGRAM TO ACCEPT DATA IN THE FORMAT AS ACCEPTED
      BY
420  REM  VIDICHART, SCIPLOT, AND CURFIT
440  REM  THIS WAS WRITTEN AS A GENERAL USE PROGRAM
460  REM    04-AUG-82     P.K.WITTMAN  UPDATED 23-AUG-82

480  REM
500  POKE 33,40
520  DIM A1(1100),A2(1100),B1(1100),B2(1100)
540  HOME
560 G$ =  CHR$ (223)
580  PRINT "DATA FILE"
600 CV =  PEEK (37)
620  POKE 36,10
640  POKE 37,CV: VTAB CV: PRINT "<";MM$;">"
660 NM$ = MM$
680 NM =  LEN (NM$)
690 KK = 13 + NM
700  POKE 37,CV: POKE 36,12 + NM: VTAB CV: GOSUB 10000
710 NM$ = A$
715  PRINT  CHR$ (13)
720 G1 =  LEN (NM$)
740  IF G1 = 0 THEN 780
760 MM$ = NM$
780  PRINT "X,Y PAIRS"
800 CV =  PEEK (37)
820  POKE 36,10
840  POKE 37,CV: VTAB CV: PRINT "<";XY$;">"
860 SD$ = XY$
880 SD =  LEN (SD$)
890 KK = 13 + SD
900  POKE 37,CV: POKE 36,12 + SD: VTAB CV: GOSUB 10000
910 SD$ = A$
915  PRINT  CHR$ (13)
920 G2 =  LEN (SD$)
940  IF G2 = 0 THEN 980
960 XY$ = SD$
```

```
980  IF  LEFT$ (XY$,1) <  > "Y" THEN 1460
1000  PRINT  CHR$ (4);"OPEN ";MM$
1020  PRINT  CHR$ (4);"READ ";MM$
1040  INPUT LE
1060  FOR Z = 0 TO (LE - 1) / 2
1080  INPUT B1(Z)
1100  INPUT A1(Z)
1120  NEXT Z
1140  PRINT  CHR$ (4);"CLOSE ";MM$
1160  PRINT "LIST DATA?"
1180 CV =  PEEK (37)
1200  POKE 36,11
1220  POKE 37,CV: VTAB CV: PRINT "<";LL$;">"
1240 LS$ = LL$
1260 LS =  LEN (LS$)
1270 KK = 14 + LS
1280  POKE 37,CV: POKE 36,13 + LS: VTAB CV: GOSUB 10000
1290 LS$ = A$
1295  PRINT  CHR$ (13)
1300 G3 =  LEN (LS$)
1320  IF G3 = 0 THEN 1360
1340 LL$ = LS$
1360  IF  LEFT$ (LL$,1) <  > "Y" THEN 2060
1380  FOR Z = 0 TO LE - 1
1400  PRINT Z; TAB( 10);A1(Z); TAB( 20);B1(Z)
1420  NEXT Z
1440  GOTO 2060
1460  PRINT "1ST X VALUE?"
1480 CV =  PEEK (37)
1500  POKE 36,13
1520  POKE 37,CV: VTAB CV: PRINT "<";Z1$;">"
1540 X1$ = Z1$
1560 X1 =  LEN (X1$)
1570 KK = 16 + X1
1580  POKE 37,CV: POKE 36,15 + X1: VTAB CV: GOSUB 10000
1590 X1$ = A$
1595  PRINT  CHR$ (13)
1600 G4 =  LEN (X1$)
1620  IF G4 = 0 THEN 1660
1640 Z1$ = X1$
1660  PRINT "X INCREMENT?"
1680 CV =  PEEK (37)
1700  POKE 36,13
1720  POKE 37,CV: VTAB CV: PRINT "<";Z2$;">"
1740 X2$ = Z2$
1760 X2 =  LEN (X2$)
1770 KK = 16 + X2
1780  POKE 37,CV: POKE 36,15 + X2: VTAB CV: GOSUB 10000
1790 X2$ = A$
1795  PRINT  CHR$ (13)
1800 G5 =  LEN (X2$)
1820  IF G5 = 0 THEN 1860
```

```
1840 Z2$ = X2$
1860 XX =  VAL (Z1$)
1880  PRINT  CHR$ (4);"OPEN ";MM$
1900  PRINT  CHR$ (4);"READ ";MM$
1920  INPUT LE
1940  FOR Z = 0 TO LE - 1
1960  INPUT A1(Z)
1980 B1(Z) = XX:XX = XX +  VAL (Z2$)
2000  NEXT Z
2020  PRINT  CHR$ (4);"CLOSE ";MM$
2040  GOTO 1160
2060  REM FIND MAX & MIN FOR BOTH X & Y
2080 M1X = A1(0):M2X = A1(0):M3Y = B1(0):M4Y = B1(0)
2100  FOR Z = 0 TO LE - 1
2120  IF A1(Z) < M1X THEN M1X = A1(Z)
2140  IF A1(Z) > M2X THEN M2X = A1(Z)
2160  IF B1(Z) < M3Y THEN M3Y = B1(Z)
2180  IF B1(Z) > M4Y THEN M4Y = B1(Z)
2200  NEXT Z
2220  PRINT "X MIN,MAX ";M3Y;" ";M4Y;"  Y MIN,MAX ";M1X;"
    ";M2X
2240  PRINT
2260  PRINT MM$" CONTAINS 0 TO ";LE - 1;" POINTS"
2280  PRINT
2300  PRINT " WHAT RANGE OF X TO EXAMINE ?"
2320  PRINT "FIRST SUBSCRIPT?"
2340 CV =  PEEK (37)
2360  POKE 36,17
2380  POKE 37,CV: VTAB CV: PRINT "<";S1$;">"
2400 XC$ = S1$
2420 T1 =  LEN (XC$)
2430 KK = 20 + T1
2440  POKE 37,CV: POKE 36,19 + T1: VTAB CV: GOSUB 10000
2450 XC$ = A$
2455  PRINT  CHR$ (13)
2460 G6 =  LEN (XC$)
2480  IF G6 = 0 THEN 2520
2500 S1$ = XC$
2520  PRINT "LAST SUBSCRIPT?"
2540 CV =  PEEK (37)
2560  POKE 36,16
2580  POKE 37,CV: VTAB CV: PRINT "<";S2$;">"
2600 XD$ = S2$
2620 T2 =  LEN (XD$)
2640  POKE 37,CV: POKE 36,18 + T2: VTAB CV: INPUT "";XD$
2660 G7 =  LEN (XD$)
2680  IF G7 = 0 THEN 2720
2700 S2$ = XD$
2720 XC =  VAL (S1$):XD =  VAL (S2$)
2740  IF XD < LE - 1 THEN 2820
2760  FOR Z = (LE) TO XD
```

```
2780 B1(Z) = Z +  VAL (Z1$)
2800  NEXT Z
2820 M1X = A1(XC):M2X = A1(XC):M3Y = B1(XC):M4Y = B1(XC)
2840  FOR Z = XC TO XD
2860  IF A1(Z) < M1X THEN M1X = A1(Z)
2880  IF A1(Z) > M2X THEN M2X = A1(Z)
2900  IF B1(Z) < M3Y THEN M3Y = B1(Z)
2920  IF B1(Z) > M4Y THEN M4Y = B1(Z)
2940  NEXT Z
2960  PRINT " X MIN,MAX ";M3X;" ";M4X;"   Y MIN,MAX ";M1Y;
    " ";M2Y
2980  PRINT "SCALE & PLOT THIS X RANGE"
3000 CV =  PEEK (37)
3020  POKE 36,26
3040  POKE 37,CV: VTAB CV: PRINT "<";NT$;">"
3060 NS$ = NT$
3080 NS =  LEN (NS$)
3090 KK = 28 + NS
3100  POKE 37,CV: POKE 36,28 + NS: VTAB CV: GOSUB 10000
3110 NS$ = A$
3115  PRINT  CHR$ (13)
3120 G9 =  LEN (NS$)
3140  IF G9 = 0 THEN 3180
3160 NT$ = NS$
3180  IF  LEFT$ (NT$,1) <  > "Y" THEN 2300
3200  PRINT
3220  PRINT "X AXIS LABEL?"
3240 CV =  PEEK (37)
3260  POKE 36,14
3280  POKE 37,CV: VTAB CV: PRINT "<";XQ$;">"
3300 XL$ = XQ$
3320 XL =  LEN (XL$)
3330 KK = 17 + XL
3340  POKE 37,CV: POKE 36,16 + XL: VTAB CV: GOSUB 10000
3350 XL$ = A$
3355  PRINT  CHR$ (13)
3360 H1 =  LEN (XL$)
3380  IF H1 = 0 THEN 3420
3400 XQ$ = XL$
3420 XL =  LEN (XQ$)
3440 XK =  INT ((1885 - (XL * 24)) / 2) + 155
3460  PRINT "X RANGE IS ";(XD - XC + 1);" FROM ";M3;" TO "
    ;M4
3480  PRINT "HOW MANY X TICK MARKS?"
3500 CV =  PEEK (37)
3520  POKE 36,23
3540  POKE 37,CV: VTAB CV: PRINT "<";XN$;">"
3560 XE$ = XN$
3580 T3 =  LEN (XN$)
3590 KK = 26 + T3
3600  POKE 37,CV: POKE 36,25 + T3: VTAB CV: GOSUB 10000
3610 XE$ = A$
3615  PRINT  CHR$ (13)
```

```
3620 G8 =  LEN (XE$)
3640  IF G8 = 0 THEN 3680
3660 XN$ = XE$
3680 VE =  VAL (XN$) - 0
3700 XF = B1(XC):XG = B1(XD)
3720  PRINT "X TICK MARKS OCCUR EVERY ";((M4 - M3) + 0) /
   VE;" UNITS"
3740  PRINT "INCREMENT FOR X TICK LABEL?"
3760 CV =  PEEK (37)
3780  POKE 36,28
3800  POKE 37,CV: VTAB CV: PRINT "<";XP$;">"
3820 XH$ = XP$
3840 T4 =  LEN (XP$)
3850 KK = 31 + T4
3860  POKE 37,CV: POKE 36,30 + T4: VTAB CV: GOSUB 10000
3870 XH$ = A$
3875  PRINT  CHR$ (13)
3880 H2 =  LEN (XH$)
3900  IF H2 = 0 THEN 3940
3920 XP$ = XH$
3940 VH =  VAL (XP$)
3960  PRINT
3980  PRINT "Y AXIS LABEL?"
4000 CV =  PEEK (37)
4020  POKE 36,14
4040  POKE 37,CV: VTAB CV: PRINT "<";YQ$;">"
4060 YL$ = YQ$
4080 YL =  LEN (YL$)
4090 KK = 17 + YL
4100  POKE 37,CV: POKE 36,16 + YL: VTAB CV: GOSUB 10000
4110 YL$ = A$
4115  PRINT  CHR$ (13)
4120 H3 =  LEN (YL$)
4140  IF H3 = 0 THEN 4180
4160 YQ$ = YL$
4180 YL =  LEN (YQ$)
4200 YK =  INT ((1275 - (YL * 24)) / 2) + 135
4220  PRINT "SCALE Y DATA BETWEEN WHAT VALUES ?"
4240  PRINT "Y MINIMUM VALUE?"
4260 CV =  PEEK (37)
4280  POKE 36,17
4300  POKE 37,CV: VTAB CV: PRINT "<";S3$;">"
4320 YF$ = S3$
4340 T5 =  LEN (YF$)
4350 KK = 20 + T5
4360  POKE 37,CV: POKE 36,19 + T5: VTAB CV: GOSUB 10000
4370 YF$ = A$
4375  PRINT  CHR$ (13)
4380 H4 =  LEN (YF$)
4400  IF H4 = 0 THEN 4440
4420 S3$ = YF$
4440  PRINT "Y MAXIMUM VALUE?"
4460 CV =  PEEK (37)
```

```
4480  POKE 36,17
4500  POKE 37,CV: VTAB CV: PRINT "<";S4$;">"
4520 YG$ = S4$
4540 T6 =  LEN (YG$)
4550 KK = 20 + T6
4560  POKE 37,CV: POKE 36,19 + T6: VTAB CV: GOSUB 10000
4570 YG$ = A$
4575  PRINT  CHR$ (13)
4580 H5 =  LEN (YG$)
4600  IF H5 = 0 THEN 4640
4620 S4$ = YG$
4640 VG =  VAL (S4$):VF =  VAL (S3$)
4660 MY = VG
4680  PRINT "Y RANGE IS ";(VG - VF + 1);" FROM ";VF;" TO "
     ;VG
4700  PRINT "HOW MANY Y TICK MARKS?"
4720 CV =  PEEK (37)
4740  POKE 36,23
4760  POKE 37,CV: VTAB CV: PRINT "<";YN$;">"
4780 YE$ = YN$
4800 T7 =  LEN (YN$)
4810 KK = 26 + T7
4820  POKE 37,CV: POKE 36,25 + T7: VTAB CV: GOSUB 10000
4830 YE$ = A$
4835  PRINT  CHR$ (13)
4840 H6 =  LEN (YE$)
4860  IF H6 = 0 THEN 4900
4880 YN$ = YE$
4900 YT =  VAL (YN$)
4920  PRINT "Y TICK MARKS OCCUR EVERY ";((VG - VF + 1)) /
     YT;" UNITS"
4940  PRINT "INCREMENT FOR Y TICK LABEL?"
4960 CV =  PEEK (37)
4980  POKE 36,28
5000  POKE 37,CV: VTAB CV: PRINT "<";YP$;">"
5020 YH$ = YP$
5040 T8 =  LEN (YH$)
5050 KK = 31 + T8
5060  POKE 37,CV: POKE 36,30 + T8: VTAB CV: GOSUB 10000
5070 YH$ = A$
5075  PRINT  CHR$ (13)
5080 H7 =  LEN (YH$)
5100  IF H7 = 0 THEN 5140
5120 YP$ = YH$
5140 YS =  VAL (YP$)
5160 XA = B1(XC):YA = VF:XB = B1(XC):YB = VF
5180 YB$ =  STR$ (VF)
5200 IY = ((VG - VF) + 1) / YT
5220 XB$ =  STR$ (XF)
5240 IX = ((XG - XF) + 0) / VE
5260 RX = (MY - VF) + 1
5280 RY = (M4Y - M3Y)
```

```
5300 SX = (( INT (1050 / YT) * YT) / RX):SY = (( INT (1595
     / VE) * VE) / RY)
5320  FOR Z = XC TO XD
5340 A2(Z) =  INT ((A1(Z) - VF) * SX + 225)
5360  IF A2(Z) >  INT ( INT ((1050 / YT)) * YT) + 225 THEN
     A2(Z) =  INT ( INT ((1050 / YT)) * YT) + 225
5380  IF A2(Z) < 225 THEN A2(Z) = 225
5400 B2(Z) =  INT ((B1(Z) - M3Y) * SY + 290)
5420  IF B2(Z) >  INT ( INT ((1595 / VE)) * VE) + 290 THEN
     B2(Z) =  INT ( INT ((1595 / VE)) * VE) + 290
5440  IF B2(Z) < 290 THEN B2(Z) = 290
5460  NEXT Z
5480  PRINT "LIST SCALED DATA?"
5500 CV =  PEEK (37)
5520  POKE 36,18
5540  POKE 37,CV: VTAB CV: PRINT "<";L3$;">"
5560 L2$ = L3$
5580 L2 =  LEN (L2$)
5590 KK = 21 + L2
5600  POKE 37,CV: POKE 36,20 + L2: VTAB CV: GOSUB 10000
5610 L2$ = A$
5615  PRINT  CHR$ (13)
5620 H8 =  LEN (L2$)
5640  IF H8 = 0 THEN 5680
5660 L3$ = L2$
5680  IF  LEFT$ (L3$,1) <  > "Y" THEN 5760
5700  FOR Z = XC TO XD
5720  PRINT Z; TAB( 10);A2(Z); TAB( 20);B2(Z)
5740  NEXT Z
5760 XM =  INT ( INT ((1595 / VE)) * VE) + 290
5780 YM =  INT ( INT ((1050 / YT)) * YT) + 225
5800  PRINT  CHR$ (4);"PR#2"
5820  PRINT ";:I 21 100"
5840  PRINT "H"
5860  PRINT "AOU290 225"
5880  PRINT "D";XM;" 225 290 225 290 ";YM;" 290 225"
5900  PRINT "U"
5920 XI =  INT (1595 / VE)
5940 XJ = 290
5960  FOR X = 0 TO VE
5980  PRINT "AU";XJ;" 235"
6000  PRINT "D";XJ;" 225"
6020  PRINT "AU"
6040  GOSUB 8660
6060 XJ = XJ + XI
6080  NEXT X
6100  PRINT "U";XK;" 120"
6120  PRINT " S12 ";XQ$
6140  PRINT G$
6160 YI =  INT (1050 / YT)
6180 YJ = 225
6200  FOR Q = 0 TO YT
```

```
6220  PRINT "U290 ";YJ
6240  PRINT "D300 ";YJ
6260  PRINT "U"
6280  GOSUB 8920
6300 YJ = YJ + YI
6320  NEXT Q
6340  PRINT "U160 ";YK
6360  PRINT "S42 ";YQ$
6380  PRINT G$
6400  PRINT "U290 225"
6420  PRINT B2(XC);" ";A2(XC)
6440  FOR Z = XC + 1 TO XD
6460  PRINT "D";B2(Z);" ";A2(Z)
6480  NEXT Z
6500  PRINT "U"
6520  PRINT "H"
6540  PRINT  CHR$ (4);"PR#O"
6560  PRINT "LABEL THE PLOT?"
6580 CV =  PEEK (37)
6600  POKE 36,16
6620  POKE 37,CV: VTAB CV: PRINT "<";LQ$;">"
6640 LP$ = LQ$
6660 T9 =  LEN (LP$)
6670 KK = 19 + T9
6680  POKE 37,CV: POKE 36,18 + T9: VTAB CV: GOSUB 10000
6690 LP$ = A$
6695  PRINT  CHR$ (13)
6700 H9 =  LEN (LP$)
6720  IF H9 = O THEN 6760
6740 LQ$ = LP$
6760  PRINT "THIS IS A PLOT OF FILE ";NM$
6780  IF  LEFT$ (LQ$,1) <  > "Y" THEN 8180
6800  REM  HEADING FOR PLOT
6820  PRINT "THREE LINES OF TEXT (MAX 25 CHAR)"
6840  PRINT "       ARE POSSIBLE"
6860  PRINT "FIRST LINE?"
6880 CV =  PEEK (37)
6900  POKE 36,12
6920  POKE 37,CV: VTAB CV: PRINT "<";W1$;">"
6940 W2$ = W1$
6960 W2 =  LEN (W2$)
6970 KK = 15 + W2
6980  POKE 37,CV: POKE 36,14 + W2: VTAB CV: GOSUB 10000
6990 W2$ = A$
6995  PRINT  CHR$ (13)
7000 J1 =  LEN (W2$)
7020  IF J1 = O THEN 7060
7040 W1$ = W2$
7060  PRINT "SECOND LINE?"
7080 CV =  PEEK (37)
7100  POKE 36,13
7120  POKE 37,CV: VTAB CV: PRINT "<";W3$;">"
```

```
7140 W4$ = W3$
7160 W4 =  LEN (W4$)
7170 KK = 16 + W4
7180  POKE 37,CV: POKE 36,15 + W4: VTAB CV: GOSUB 10000
7190 W4$ = A$
7195  PRINT  CHR$ (13)
7200 J2 =  LEN (W4$)
7220  IF J2 = 0 THEN 7260
7240 W3$ = W4$
7260  PRINT "THIRD LINE?"
7280 CV =  PEEK (37)
7300  POKE 36,12
7320  POKE 37,CV: VTAB CV: PRINT "<";W5$;">"
7340 W6$ = W5$
7360 W6 =  LEN (W6$)
7370 KK = 15 + W6
7380  POKE 37,CV: POKE 36,14 + W6: VTAB CV: GOSUB 10000
7390 W6$ = A$
7395  PRINT  CHR$ (13)
7400 J3 =  LEN (W6$)
7420  IF J3 = 0 THEN 7460
7440 W5$ = W6$
7460  PRINT "X INCHES FROM ORIGIN?"
7480 CV =  PEEK (37)
7500  POKE 36,22
7520  POKE 37,CV: VTAB CV: PRINT "<";I1$;">"
7540 I2$ = I1$
7560 I2 =  LEN (I2$)
7570 KK = 25 + I2
7580  POKE 37,CV: POKE 36,24 + I2: VTAB CV: GOSUB 10000
7590 I2$ = A$
7595  PRINT  CHR$ (13)
7600 J4 =  LEN (I2$)
7620  IF J4 = 0 THEN 7660
7640 I1$ = I2$
7660  PRINT "Y INCHES FROM ORIGIN?"
7680 CV =  PEEK (37)
7700  POKE 36,22
7720  POKE 37,CV: VTAB CV: PRINT "<";I3$;">"
7740 I4$ = I3$
7760 I4 =  LEN (I4$)
7780  POKE 37,CV: POKE 36,24 + I4: VTAB CV: INPUT "";I4$
7800 J5 =  LEN (I4$)
7820  IF J5 = 0 THEN 7860
7840 I3$ = I4$
7860 LX =  VAL (I1$) * 160:LY =  VAL (I3$) * 160
7880  PRINT  CHR$ (4);"PR#2"
7900  PRINT ";:I 21 100"
7920  PRINT "H"
7940  PRINT "AOU";LX + 290;" ";LY + 225
7960  PRINT "S12 ";W1$
7980  PRINT G$
```

```
8000  PRINT "AU";LX + 290;" ";LY + 190
8020  PRINT "S12 ";W3$
8040  PRINT G$
8060  PRINT "AU";LX + 290;" ";LY + 150
8080  PRINT "S12 ";W5$
8100  PRINT G$
8120  PRINT "U"
8140  PRINT "H"
8160  PRINT  CHR$ (4);"PR#0"
8180  PRINT "SAME FILE?"
8200 CV =  PEEK (37)
8220  POKE 36,11
8240  POKE 37,CV: VTAB CV: PRINT "<";Q1$;">"
8260 SF$ = Q1$
8280 SF =  LEN (SF$)
8290 KK = 14 + SF
8300  POKE 37,CV: POKE 36,13 + SF: VTAB CV: GOSUB 10000
8310 SF$ = A$
8315  PRINT  CHR$ (13)
8320 J4 =  LEN (SF$)
8340  IF J4 = 0 THEN 8380
8360 Q1$ = SF$
8380  IF  LEFT$ (Q1$,1) <  > "Y" THEN 8420
8400  GOTO 2260
8420  PRINT "ANOTHER FILE?"
8440 CV =  PEEK (37)
8460  POKE 36,14
8480  POKE 37,CV: VTAB CV: PRINT "<";Q2$;">"
8500 SA$ = Q2$
8520 SA =  LEN (SA$)
8530 KK = 17 + SA
8540  POKE 37,CV: POKE 36,16 + SA: VTAB CV: GOSUB 10000
8550 SA$ = A$
8555  PRINT  CHR$ (13)
8560 J5 =  LEN (SA$)
8580  IF J5 = 0 THEN 8620
8600 Q2$ = SA$
8620  IF  LEFT$ (Q2$,1) <  > "N" THEN 540
8640  HOME : END
8660  IF XB / VH <  > (XA / VH) THEN 8860
8680  IF XB = XG + X2 THEN 8860
8700 XA = XA + VH
8720 X5 =  LEN (XB$)
8740  PRINT "U";XJ - ((X5 / 2) * 24);" 175"
8760  PRINT "S12 ";XB$
8780  PRINT G$
8800  PRINT "U";XJ;" 245"
8820  PRINT "D";XJ;" 225"
8840  PRINT "U"
8860 XB = XB + IX
8880 XB$ =  STR$ (XB)
8900  RETURN
```

```
8920  REM
8940  IF YB / YS <  > (YA / YS) THEN 9140
8960  IF YB = VG THEN 9140
8980 YA = YA + YS
9000 Y5 =  LEN (YB$)
9020  PRINT "U";285 - (Y5 * 24);" ";YJ - 12
9040  PRINT "S12 ";YB$
9060  PRINT G$
9080  PRINT "U290 ";YJ
9100  PRINT "D310 ";YJ
9120  PRINT "U"
9140 YB = YB + IY
9160 YB$ =  STR$ (YB)
9180  RETURN
10000  REM  INPUT ROUTINE
10020 A$ = ""
10040  GET I$
10060 I =  ASC (I$)
10070  IF I = 13 THEN 10160
10080 A$ = A$ + I$: HTAB (KK): PRINT A$;
10100  IF I = 13 THEN 10160
10120  IF I = 3 THEN  STOP
10140  GOTO 10040
10160  REM
10180  RETURN
```

APPENDIX 5
DIFFRACTED STIMULATED EMISSION

In the course of becoming familar with the operation of both the nitrogen laser and the dye laser, the phenomenon of diffracted stimulated emission was investigated. This work was instigated by a paper by Stepowski (80) which appeared in 1979.

In this paper, it was shown theoretically that diffracted stimulated emission should occur at certain angles when a medium is probed with intersecting dye laser beams capable of exciting a certain species in the medium. This was of great interest because it is well-known that the stimulated emission rate can be considerably greater than the spontaneous emission rate in all cases where the radiational excitation rate exceeds the collisional quenching rate plus the spontaneous emission rate. Unfortunately, with a single laser beam, stimulated emission is difficult to detect because it occurs in the same direction and with the same phase and polarization as the exciting laser beam (81). By splitting the exciting laser beam into two equivalent beams which intersect at angle 2θ in the medium of interest and measuring the diffracted stimulated emission at an angle of 3θ (or 5θ, 7θ, etc.), it is possible to avoid the difficult (impossible) problem of separating the stimulated emission from the incident single laser beam.

Therefore, an optical system was designed and constructed to produce the conditions required to cause the production of diffracted stimulated emission. Described is the empirical study of diffracted stimulated emission and the problems associated with it. A nitrogen laser-pumped dye laser with Rhodamine 590 tuned to 589.6 nm (1.5 mJ at 20 Hz) was used as the excitation source. The dye laser beam was split into two beams using a quartz plate beam splitter. The orthogonal beam was directed through the atom reservoir (in this work, an air-acetylene flame) by means of a front-surface planar mirror. The beam passing through the beam splitter was directed via a set of four front-surface planar mirrors into the atom reservoir in such a manner as to have spatial overlap with the orthogonal beam. The four mirrors had micrometer adjustments which served to change the beam path length in order to achieve the required temporal and spatial phase matching of the two beams (see Figure 36). A photomultiplier tube (R955, Hamamatsu, Middlesex, NJ) was mounted onto a JY H-10 monochromator (ISA, Metuchen, NJ) with geometric slits of 0.05 mm (bandpass of 0.4 nm). The monochromator was fixed onto a rotary micrometer mount whose axial center coincided with the volume in the flame where the two laser beams crossed (see Figure 37). The flame produced approximately 2.6×10^{16} Na atoms/cm^3 from a 1000 ppm Na (NaCl) solution.

Figure 36

Block diagram of experimental system used to produce diffracted stimulated emission.

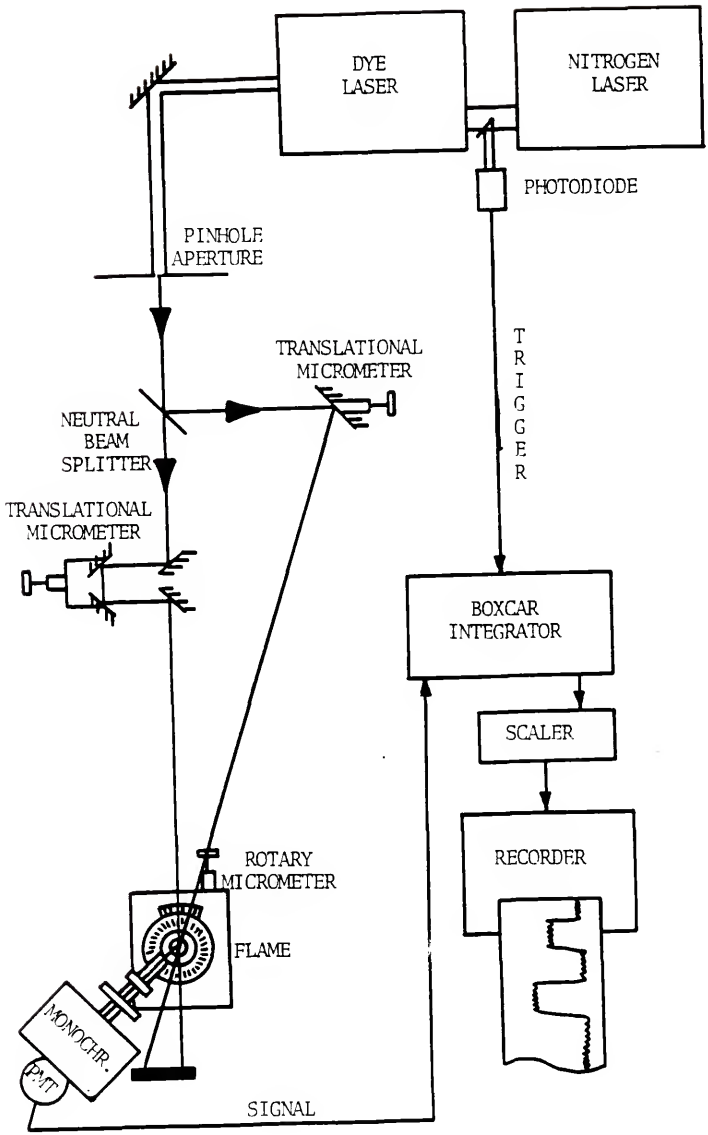
DYE
LASER
NITROGEN
LASER
PHOTODIODE
PINHOLE
APERTURE
TRANSLATIONAL
MICROMETER
TRIGGER
NEUTRAL
BEAM
SPLITTER
TRANSLATIONAL
MICROMETER
BOXCAR
INTEGRATOR
SCALER
RECORDER
ROTARY
MICROMETER
FLAME
MONOCHR.
PMT
SIGNAL

Figure 37

Detailed view of the flame and detector geometry in the diffracted stimulated emission system.

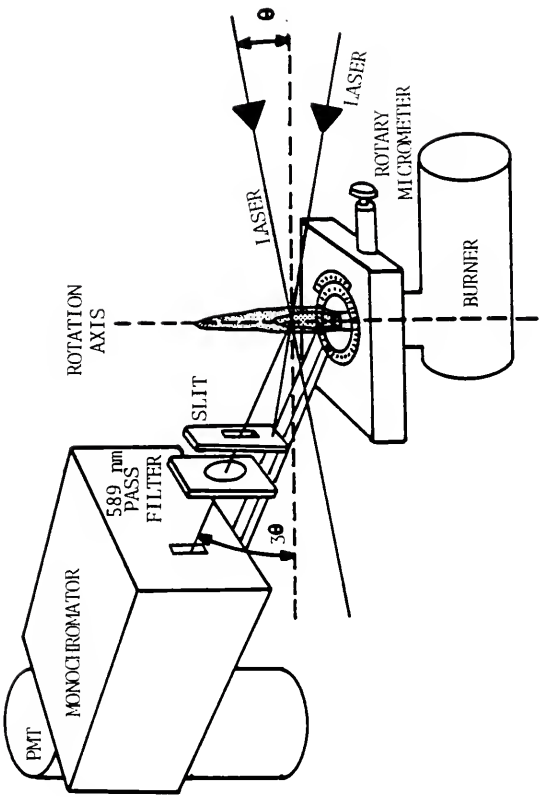
θ
LASER
LASER
ROTARY
MICROMETER
BURNER
ROTATION
AXIS
SLIT
589 nm
PASS
FILTER
3θ
MONOCHROMATOR
PMT

For a crossing angle of $\theta = 8^{\circ}54'$, diffracted stimulated emission is expected at $26^{\circ}02'$; it was actually found at $25^{\circ}50'$. There was great difficulty in obtaining the signal because the smallest amount of movement in the optical mounts as well as the optical table would upset the critical alignment required for temporal and spatial overlap. The laser was located on a separate optical table from the atom reservoir where the actual crossing of the beams was achieved. Ideally, all components should be on a single vibrationally isolated optical table. Additionally, the mirrors, beam splitter, burner and monochromator were positioned on optical rails using locally constructed mounting risers, which allowed horizontal and vertical adjustment although not on a micrometer scale. It was the alignment limitation which is the single greatest drawback to the analytical use of diffracted stimulated emission. However, even if this problem could be minimized, the signals from diffracted stimulated emission would still be much weaker than those of fluorescence (see Table A5-1). Because the signals were weak for a 1000 ppm Na solution and stimulated emission intensity is proportional to the square of the number of excitable species present, diffracted stimulated emission is not expected to be of much use in trace analytical measurements.

TABLE A5-1

Signal levels for sodium fluorescence and diffracted stimulated emission at 589.6 nm[a]

Sample Solution	Fluorescence (R.U.)[c]	Diff. Stim. Em. (R.U.)[c]
1000 ppm Na	78	5
1000 ppm Na[a]	80	50

[a]All measurements taken at 3θ angle.

[b]This measurement taken on different date and points to the critical influence of precise alignment.

[c]R.U. = relative units.

REFERENCES

1. B.V. L'vov, Inzh. Fiz. Zh. 2, 44 (1959).
2. B.V. L'vov, Inzh. Fiz. Zh. 2, 56 (1959).
3. B.V. L'vov, Spectrochom. Acta 17, 761 (1961).
4. B.V. L'vov, Zavodsk. Lab. 28, 931 (1962).
5. B.V. L'vov, Pure Appl. Chem. 23, 11 (1970).
6. J.P. Matousek and B.J. Stevens, Clin. Chem. 17, 363 (1971).
7. F.J.M.J. Maessen and F.D. Posma, Anal. Chem. 46, 1439 (1974).
8. F.D. Posma, H.C. Smit and A.F. Rooze, Anal. Chem. 47, 2087 (1975).
9. G. Torsi and G. Tessari, Anal. Chem. 45, 1812 (1973).
10. D.J. Johnson, B.L.Sharp, T.S. West and R.M. Dagnall, Anal. Chem. 47, 1234 (1975).
11. B.V. L'vov, ABSORPTION SPECTROCHEMICAL METHODS OF ANALYSIS, Adam Hilger, London (1970).
12. J. Aggett and A.J. Sprott, Anal. Chim. Acta 72, 49 (1974).
13. W.K. Robbins, Anal. Chem. 46, 2177 (1974).
14. D.C. Manning and R.D. Ediger, A.A. Newslett. 15, 42 (1976).
15. C.W. Fuller, Analyst 99, 739 (1974).
16. S.L. Paveri-Fontana, G. Terrasi and G. Torsi, Anal. Chem. 46, 1032 (1974).
17. W.C. Campbell and J.M. Ottaway, Talanta 21, 837 (1974).
18. D. Alger, R.G. Anderson, I.S. Maines and T.S. West, Anal. Chim. Acta 57, 271 (1971).

19. G. Bowdin, M. Chaput and L. Feve, Spectrochim. Acta 26B, 425 (1971).

20. J. Aggett and T.S. West, Anal. Chim. Acta 55, 439 (1971).

21. L. Ebdon, G.F. Kirkbright and T.S. West, Talanta 19, 1301 (1972).

22. R.D. Reeves, B.M. Patel, C.J. Molnar and J.D. Winefordner, Anal. Chem. 45, 246 (1973).

23. R.E. Sturgeon and C.L. Chakrabarti, Prog. Analyt. Atom. Spectrosc. 1, 9 (1979).

24. A. Syty, Crit. Rev. Anal. Chem. 4, 155 (1974).

25. R. Woodriff, Appl. Spectrosc. 28, 413 (1974).

26. G.M. Heiftje, T.R. Copeland and D.R. deOlivares, Anal. Chem. 48, 142R (1976).

27. C.T.J. Alkemade, PROC. XTH COLLOQ. SPECTR. INTERN., E.R. Lippincott and M. Margoshes, Editors, Spartan Books, Washington, D.C. (1963).

28. J.D. Winefordner and T.J. Vickers, Anal. Chem. 36, 161 (1964).

29. J.D. Winefordner and R.A. Staab, Anal. Chem. 36, 161 (1964).

30. P.P. Sorokin and J.R. Lankard, IBM J. Res Develop. 10, 162 (1966).

31. F.P. Schafer, W. Schmidt and J. Volze, J. Appl. Phys. Lett. 9, 306 (1966).

32. L.M. Fraser and J.D. Winefordner, Anal. Chem. 43, 1693 (1971).

33. M.A. Bolshov, A.V. Zybin and I.I. Smirenkina, Spectrochim. Acta 36B, 1143 (1981).

34. N. Omenetto, Editor, ANALYTICAL LASER SPECTROSCOPY, Wiley, New York (1979).

35. S.I.Weeks, H.J. Haraguchi and J.D. Winefordner, Anal. Chem. 50, 360 (1978).

36. G. Zizak, J.D.Bradshaw and J.D. Winefordner, Appl. Opt. 19, 3631 (1980).

37. J.W. Daily, Appl. Opt. 17, 225 (1978).

38. R.B. Green, R.A. Keller, G.G. Luther, and J.C. Travis, J. Am. Chem. Soc. 98, 8517 (1976).

39. M.B. Blackburn and J.M. Mermet, Appl. Opt. 18, 1804 (1980).

40. M.S. Epstein, S. Bayer, J. Bradshaw, E. Voigtman and J.D. Winefordner, Spectrochim. Acta 35B, 233 (1980).

41. M.S. Epstein, J. Bradshaw, S. Bayer, J. Bower, E. Voigtman and J. D. Winefordner, Appl. Spectrosc. 34, 372 (1980).

42. B.M. Patel, R.D. Reeves, R.F. Browner, C.J. Molnar and J.D. Winefordner, Appl. Spectrosc. 27, 171 (1973).

43. M.A. Bolshov, A.V. Zybin, L.A. Zybina, V.G. Koloshnikov and I.A. Majorov, Spetrochim. Acta 31B, 493 (1976).

44. S. Neuman and M. Kriese, Spectrochim. Acta 29B, 127 (1974).

45. J.P. Hohimer and P.J. Hargis, Appl. Phys. Lett. 30, 344 (1977).

46. M.A. Bolshov, A.V.Zybin and I.I. Smirenkina, Spectrochim. Acta 36B, 1143 (1981).

47. B.V. L'vov, Zh. Prikl. Spektrosk. 8, 517 (1968).

48. B.V. L'vov, Spectrochim. Acta 33B, 153 (1978).

49. B.V. L'vov, D.A. Katskov and G.G. Lebedev, Zh. Prikl. Spektrosk. 9, 558 (1968).

50. B.V. L'vov, L.P. Krugkikova and G.V. Plyushch, Zh. Prikl. Spektrosk. 15, 975 (1971).

51. A.C.G. Mitchell and M.W. Zemansky, RESONANCE RADIATION AND EXCITED ATOMS, Cambridge Univ. Press, Cambridge, England (1961).

52. P. Pringsheim, FLUORESCENCE AND PHOSPHORESCENCE, Interscience Publishers, New York (1949).

53. N. Omenetto and J.D. Winefordner, Appl. Spectrsc. 26, 555 (1972).

54. L.M. Fraser, Ph.D. Dissertation, University of Florida, (1972).

55. J.D. Winefordner, J. Chem. Ed. 55, 72 (1978).

56. G.D. Boutilier, M.B. Blackburn, J.M. Mermet, S.J. Weeks, H. Haraguchi, J.D. Winefordner and N. Omenetto, Appl. Opt. 17, 2291 (1978).

57. J.N. Bower, Ph.D. Dissertation, University of Florida, (1979).

58. W.R. Ware, "Transient Luminescence Measurements" in CREATION AND DETECTION OF THE EXCITED STATE, Vol. 1, Part A, A.A. Lamole, Editor, Marcel Dekker, New York (1971).

59. N. Omenetto and J.D. Winefordner, Prog. Analyt. Atom. Spectrosc. 2, 151 (1979).

60. D.R. Jenkins, Proc. Roy. Soc. Ser. A 306, 413 (1966).

61. H.P. Hooyermayers and P.J. Lijnse, J. Quant. Spectrosc. Radiat. Transfer 9, 995 (1969).

62. P.J. Lijnse and R.J. Elsenaar, J. Quant. Spectrosc. Radiat. Transfer 12, 1115 (1972).

63. C.Th.J. Alkemade, Tj. Hollander, W. Snelleman and P.J. Th. Zeegers, METAL VAPOURS IN FLAMES, Pergamon Press, New York (1982).

64. R. Mavrodineanu and H. Boiteaux, FLAME SPECTROSCOPY, Wiley and Sons, New York (1965).

65. W.F. Meggers, C.H. Corliss and B.F. Schriber, TABLES OF SPECTRAL-LINE INTENSITIES, NBS Monograph 32, Part I, US Government Printing Office, Washington, D.C., (1961).

66. M.L. Parsons, B.W. Smith and G.E. Bentley, HANDBOOK OF FLAME SPECTROSCOPY, Plenum Press, New York (1975).

67. P. Bennett, N. Omenetto and G. Rossi, Appl. Spectrosc. 25, 57 (1971).

68. M.S. Epstein, S. Bayer, J. Bradshaw, E. Voigtman and J.D. Winefordner, Spectrochim. Acta 35B, 233 (1980).

69. T.F. Wynn, Jr., M.S. Thesis, University of Flordia, (1980).

70. J.D. Winefordner, Chem. Tech. 5, 123 (1975).

71. R.F. Browner, Analyst 99, 617 (1974).

72. C.J. Molnar, Ph.D. Dissertation, University of Florida, (1974).

73. R.E. Russo and G.M. Hieftje, Appl. Spectrosc. 36, 92 (1982).

74. M.A. Bolshov, A.V. Zybin, V.G. Koloshnikov and M.V. Vasnetsov, Spectrochim. Acta 36B, 345 (1981).

75. E. Voigtman and D. Bolton, University of Florida, private communication, March 1981.

76. E. Voigtman, University of Florida, private communication, March 1981.

77. P. Wittman, J. Bower, J.J. Horvath, A. Ullman and J.D. Winefordner, Can. J. Spectrosc. 26, 212 (1981).

78. R. Stair, R.G. Johnson and E.W. Halback, J. Research 64A, 291 (1960).

79. R.L. Cochran and G.M. Hieftje, Anal. Chem. 49, 2040 (1977).

80. D. Stepowski, Appl. Opt. 18, 3967 (1979).

81. A.P. Thorne, SPECTROPHYSICS, Wiley and Sons, New York (1974).

BIOGRAPHICAL SKETCH

Philip Kirk Wittman was born May 11, 1956, in Williamsport, Pennsylvania. In June, 1974, he was graduated from Montoursville Area High School in Montoursville, Pennsylvania. In May, 1978, he was graduated from Lycoming College in Williamsport, Pennsylvania, with a Bachelor of Arts degree in chemistry. In September, 1978, he entered the Graduate School at the University of Florida in Gainesville, Florida.

He is a member of the American Chemical Society (Analytical Division), the American Institute of Chemists and the Society for Applied Spectroscopy.

I certify that I have read this study and that in my opinion it conforms to acceptable standards of scholarly presentation and is fully adequate, in scope and quality, as a dissertation for the degree of Doctor of Philosophy.

James D. Winefordner, Chairman
Graduate Research Professor
of Chemistry

I certify that I have read this study and that in my opinion it conforms to acceptable standards of scholarly presentation and is fully adequate, in scope and quality, as a dissertation for the degree of Doctor of Philosophy.

Gerhard M. Schmid
Associate Professor of Chemistry

I certify that I have read this study and that in my opinion it conforms to acceptable standards of scholarly presentation and is fully adequate, in scope and quality, as a dissertation for the degree of Doctor of Philosophy.

John G. Dorsey
Assistant Professor of Chemistry

I certify that I have read this study and that in my opinion it conforms to acceptable standards of scholarly presentation and is fully adequate, in scope and quality, as a dissertation for the degree of Doctor of Philosophy.

W. Emmett Bolch
Professor of Environmental
Engineering Sciences

I certify that I have read this study and that in my opinion it conforms to acceptable standards of scholarly presentation and is fully adequate, in scope and quality, as a dissertation for the degree of Doctor of Philosophy.

Paul Urone
Professor Emeritus of
Environmental Engineering Sciences

This dissertation was submitted to the Graduate Faculty of the Department of Chemistry in the College of Liberal Arts and Sciences and to the Graduate Council, and was accepted as partial fulfillment of the requirements for the degree of Doctor of Philosophy.

Dean, Graduate School

UNIVERSITY OF FLORIDA
3 1262 08553 1621